



Pedro Henrique Milet Pinheiro Pereira

Domino tilings of three-dimensional regions

Tese de Doutorado

Thesis presented to the Programa de Pós-Graduação em Matemática of the Departamento de Matemática, PUC-Rio as partial fulfillment of the requirements for the degree of Doutor em Matemática.

Advisor: Prof. Nicolau Corção Saldanha

Rio de Janeiro
February 2015



Pedro Henrique Milet Pinheiro Pereira

Domino tilings of three-dimensional regions

Thesis presented to the Programa de Pós-Graduação em Matemática of the Departamento de Matemática do Centro Técnico Científico da PUC-Rio, as partial fulfillment of the requirements for the degree of Doutor.

Prof. Nicolau Corção Saldanha

Advisor

Departamento de Matemática – PUC-Rio

Prof. Carlos Gustavo Tamm de Araújo Moreira

Instituto Nacional de Matemática Pura e Aplicada – IMPA

Prof. Carlos Tomei

Departamento de Matemática – PUC-Rio

Prof. Robert David Morris

Instituto Nacional de Matemática Pura e Aplicada – IMPA

Prof. Roberto Imbuzeiro Moraes Felinto de Oliveira

Instituto Nacional de Matemática Pura e Aplicada – IMPA

Prof. Thomas Maurice Lewiner

Departamento de Matemática – PUC-Rio

Profa. Juliana Abrantes Freire

Departamento de Matemática – PUC-Rio

José Eugenio Leal

Coordinator of the Centro Técnico Científico – PUC-Rio

Rio de Janeiro, February 5th, 2015

Pedro Henrique Milet Pinheiro Pereira

The author completed his undergraduate studies in Mathematics at PUC-Rio in 2009, and obtained the degree of Mestre from PUC-Rio in 2011.

Bibliographic data

Pereira, Pedro Henrique Milet Pinheiro

Domino tilings of three-dimensional regions / Pedro Henrique Milet Pinheiro Pereira ; advisor: Nicolau Corção Saldanha. – 2015.

97 f. : il. (color.) ; 30 cm

Tese (doutorado)–Pontifícia Universidade Católica do Rio de Janeiro, Departamento de Matemática, 2015.

Inclui bibliografia

1. Matemática – Teses. 2. Coberturas tridimensionais. 3. Dominós. 4. Dímeros. 5. Acessibilidade por flips. 6. Conectividade por movimentos locais. 7. Writhe. 8. Teoria dos nós. I. Saldanha, Nicolau Corção. II. Pontifícia Universidade Católica do Rio de Janeiro. Departamento de Matemática. III. Título.

CDD: 510

Acknowledgments

To CNPq, FAPERJ and PUC-Rio, whose support made this research possible.

To my advisor, Prof. Nicolau Corção Saldanha, for his patience, support and willingness to share his knowledge.

To the Department of Mathematics, Kátia and Creuza in particular, for their availability and efficiency in helping in various situations.

To my family, for their constant love and support.

Abstract

Pereira, Pedro Henrique Milet Pinheiro; Saldanha, Nicolau Corção. **Domino tilings of three-dimensional regions**. Rio de Janeiro, 2015. 97p. Tese de Doutorado — Departamento de Matemática, Pontifícia Universidade Católica do Rio de Janeiro.

In this thesis, we consider domino tilings of three-dimensional regions, especially those of the form $\mathcal{D} \times [0, N]$. In particular, we investigate the connected components of the space of tilings of such regions by flips, the local move performed by removing two adjacent dominoes and placing them back in the only other possible position. For regions of the form $\mathcal{D} \times [0, 2]$, we define a polynomial invariant $P_t(q)$ that characterizes tilings that are “almost in the same connected component”, in a sense discussed in the thesis. We also prove that the space of domino tilings of such a region is connected by flips and trits, a local move performed by removing three adjacent dominoes, no two of them parallel, and placing them back in the only other possible position. For the general case, the invariant is an integer, the twist, to which we give a simple combinatorial formula and an interpretation via knot theory; we also prove that the twist has additive properties for suitable decompositions of a region. Finally, we investigate the range of possible values for the twist of tilings of an $L \times M \times N$ box.

Keywords

Three-dimensional tilings; Dominoes; Dimers; Flip accessibility; Connectivity by local moves; Writhe; Knot theory;

Resumo

Pereira, Pedro Henrique Milet Pinheiro; Saldanha, Nicolau Corção. **Coberturas de regiões tridimensionais por dominós**. Rio de Janeiro, 2015. 97p. Tese de Doutorado — Departamento de Matemática, Pontifícia Universidade Católica do Rio de Janeiro.

Nessa tese, consideramos coberturas de regiões tridimensionais por dominós, especialmente as da forma $\mathcal{D} \times [0, N]$. Em particular, nós investigamos as componentes conexas do espaço de coberturas desse tipo de região por flips, o movimento local que consiste em remover dois dominós paralelos adjacentes e colocá-los de volta na única outra posição possível. Para regiões da forma $\mathcal{D} \times [0, 2]$, nós definimos um invariante polinomial $P_t(q)$ que caracteriza coberturas que estão “quase na mesma componente conexa”, num sentido discutido na tese. Também provamos que o espaço de coberturas desse tipo de região é conexo por flips e trits, um movimento local que consiste em remover três dominós adjacentes e ortogonais entre si e colocá-los de volta na única outra posição possível. No caso geral, o invariante é um inteiro, o twist, para o qual damos uma fórmula combinatória simples, bem como uma interpretação via teoria dos nós; também provamos que o twist tem propriedades aditivas para decomposições adequadas de uma região. Por fim, investigamos também o conjunto de valores que são twists de coberturas de uma caixa $L \times M \times N$.

Palavras-chave

Coberturas tridimensionais; Dominós; Dímeros; Acessibilidade por flips; Conectividade por movimentos locais; Writhe; Teoria dos nós;

Contents

1	Introduction	8
2	Definitions and Notation	13
3	The two-floored case	16
3.1	Duplex regions	16
3.2	General two-story regions	19
3.3	The effect of trits on P_t	21
3.4	Examples	22
3.5	The invariant in more space	26
3.6	Connectivity by flips and trits	35
3.7	The invariant when more floors are added	37
4	The general case	41
4.1	The twist for cylinders	41
4.2	Topological groundwork for the twist	47
4.3	Writhe formula for the twist	56
4.4	Different directions of projection	59
4.5	Additive properties and proof of Theorem 3	69
4.6	Embeddable regions	71
4.7	The twist for duplex regions	73
4.8	Examples and counterexamples	76
5	Possible values of the twist	79
5.1	Asymptotic lower bounds	80
5.2	General bounds for boxes	85
	Glossary	93

1

Introduction

Towards the end of the twentieth century, a lot has been said about tilings of two-dimensional regions by a number of different pieces: in particular, the so-called *domino* and *lozenge* tilings have received a lot of attention.

Kasteleyn [12] showed that the number of domino tilings of a plane region can be calculated via the determinant of a matrix. Conway [6] discovered a technique using groups, that in a number of interesting cases can be used to decide whether a given region can be tessellated by a set of given tiles. Thurston [23] introduced height functions, and proposed a linear time algorithm for solving the problem of tileability of simply connected plane regions by dominoes. In a more probabilistic direction, Jockusch, Propp and Shor [11, 5] studied random tilings of the so-called Aztec Diamond (introduced in [7]), and showed the Arctic Circle Theorem. Richard Kenyon and Andrei Okounkov also studied random tilings and, in particular, their relation to Harnack curves [14, 13]. The concept of a flip is important in the context of dominoes as well as in that of lozenges. In both cases, two tilings of a simply connected region can always be joined by a sequence of flips (see [22] for an overview). Also, see [21] for considerations on flip connectivity in more general two-dimensional regions.

However, in comparison, much less is known about tilings of three-dimensional regions. Hammersley [10] proved results concerning the asymptotic behavior of the number of brick tilings of a d -dimensional box when all dimensions go to infinity. In particular, his results imply that the limit $\ell_3 = \lim_{n \rightarrow \infty} \frac{\log f(2n)}{(2n)^3}$, where $f(n)$ is the number of tilings of an $n \times n \times n$ box, exists and is finite; as far as we know, its exact value is not yet known, but several upper and lower bounds have been established for ℓ_3 (see [4] and [8] for more information on this topic). Randall and Yngve [20] considered tilings of “Aztec” octahedral and tetrahedral regions with triangular prisms, which generalize domino tilings to three dimensions; they were able to carry over to this setting many of the interesting properties from two dimensions, e.g., height functions and connectivity by local moves. Linde, Moore and Nordahl

[15] considered families of tilings that generalize rhombus (or lozenge) tilings to n dimensions, for any $n \geq 3$. Bodini [3] considered tileability problems of pyramidal polycubes. Pak and Yang [19] studied the complexity of the problems of tileability and counting for domino tilings in three and higher dimensions, and proved some hardness results in this respect.

Others have considered difficulties with connectivity by local moves in dimension higher than two (see, e.g., [20]). We propose a few related algebraic invariants that could help understand the structure of connected components by flips in dimension three.

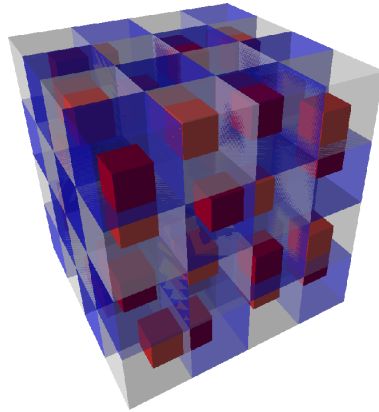


Figure 1.1: A tiling of a $4 \times 4 \times 4$ box.

This thesis contains material from the preprints [17] and [18]. In this thesis, we investigate tilings of contractible cubulated regions (that is, a finite union of unit cubes with vertices in \mathbb{R}^2) by *domino brick* pieces, or *dominoes*, which are $2 \times 1 \times 1$ rectangular cuboids, in one of the three possible rotations. An example of such a tiling is shown in Figure 1.1. While this 3D representation of tilings may be attractive, it is also somewhat difficult to work with. Hence, we prefer to work with a 2D representation of tilings, which is shown in Figure 1.2.

A key element in our study is the concept of a *flip*, which is a straightforward generalization of the two-dimensional one. We perform a flip on a tiling by removing two (adjacent and parallel) domino bricks and placing them back in the only possible different position. The removed pieces form a $2 \times 2 \times 1$ slab, in one of three possible directions (see Figure 1.3).

We also study the *trit*, which is a move that happens within a $2 \times 2 \times 2$ cube with two opposite “holes”, and which has an orientation (positive or negative: see Chapter 2). More precisely, we remove three dominoes, no two of them parallel, and place them back in the only other possible configuration (see Figure 1.4).

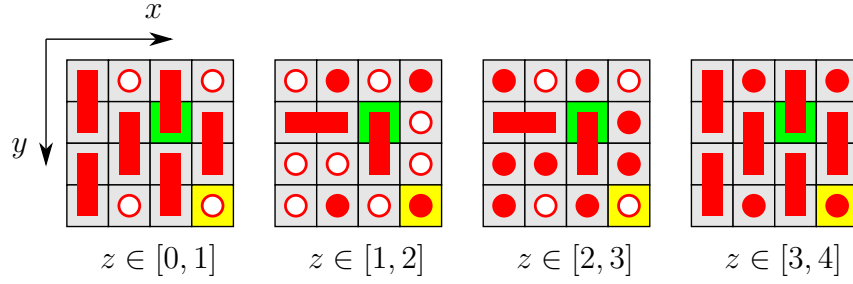


Figure 1.2: A tiling of the box $\mathcal{B} = [0, 4] \times [0, 4] \times [0, 4]$ box in our notation. The x and y axis are drawn, and z points towards the paper, so that floors to the right have higher z coordinates. Dominoes that are parallel to the x or y axis are represented as 2D dominoes, since they are contained in a single floor. Dominoes parallel to the z axis are represented as circles, with the following convention: if the corresponding domino connects a floor with the floor to the left of it, the circle is painted red; otherwise, it is painted white. Thus, for example, in Figure 1.2, each of the four white circles on the leftmost floor represents the same domino as the red circles on the floor directly to the right of it. The squares highlighted in yellow represent cubes whose centers have the same x and y coordinates. Notice the top two yellow cubes are connected by a domino parallel to the z axis, as well as the bottom two. The squares highlighted in green also represent cubes whose center have the same x and y coordinates, but the dominoes involving these cubes are not parallel to the z axis.

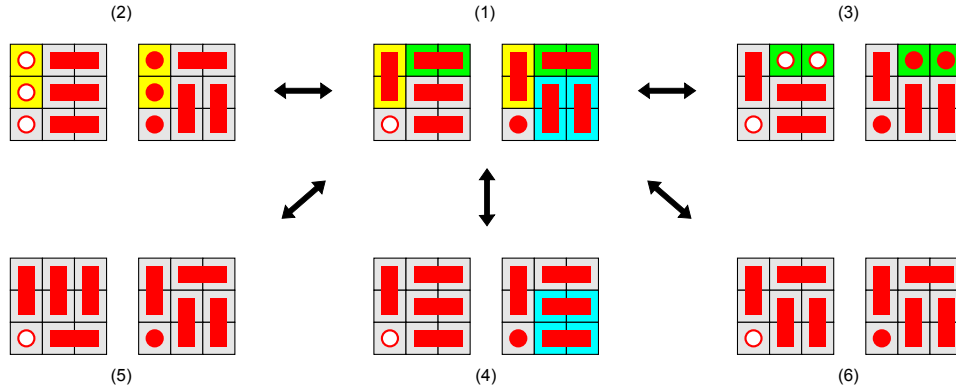


Figure 1.3: All flips available in tiling (1). The $2 \times 2 \times 1$ slabs involved in the flips taking (1) to (2), (3) and (4) are highlighted: they illustrate the three possible relative positions of dominoes in a flip.

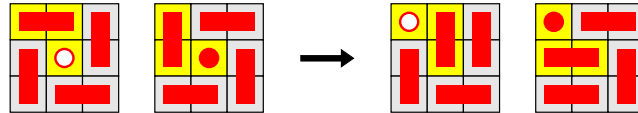


Figure 1.4: An example of a negative trit. The affected cubes are highlighted in yellow.

A (*cubiculated*) *cylinder* or *multiplex* is a region of the form $\mathcal{D} \times [0, N]$ (possibly rotated), where $\mathcal{D} \subset \mathbb{R}^2$ is a simply connected planar region with connected interior. When $N = 2$, the region is called a *duplex region*. A cubiculated region \mathcal{R} is a *two-story region* if it is contained in a set of the form $\mathbb{R}^2 \times [0, 2]$, possibly rotated, and such that the sets $\mathcal{R} \cap (\mathbb{R}^2 \times [0, 1])$ and $\mathcal{R} \cap (\mathbb{R}^2 \times [1, 2])$ are both connected and simply connected.

In view of the situation with plane tilings, one might expect that the space of domino brick tilings of a simple three-dimensional region, say, an $L \times M \times N$ box, would be connected by flips. This turns out not to be the case, as the spaces of domino brick tilings of even relatively small boxes are already not flip-connected. In Chapter 3, we introduce an algebraic invariant for tilings of two-story regions. This invariant is a polynomial $P_t \in \mathbb{Z}[q, q^{-1}]$ associated with each tiling t such that if two tilings t_1, t_2 are in the same flip connected component, then $P_{t_1} = P_{t_2}$. The converse is not necessarily true; however, it is almost true, in a sense that we shall discuss later. We shall prove the following theorems in Chapter 3:

Theorem 1. *The polynomial $P_t(q)$, defined in Sections 3.1 and 3.2, has the following properties:*

- (i) *If t_0 and t_1 are tilings of a two-story region that lie in the same flip connected component, then $P_{t_0} = P_{t_1}$.*
- (ii) *If \mathcal{R} is a duplex region and t_0 and t_1 are two tilings of \mathcal{R} , then $P_{t_0} = P_{t_1}$ if and only if there exists a box with two floors \mathcal{B} such that the embeddings of t_0 and t_1 in \mathcal{B} lie in the same flip connected component.*
- (iii) *If \mathcal{R}, t_0, t_1 are as above and $P'_{t_0}(1) = P'_{t_1}(1)$, then there exists a box with four floors \mathcal{B} such that the embeddings of t_0 and t_1 in \mathcal{B} lie in the same flip connected component.*

Theorem 2. *The trit has the following properties in two-story regions:*

- (i) *If t_0 and t_1 are two tilings of a two-story region and t_1 can be reached from t_0 after a single positive trit, then $P_{t_1}(q) - P_{t_0}(q) = q^k(q - 1)$ for some $k \in \mathbb{Z}$; as a consequence, $P'_{t_1}(1) - P'_{t_0}(1) = 1$.*
- (ii) *The space of domino brick tilings of a duplex region is connected by flips and trits. In other words, if t_0 is any tiling of such a region and t_1 is any other tiling of the same region, then there exists a sequence of flips and trits that take t_0 to t_1 .*

However, the construction for $P_t(q)$ no longer makes sense for more general regions. Chapter 4 discusses an invariant, the twist, defined for cylinders. The definitions of twist are somewhat technical and involve a relatively lengthy discussion. We shall give two different but equivalent definitions: the first one, given in Section 4.1, is a sum over pairs of dominoes. At first sight, this formula gives a number in $\frac{1}{4}\mathbb{Z}$ and depends on a choice of axis. However, it turns out that, for cylinders, this number is an integer, and different choices of axis yield the same result. The proof of this claim will be completed in Section 4.4, and it relies on the second definition, which uses the concepts of writhe and linking number from knot theory (see, e.g., [1]). In particular, we prove the following:

Theorem 3. *Let \mathcal{R} be a cylinder, and t a tiling of \mathcal{R} . The twist $\text{Tw}(t)$ is an integer with the following properties:*

- (i) *If a tiling t_1 is reached from t_0 after a flip, then $\text{Tw}(t_1) = \text{Tw}(t_0)$.*
- (ii) *If a tiling t_1 is reached from t_0 after a single positive trit, then $\text{Tw}(t_1) - \text{Tw}(t_0) = 1$.*
- (iii) *If \mathcal{R} is a duplex region, then $\text{Tw}(t) = P'_t(1)$ for any tiling t of \mathcal{R} .*
- (iv) *Suppose a cylinder $\mathcal{R} = \bigcup_{1 \leq i \leq m} \mathcal{R}_i$, where each \mathcal{R}_i is a cylinder (they need not have the same axis) and such that $i \neq j \Rightarrow \text{int}(\mathcal{R}_i) \cap \text{int}(\mathcal{R}_j) \neq \emptyset$. Then there exists a constant $K \in \mathbb{Z}$ such that, for any family $(t_i)_{1 \leq i \leq n}$, t_i a tiling of \mathcal{R}_i ,*

$$\text{Tw} \left(\bigsqcup_{1 \leq i \leq m} t_i \right) = K + \sum_{1 \leq i \leq m} \text{Tw}(t_i).$$

Finally, Chapter 5 discusses the possible range values for the twist of tilings of a given region. The main result of the chapter is the following theorem:

Theorem 4. *For a box \mathcal{B} , set $\text{Tw}(\mathcal{B}) = \{\text{Tw}(t) | t \text{ tiling of } \mathcal{B}\}$, and let $\text{Tw}_{\max}(L, M, N) = \max \text{Tw}([0, L] \times [0, M] \times [0, N])$. If $L, M, N \geq 2$, with at least two of the three dimensions strictly larger than 2 (and at least one of them even), then*

$$C_0 L M N \min(L, M, N) \leq \text{Tw}_{\max}(L, M, N) \leq C_1 L M N \min(L, M, N),$$

where $C_0 = 1/162$ and $C_1 = 1/16$. Moreover,

$$\limsup_{L, M, N \rightarrow \infty} \frac{\text{Tw}_{\max}(L, M, N)}{L M N \min(L, M, N)} = \frac{1}{16} \text{ but } \liminf_{L, M, N \rightarrow \infty} \frac{\text{Tw}_{\max}(L, M, N)}{L M N \min(L, M, N)} \leq \frac{1}{24}.$$

2

Definitions and Notation

This short chapter contains general notations and conventions that are used throughout the thesis, although we might postpone definitions that involve a lengthy discussion or are intrinsic of a given chapter or section.

If n is an integer, n^\sharp will denote $n + \frac{1}{2}$ (in music theory, D^\sharp is a half tone higher than D in pitch). We also define \mathbb{Z}^\sharp to be the set $\{n^\sharp | n \in \mathbb{Z}\}$.

Given $\vec{v}_1, \vec{v}_2, \vec{v}_3 \in \mathbb{R}^3$, $\det(\vec{v}_1, \vec{v}_2, \vec{v}_3) = \vec{v}_1 \cdot (\vec{v}_2 \times \vec{v}_3)$ denotes the determinant of the $3 \times 3 \times 3$ matrix whose i -th line is \vec{v}_i , $i = 1, 2, 3$. If $\beta = (\vec{\beta}_1, \vec{\beta}_2, \vec{\beta}_3)$ is a basis, write $\det(\beta) = \det(\vec{\beta}_1, \vec{\beta}_2, \vec{\beta}_3)$.

We denote the three canonical basis vectors as $\vec{i} = (1, 0, 0)$, $\vec{j} = (0, 1, 0)$ and $\vec{k} = (0, 0, 1)$. We denote by $\Delta = \{\vec{i}, \vec{j}, \vec{k}\}$ the set of canonical basis vectors, and $\Phi = \{\pm\vec{i}, \pm\vec{j}, \pm\vec{k}\}$. Let $\mathbf{B} = \{\beta = (\vec{\beta}_1, \vec{\beta}_2, \vec{\beta}_3) | \vec{\beta}_i \in \Phi, \det(\beta) = 1\}$ be the set of positively oriented bases with vectors in Φ .

A *basic cube* is a closed unit cube in \mathbb{R}^3 whose vertices lie in \mathbb{Z}^3 . For $(x, y, z) \in \mathbb{Z}^3$, the notation $C(x^\sharp, y^\sharp, z^\sharp)$ denotes the basic cube $(x, y, z) + [0, 1]^3$, i.e., the closed unit cube whose center is $(x^\sharp, y^\sharp, z^\sharp)$; it is *white* (resp. *black*) if $x + y + z$ is even (resp. odd). If $C = C(x^\sharp, y^\sharp, z^\sharp)$, define $\text{color}(C) = (-1)^{x+y+z+1}$, or, in other words, 1 if C is black and -1 if C is white. A *region* is a finite union of basic cubes. A *domino brick* or *domino* is the union of two basic cubes that share a face. A *tiling* of a region is a covering of this region by dominoes with pairwise disjoint interiors.

We sometimes need to refer to planar objects. Let π denote either \mathbb{R}^2 or a *basic plane* contained in \mathbb{R}^3 , i.e., a plane with equation $x = k$, $y = k$ or $z = k$ for some $k \in \mathbb{Z}$. A *basic square in π* is a unit square $Q \subset \pi$ with vertices in \mathbb{Z}^2 (if $\pi = \mathbb{R}^2$) or \mathbb{Z}^3 . A *planar region $D \subset \pi$* is a finite union of basic squares.

A region \mathcal{R} is a *cubiculated cylinder* or *multiplex region* if there exist a basic plane π with normal vector $\vec{v} \in \Delta$, a simply connected planar region $\mathcal{D} \subset \pi$ with connected interior and a positive integer N such that

$$\mathcal{R} = \mathcal{D} + [0, N]\vec{v} = \{p + s\vec{v} | p \in \mathcal{D}, s \in [0, N]\};$$

we usually call \mathcal{R} a *cylinder* or *multiplex* for brevity. The cylinder \mathcal{R} above has base \mathcal{D} , axis \vec{v} and depth N . For instance, a cylinder with axis \vec{k} and depth N can be written as $\mathcal{D} \times [k, k + N]$, where $\mathcal{D} \subset \mathbb{R}^2$. A \vec{v} -cylinder means a cylinder with axis \vec{v} . A *duplex region* or *duplex* is a cylinder with depth 2 (and hence the alternative name of multiplex for cylinders).

We sometimes want to point out that the hypothesis of simple connectivity (of a cylinder) is not being used: therefore, a *pseudocylinder* (or *pseudomultiplex*) with base \mathcal{D} , axis \vec{v} and depth N has the same definition as above, except that the planar region $\mathcal{D} \subset \pi$ is only assumed to have connected interior (and is not necessarily simply connected).

A *box* is a region of the form $\mathcal{B} = [L_0, L_1] \times [M_0, M_1] \times [N_0, N_1]$, where $L_i, M_i, N_i \in \mathbb{Z}$. Boxes are special cylinders, in the sense that we can take any vector $\vec{v} \in \Delta$ as the axis. In fact, boxes are the only regions that satisfy the definition of cylinder for more than one axis.

Regarding notation, Figures 1.2, 1.3 and 1.4 were drawn with $\beta = (\vec{i}, \vec{j}, \vec{k})$ in mind. However, any $\beta \in \mathbf{B}$ allows for such representations, as follows: we draw $\vec{\beta}_3$ as perpendicular to the paper (pointing towards the paper). If $\pi = \vec{\beta}_3^\perp$, we then draw each floor $\mathcal{R} \cap (\pi + [n, n+1]\vec{\beta}_3)$ as if it were a plane region. Floors are drawn from left to right, in increasing order of n .

The *flip connected component* of a tiling t of a region \mathcal{R} is the set of all tilings of \mathcal{R} that can be reached from t after a sequence of flips.

Suppose t is a tiling of a region \mathcal{R} , and let $\mathcal{B} = [l, l+2] \times [m, m+2] \times [n, n+2]$, with $l, m, n \in \mathbb{N}$. Suppose $\mathcal{B} \cap \mathcal{R}$ contains exactly three dominoes of t , no two of them parallel: notice that this intersection can contain six, seven or eight basic cubes of \mathcal{R} . Also, a rotation (it can even be a rotation, say, in the XY plane), can take us either to the left drawing or to the right drawing in Figure 2.1.



Figure 2.1: The anatomy of a positive trit (from left to right). The trit that takes the right drawing to the left one is a negative trit. The squares with no dominoes represent basic cubes that may or may not be in \mathcal{R} (see Figure 1.4 for an example).

If we remove the three dominoes of t contained in $\mathcal{B} \cap \mathcal{R}$, there is only one other possible way we can place them back. This defines a move that takes t to a different tiling t' by only changing dominoes in $\mathcal{B} \cap \mathcal{R}$: this move is called a *trit*. If the dominoes of t contained in $\mathcal{B} \cap \mathcal{R}$ form a plane rotation of the

left drawing in Figure 2.1, then the trit is *positive*; otherwise, it's *negative*. Notice that the sign of the trit is unaffected by translations (colors of cubes don't matter) and rotations in \mathbb{R}^3 (provided that these transformations take \mathbb{Z}^3 to \mathbb{Z}^3). A reflection, on the other hand, switches the sign (the drawing on the right can be obtained from the one on the left by a suitable reflection).

3

The two-floored case

A *two-story region* is a connected and simply connected region $\mathcal{R} \subset \pi + [0, 2]\vec{u}$, where π is a basic plane with normal $\vec{u} \in \Delta$, such that both sets $\mathcal{R} \cap (\pi + [0, 1]\vec{u})$ and $\mathcal{R} \cap (\pi + [1, 2]\vec{u})$ are simply connected. We often think of these two sets as the two “floors” of \mathcal{R} . In this chapter (unlike the next), rotations will not play an important role, so we shall assume that $\pi = \mathbb{R}^2 \times \{0\}$ and $\vec{u} = \vec{k}$. Likewise, duplex regions will be assumed to have axis \vec{k} , and will often be denoted $\mathcal{D} \times [0, 2]$ where $\mathcal{D} \subset \mathbb{R}^2$ has connected interior and is simply connected.

Most of the material in this chapter is also covered in [17].

3.1

Duplex regions

Let $\mathcal{D} \subset \mathbb{R}^2$ be a quadriculated simply connected plane region, and let $\mathcal{R} = \mathcal{D} \times [0, 2] \subset \mathbb{R}^3$ be a duplex region. Our goal throughout this section is to associate to each tiling t of \mathcal{R} a polynomial $P_t \in \mathbb{Z}[q, q^{-1}]$ which always coincides for tilings in the same flip connected component.

Consider the two floors of a tiling t of \mathcal{R} , each dimer of t being oriented from the white cube that it contains to the black one, as illustrated in the left of Figure 3.1. If we project the dimers of t to the plane $z = 0$, we will see two plane tilings of \mathcal{D} with *jewels* (which occupy exactly one square), which are the projections of dimers parallel to \vec{k} , as shown in Figure 3.1. A white (resp. black) jewel is a jewel that happens in a white (resp. black) square; we write $\text{color}(j) = 1$ if j is black, and -1 if it is white.

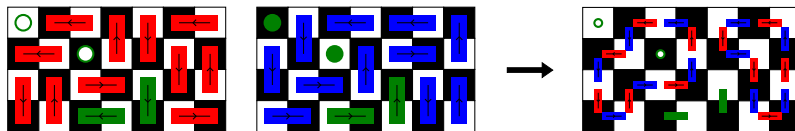


Figure 3.1: A tiling of a $7 \times 4 \times 2$ box and its associated drawing. The associated drawing has two jewels and four cycles, two of which are trivial ones. The jewels have opposite color, and both cycles spin counterclockwise.

Thus, the resulting drawing can be seen as a set of disjoint plane cycles (projections of dimers that are not parallel to $\vec{\mathbf{k}}$ maintain their orientations) together with jewels. A cycle is called *trivial* if it has length 2. In order to construct P_t , consider a jewel j , and let $k_t(j) = \sum_{\gamma} \text{wind}(\gamma, j)$, where the sum is taken over all the cycles γ in the associated drawing, and $\text{wind}(\gamma, j)$ denotes the winding number of γ around j . Then

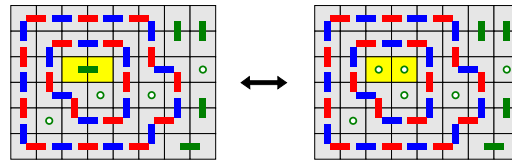
$$P_t(q) = \sum_j \text{color}(j) q^{k_t(j)}.$$

For instance, for the tiling t in Figure 3.1, $P_t(q) = q - 1$. For now, define the twist of a tiling to be $\text{Tw}(t) = P'_t(1)$. (see Chapter 4 for a general definition).

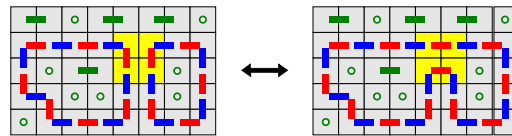
We now show that P_t is, in fact, flip invariant.

Proposition 3.1. *Let \mathcal{R} be a duplex region, and let t_0 be a tiling of \mathcal{R} . If t_1 is obtained from t_0 by performing a single flip on t_0 , then $P_{t_1} = P_{t_0}$.*

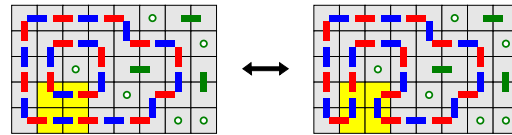
Proof. Let us consider the tiling t_0 and its associated drawing as a plane tiling with jewels; we want to see how this drawing is altered by a single flip. We will split the proof into cases, and the reader may find it easier to follow by looking at Figure 3.2.



(a) Case 1: $P_t(q) = 1 - q^{-2}$ in both tilings



(b) Case 2.1: $P_t(q) = q - 1$ in both tilings. Both cycles must have the same orientation to allow a flip.



(c) Case 2.2: $P_t(q) = q - 1$ in both tilings. Notice that the two nested cycles must have opposite orientation.

Figure 3.2: Examples illustrating the effects of flips in each of the cases. The flip positions are highlighted in yellow.

Case 1. *A flip that takes two non- $\vec{\mathbf{k}}$ dominoes which are in the same position in both floors to two adjacent $\vec{\mathbf{k}}$ dominoes (or the reverse of this flip)*

The non- \vec{k} dominoes have no contribution to P_{t_0} . On the other hand, the two \vec{k} dominoes that appear after the flip have opposite colors (since they are adjacent), and are enclosed by exactly the same cycles. Hence, their contributions to P_{t_1} cancel out, and thus $P_{t_0} = P_{t_1}$ in this case.

Case 2. *A flip that is completely contained in one of the floors.*

If we look at the effect of such a flip in the associated drawing, two things can happen:

- 2.1. It connects two cycles that are not enclosed in one another and have the same orientation, and creates one larger cycle with the same orientation as the original ones, or it is the reverse of such a move;
- 2.2. It connects two cycles of opposite orientation such that one cycle is enclosed by the other (or it is the reverse of such a flip). The new cycle has the same orientation as the outer cycle.

In case 2.1, a jewel is enclosed by the new larger cycle if and only if it is enclosed by exactly one of the two original cycles. Hence, its contribution is the same in both P_{t_0} and P_{t_1} .

In case 2.2, a jewel is enclosed by the new cycle if and only if it is enclosed by the outer cycle and not enclosed by the inner one. If it is enclosed by the new cycle, its contribution is the same in P_{t_0} and P_{t_1} , because the new cycle has the same orientation as the outer one. On the other hand, if a jewel j is enclosed by both cycles, their contributions to $k_t(j)$ cancel out, hence the jewel's contribution is also the same in P_{t_0} and P_{t_1} .

Hence, $P_{t_0} = P_{t_1}$ whenever t_0 and t_1 differ by a single flip. \square

Notice that in cases 2.1 and 2.2 in the proof, one or both of the cycles involved may be trivial cycles. However, this does not change the analysis.

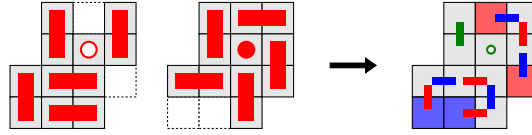


Figure 3.3: An example of tiled region with two simply connected but unequal floors. Holes in the leftmost floor are painted red in the associated drawing, while holes in the rightmost floor are painted blue.

3.2

General two-story regions

Let \mathcal{R} be a two-story region, and let \mathcal{R}' be the smallest duplex region containing \mathcal{R} . The cubes in $\mathcal{R}' \setminus \mathcal{R}$ are called *holes*. If we project the dominoes of a tiling t into the plane $z = 0$, we end up with a set of disjoint (simple) paths, some of which may be cycles, while others have loose ends: an example is showed in the left of Figure 3.3 (in that case, all nontrivial paths have loose ends).

Notice also that every white (resp. black) hole (regardless of which floor it is in) creates a loose end in the associated drawing where a domino is oriented in such a way that it is entering (resp. leaving) the square, which we call a *source* (resp. *sink*): the names source and sink do not refer to the dominoes, but instead refer to the ghost curves, which are defined below. Also, sources and sinks do not depend on the specific tiling and, since the number of black holes must equal the number of white holes, the number of sources always equals the number of sinks in a tileable region.

A *ghost curve* in the associated drawing of \mathcal{R} is a curve that connects a source to a sink and which never touches the closure of a square that is common to both floors. Since the floors are simply connected, we can always connect any source to any sink via a ghost curve: an associated drawing of a tiling t is then the “usual” associated drawing (from Section 3.1) together with a set of ghost curves such that each source and each sink is in exactly one ghost curve: this is shown in Figure 3.4.

For a two-story region \mathcal{R} , fix a set of ghost curves such that every source and every sink intersects exactly one ghost curve. Therefore, the associated drawing of each tiling t is a set of cycles and jewels, so that we may define $P_t(q)$ in the same way as we did for duplex regions. Namely, for a jewel j , let $k_t(j)$ denote the sum of the winding numbers of the newly formed cycles with respect to that jewel, and set $P_t(q) = \sum_j \text{color}(j) q^{k_t(j)}$. One important difference with respect to Section 3.1 is that the winding number of a cycle

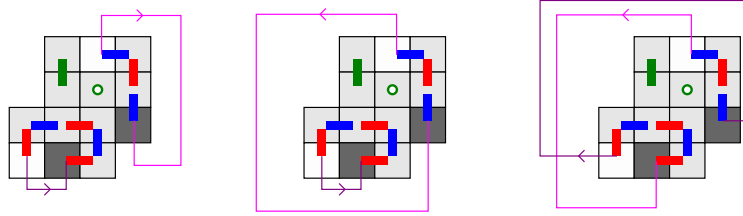


Figure 3.4: Three different ways to join sources and sinks. The sources are highlighted in very light grey (almost white), while the sinks are highlighted in dark grey. The invariants $P_t(q)$ for each case, from left to right, are 1, q and 1.

with respect to a jewel is no longer necessarily 1 or -1 , but can be any integer (see Figure 3.5).

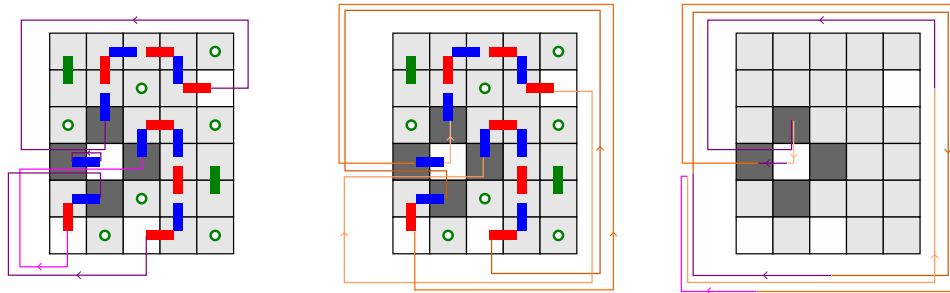


Figure 3.5: Two different ways to connect sources and sinks. The last diagram illustrates that the difference (first minus second) between these two connections forms a set of cycles, each of which has the same winding number with respect to each square where it is possible to have a jewel. In this case, this set has two cycles: one with winding number 0 and the other with winding number -1 (with respect to every square that is common to both floors). Notice that the invariant is $-2q + 1 - 2q^{-1}$ in the first diagram and $-2q^2 + q - 2$ in the second, that is, the first invariant is indeed q^{-1} times the second.

Strictly speaking, we should have made an explicit reference to the choice of ghost curves instead of simply writing P_t . However, it turns out that the following holds: if $P_{t,1}$ is the invariant associated with one choice of connection and $P_{t,2}$ is associated with another, then there exists $k \in \mathbb{Z}$ such that for every tiling t , $P_{t,1}(q) = q^k P_{t,2}(q)$.

To see this, fix a tiling t . We want to look at the contributions of a jewel to P_t for two given choices of source-sink connections. Since the exponent of the contribution of a jewel is the sum of the winding numbers of all the cycles with respect to it, it follows that the difference of exponents between two choices of connections is the sum of winding numbers of the cycles formed by putting the ghost curves from both source-sink connections together in the same picture, as illustrated in Figure 3.5. Now this sum of winding numbers is the same for every jewel: since the set of ghost curves never touches the closure of a square

common to both floors (and the intersection of the two floors is connected and simply connected), each of the newly formed cycles must enclose every jewel in the same way. Hence, the effect of changing the connection is multiplying the contribution of each jewel by the same integer power of q , and we shall simply write P_t , assuming that the choice of ghost curves is given (and fixed).

Proposition 3.2. *Let \mathcal{R} be a two-story region, and suppose t_1 is obtained from a tiling t_0 of \mathcal{R} after a single flip. Then $P_{t_0} = P_{t_1}$.*

Proof. The proof is basically the same as that of Proposition 3.1. In fact, for Case 2 (flips contained in one floor) in that proof, literally nothing changes, whereas Case 1 (flips involving jewels) can only happen in a pair of squares that are common to both floors. Since the ghost curves must never touch such squares, it follows that the pair of adjacent jewels that form a flip position have the same $k_t(j)$, hence their contributions cancel out. \square

3.3

The effect of trits on P_t

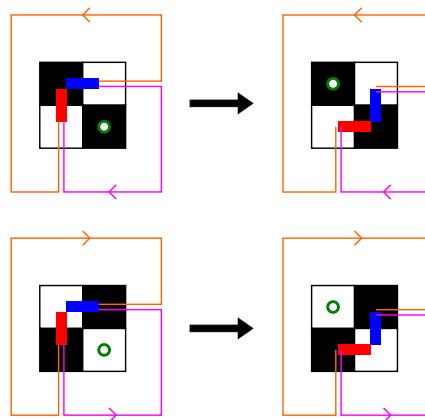


Figure 3.6: Schematic drawing of the effect of positive trits, with the magenta (shorter bottom right line) and orange lines (longer line) indicating (schematically) the two possible relative positions of the cycle γ altered by the trit (the magenta and orange segments represent cycles that may have ghostly parts or not). It is clear that, in either case, the contribution of the portrayed jewel changes from q^k to q^{k+1} if it is black, and from $-q^k$ to $-q^{k-1}$ if it is white.

We now turn our attention to the effect of a trit on P_t . By looking at Figure 3.6, we readily observe that a trit affects only the contribution of the jewel j that takes part in the trit (a trit always changes the position of precisely one jewel, since it always involves exactly one domino parallel to \vec{k}). Furthermore, it either pulls a jewel out of a cycle, or pushes it into a cycle,

but the jewel maintains its color. Hence, if $\pm q^k$ is the contribution of j to P_t , then after a trit involving j its contribution becomes $\pm q^{k+1}$ or $\pm q^{k-1}$.

A more careful analysis, however, as portrayed in Figure 3.6, shows that a positive trit involving a black jewel always changes its contribution from q^k to q^{k+1} , and a positive trit involving a white jewel changes $-q^k$ to $-q^{k-1}$. Hence, we have proven the following:

Proposition 3.3. *Let t_0 and t_1 be two tilings of a region \mathcal{R} which has two simply connected floors, and suppose t_1 is reached from t_0 after a single positive trit. Then, for some $k \in \mathbb{Z}$,*

$$P_{t_1}(q) - P_{t_0}(q) = q^k(q - 1). \quad (3-1)$$

A closer look at Equation (3-1) shows that $\text{Tw}(t_1) - \text{Tw}(t_0) = P'_{t_1}(1) - P'_{t_0}(1) = 1$ whenever t_1 is reached from t_0 after a single positive trit. This gives the following easy corollary:

Corollary 3.4. *Let t_0 and t_1 be two tilings of a region \mathcal{R} with two simply connected floors, and suppose we can reach t_1 from t_0 after a sequence S of flips and trits. Then*

$$\#(\text{positive trits in } S) - \#(\text{negative trits in } S) = \text{Tw}(t_1) - \text{Tw}(t_0).$$

3.4

Examples

For the examples below, we wrote programs in the C^{\#} language.

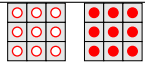
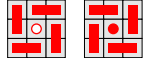
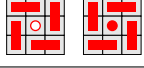
Connected Component	Number of tilings	Tiling	$P_t(q)$	$\text{Tw}(t)$
0	227		-1	0
1	1		$-q$	-1
2	1		$-q^{-1}$	1

Table 3.1: Flip connected components of a $3 \times 3 \times 2$ box.

Example 3.5 (The $3 \times 3 \times 2$ box). *The $3 \times 3 \times 2$ box is the smallest box whose space of domino tilings is not connected by flips (this can be proved using*

techniques from Chapter 4), and it has 229 tilings: the tiling t shown in Figure 1.4 has twist -1 and is alone in its flip connected component; the tiling obtained by reflecting t on the plane $z = 1$ has twist 1 (and is also alone in its flip connected component). The third component contains the remaining 227 tilings, with twist 0 . This information is summarized in Table 3.1. Finally, the space of tilings is connected by flips and trits (via the trit shown in 1.4 and its reflection).

Example 3.6 (The $7 \times 3 \times 2$ box). The $7 \times 3 \times 2$ box has a total of 880163 tilings, and thirteen flip connected components. Table 3.2 contains information about the invariants of these connected components.

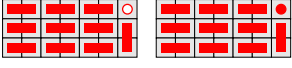
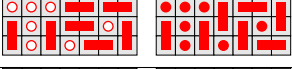
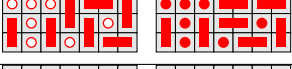
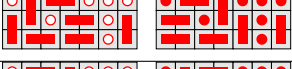
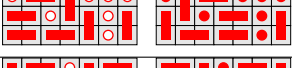
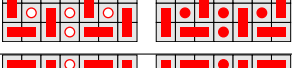
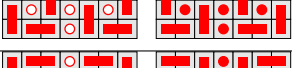
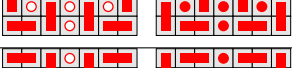
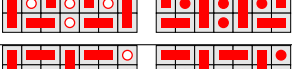
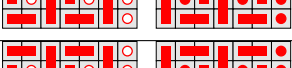
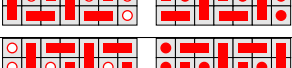
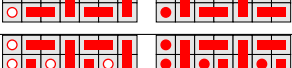
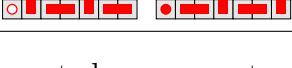
Connected Component	Number of tilings	Tiling	$P_t(q)$	$\text{Tw}(t)$
0	856617		-1	0
1	8182		$-q$	-1
2	8182		$-q^{-1}$	1
3	3565		$-2 + q^{-1}$	-1
4	3565		$q - 2$	1
5	9		$-2q + 1$	-2
6	9		$1 - 2q^{-1}$	2
7	7		$-q + 1 - q^{-1}$	0
8	7		$-q + 1 - q^{-1}$	0
9	5		$-q - 1 + q^{-1}$	-2
10	5		$q - 1 - q^{-1}$	2
11	5		$-q - 1 + q^{-1}$	-2
12	5		$q - 1 - q^{-1}$	2

Table 3.2: Flip connected components of a $7 \times 3 \times 2$ box.

We readily notice that the invariant does a good job of separating flip connected components, albeit not a perfect one: the pairs of connected components 7 and 8, 9 and 11, and 10 and 12 have the same $P_t(q)$.

Figure 3.7 shows a diagram of the flip connected components, arranged by their twists. We also notice that we can always reach a tiling from any other

via a sequence of flips and trits.

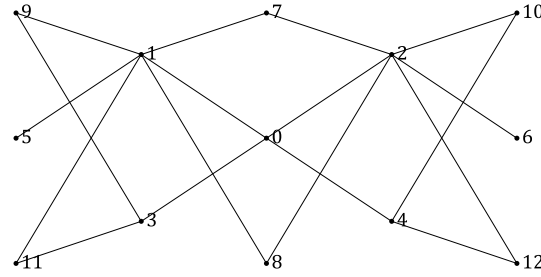


Figure 3.7: Flip connected components of the $7 \times 3 \times 2$ box, arranged by twist in increasing order. The numbering is the same as in table 3.2, and two dots A and B are connected if there exists a trit that takes a tiling in connected component A to a tiling in connected component B . As we proved earlier, a trit from left to right in the diagram is always a positive trit; and a trit from right to left is always a negative one.

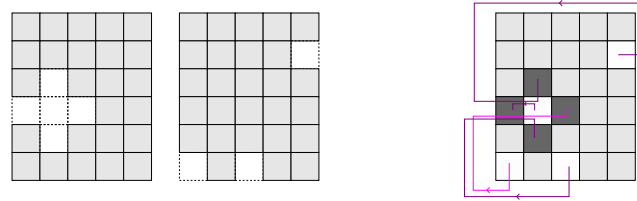


Figure 3.8: A region with two unequal floors, together with a choice of connections between the sources and the sinks. This choice of connections is the one used for the calculations in Table 3.3.

Example 3.7 (A region with two unequal floors). *Figure 3.8 shows a region with two unequal floors, together with a choice of how to join sources and sinks. It has 642220 tilings, and 30 connected components.*

Table 3.3 shows some information about these components and Figure 3.9 shows a diagram of the flip connected components, arranged by their twists. This graph is not as symmetric as the one in the previous example; nevertheless, the space of tilings is also connected by flips and trits in this case.

Connected Component	Number of tilings	$P_t(q)$	$\text{Tw}(t)$
0	165914	$-2q - q^{-1}$	-1
1	153860	$-q - 1 - q^{-1}$	0
2	92123	$-2q - 1$	-2
3	56936	$-q - 1 - q^{-2}$	1
4	50681	$-q - 2$	-1
5	41236	$-2q - q^{-2}$	0
6	17996	$-2 - q^{-1}$	1
7	13448	$-q - 2q^{-1}$	1
8	11220	$-3q$	-3
9	8786	$-2 - q^{-2}$	2
10	7609	$-q - q^{-1} - q^{-2}$	2
11	6423	$-2q + 1 - 2q^{-1}$	0
12	4560	$-3q + 1 - q^{-1}$	-2
13	4070	-3	0
14	3299	$-2q + 1 - q^{-1} - q^{-2}$	1
15	2097	$-1 - 2q^{-1}$	2
16	1382	$-1 - q^{-1} - q^{-2}$	3
17	221	$-q + 1 - 3q^{-1}$	2
18	137	$-q + 1 - 2q^{-1} - q^{-2}$	3
19	51	$-3q^{-1}$	3
20	48	$-2q - 1$	-2
21	36	$-2q^{-1} - q^{-2}$	4
22	17	$-3q^{-1}$	3
23	17	$-2q^{-1} - q^{-2}$	4
24	16	$-1 - 2q^{-1}$	2
25	16	$-1 - q^{-1} - q^{-2}$	3
26	12	$-2q + 2 - 3q^{-1}$	1
27	7	$-2q + 2 - 2q^{-1} - q^{-2}$	2
28	1	$1 - 4q^{-1}$	4
29	1	$1 - 3q^{-1} - q^{-2}$	5

Table 3.3: Information about the flip connected components of the region \mathcal{R} from Figure 3.8.

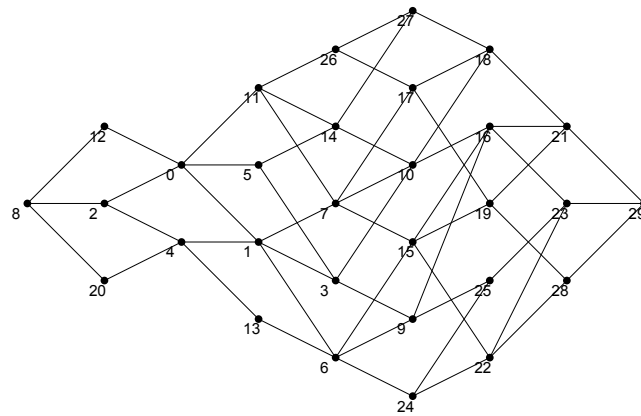


Figure 3.9: Graph with 30 vertices, each one representing a connected component of the region. As in Figure 3.7, two vertices are connected if there exists a trit taking a tiling in one component to a tiling in the other; a trit from left to right is always positive.

3.5

The invariant in more space

We already know that tilings that are not in the same flip connected component may have the same polynomial invariant, even in the case with two equal simply connected floors (see, for instance, Example 3.6). However, as we will see in this section, this is rather a symptom of lack of space than anything else.

More precisely, suppose \mathcal{R} is a duplex region and t is a tiling of \mathcal{R} . If \mathcal{B} is an $L \times M \times 2$ box (or a two-floored box) containing \mathcal{R} , then $\mathcal{B} \setminus \mathcal{R}$ can be tiled in an obvious way (using only dominoes parallel to \vec{k}). Thus t induces a tiling \hat{t} of \mathcal{B} that contains t ; we call this tiling \hat{t} the *embedding* of t in \mathcal{B} .

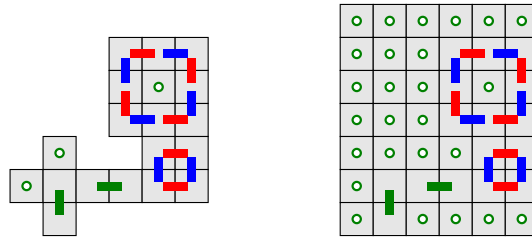


Figure 3.10: The associated drawing of a tiling, and its embedding in a $6 \times 7 \times 2$ box.

Another way to look at the embedding \hat{t} of a tiling t is the following: start with the associated drawing of t (which is a plane region), add empty squares until you get an $L \times M$ rectangle, and place a jewel in every empty square. Since the newly added jewels are outside of any cycle in \hat{t} , it follows that $P_{\hat{t}}(q) - P_t(q) = k \in \mathbb{Z}$, where k is the number of new black jewels minus the number of new white jewels (which depends only on the choice of box \mathcal{B} and not on the tiling t). Our goal for the section is to prove the following:

Proposition 3.8. *Let \mathcal{R} be a duplex region, and let t_0, t_1 be two tilings that have the same invariant, i.e., $P_{t_0} = P_{t_1}$. Then there exists a two-floored box containing \mathcal{R} such that the embeddings \hat{t}_0 and \hat{t}_1 of t_0 and t_1 lie in the same flip connected component.*

If t_0 and t_1 already lie in the same flip connected component in \mathcal{R} , then their embeddings \hat{t}_0 and \hat{t}_1 in any two-floored box will also lie in the same connected component, because you can reach \hat{t}_1 from \hat{t}_0 using only flips already available in \mathcal{R} .

Also, notice that $P_{\hat{t}_0} = P_{\hat{t}_1}$ if and only if $P_{t_0} = P_{t_1}$, because $P_{\hat{t}_1}(q) - P_{t_1}(q) = P_{\hat{t}_0}(q) - P_{t_0}(q)$. Therefore, Proposition 3.8 states that two tilings have

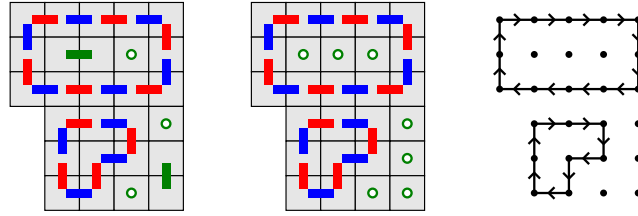


Figure 3.11: A tiling with two trivial cycles; the same tiling with the two trivial cycles flipped into jewels; and the system of cycles that corresponds to both of them.

the same invariant if and only if there exists a two-floored box where their embeddings lie in the same flip connected component.

The reader might be wondering why we're restricting ourselves to duplex regions. One reason is that for general regions with two simply connected floors, it is not always clear that you can embed them in a large box in a way that their complement is tileable, let alone tileable in a natural way.

Although it is technically possible to prove Proposition 3.8 only by looking at associated drawings, it will be useful to introduce an alternative formulation for the problem.

Let $G = G(\mathcal{R})$ be the undirected plane graph whose vertices are the centers of the squares in the associated drawing of \mathcal{R} , and where two vertices are joined by an edge if their Euclidean distance is exactly 1. A *system of cycles*, or *sock*, in G is a (finite) directed subgraph of G consisting only of disjoint oriented (simple) cycles. An *edge* of a sock is an (oriented) edge of one of the cycles, whereas a *jewel* is a vertex of G that is not contained in the system of cycles.

There is an “almost” one-to-one correspondence between the systems of cycles of G and the tilings of \mathcal{R} , which is illustrated in Figure 3.11. In fact, tilings with trivial cycles have no direct interpretation as a system of cycles; but since all trivial cycles can be flipped into a pair of adjacent jewels, we can think that every sock represents a set of tilings, all in the same flip connected component.

We would now like to capture the notion of a flip from the world of tilings to the world of socks. This turns out to be rather simple: a *flip move* on a sock is one of three types of moves that take one sock into another, shown in Figure 3.12. Notice that performing a flip move on a sock corresponds to performing one or more flips on its corresponding tiling.

A *flip homotopy* in G between two socks s_1 and s_2 is a finite sequence of flip moves taking s_1 into s_2 . If there exists a flip homotopy between two

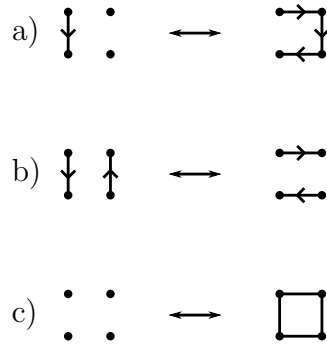


Figure 3.12: The three types of flip moves. The square in type c) is not oriented because it can have either one of the two possible orientations.

socks, they are said to be *flip homotopic* in G . Notice that two tilings are in the same flip connected component of \mathcal{R} if and only if their corresponding socks are flip homotopic in G , because every flip can be represented as one of the flip moves (and the flip that takes a trivial cycle into two jewels does not alter the corresponding sock). Figure 3.13 shows examples of flips and their corresponding flip moves.

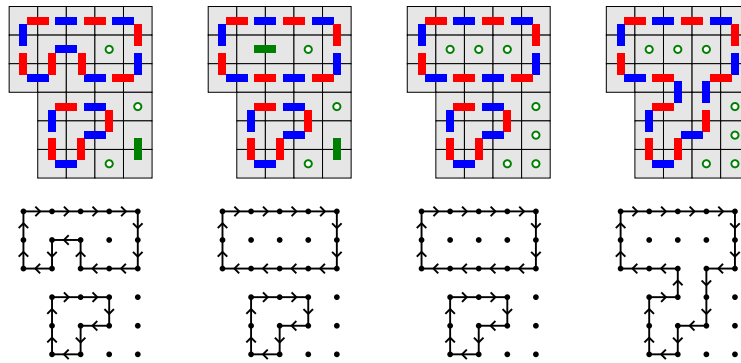


Figure 3.13: Examples of how flips affect the corresponding sock. The first flip induces a flip move of type (a), The second one does not alter the corresponding sock, and the third one induces a flip move of type (b).

One advantage of this new interpretation is that we can easily add as much space as we need without an explicit reference to a box. In fact, notice that G is a subgraph of the infinite graph \mathbb{Z}^2 , so that a sock in G is also a finite subgraph of \mathbb{Z}^2 , so that we may see it as a system of cycles in \mathbb{Z}^2 .

Lemma 3.9. *For two tilings t_0 and t_1 of a region \mathcal{R} , the following assertions are equivalent:*

- (i) *There exists a two-floored box \mathcal{B} containing \mathcal{R} such that the embeddings of t_0 and t_1 in \mathcal{B} lie in the same flip connected component.*
- (ii) *The corresponding systems of cycles of t_0 and t_1 are flip homotopic in \mathbb{Z}^2 .*

Proof. To see that (ii) implies (i), notice the following: if s_0, s_1, \dots, s_n are the socks involved in the flip homotopy between the socks of t_0 and t_1 in \mathbb{Z}^2 , let \mathcal{B} be a sufficiently large two-floored box such that $(\mathbb{Z}^2 \setminus G(\mathcal{B}))$ contains only vertices of \mathbb{Z}^2 that are jewels in all the $n+1$ socks s_0, s_1, \dots, s_n . Then the socks of t_0 and t_1 are flip homotopic in $G(\mathcal{B})$, so the embeddings of t_0 and t_1 lie in the same flip connected component.

The converse is obvious, since if the socks of t_0 and t_1 are flip homotopic in $G(\mathcal{B})$ for some two-floored box \mathcal{B} , then they are flip homotopic in \mathbb{Z}^2 . \square

A vertex $v \in \mathbb{Z}^2$ is said to be white (resp. black) if the sum of its coordinates is even (resp. odd), and we write $\text{color}(v) = -1$ (resp. 1). If s is a system of cycles in \mathbb{Z}^2 , we define the graph invariant of s as

$$P_s(q) = \sum_{j: k_s(j) \neq 0} \text{color}(j) q^{k_s(j)},$$

where $k_s(j)$ is the sum of the winding numbers of all the cycles in s (as curves) with respect to j ; this is a finite sum because the number of jewels enclosed by cycles of s is finite. Notice that if t is a tiling of \mathcal{R} and s is its corresponding sock in \mathbb{Z}^2 , $P_s(q) = P_t(q) - P_t(0)$, so that P_s is completely determined by P_t . Conversely, $P_t(q) - P_s(q) = P_t(1) - P_s(1) = P_t(0)$: since $P_t(1)$ equals the number of black squares minus the number of white squares in \mathcal{R} (thus does not depend on t), it follows that $P_t(q)$ is also completely determined by \mathcal{R} and $P_s(q)$.

A corollary of Proposition 3.1 is that if two systems of cycles s_0 and s_1 are flip homotopic in \mathbb{Z}^2 , then $P_{s_0} = P_{s_1}$. We now set out to prove that the converse also holds, which will establish Proposition 3.8.

A *boxed jewel* is a subgraph of \mathbb{Z}^2 formed by a single jewel enclosed by a number of square cycles (cycles that are squares when thought of as plane curves), all with the same orientation. Figure 3.14 shows examples of boxed jewels. Working with boxed jewels is easier, for if they have “free space” in one direction (for instance, if there are no cycles to the right of it), they can move an arbitrary even distance in that direction; the simplest case is illustrated in Figure 3.15. More complicated boxed jewels move just as easily: we first turn the outer squares into rectangles, then we move the inner boxed jewel, and finally we close the outer squares again.

An *untangled* sock is a sock that contains only boxed jewels, and such that the center of each boxed jewel is of the form $(n, 0)$ for some $n \in \mathbb{Z}$ (that is, all the enclosed jewels lie in the x axis), as illustrated in Figure 3.16. Therefore,

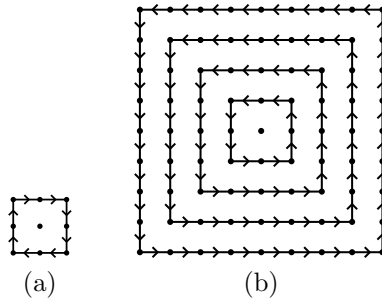


Figure 3.14: Two examples of boxed jewels.

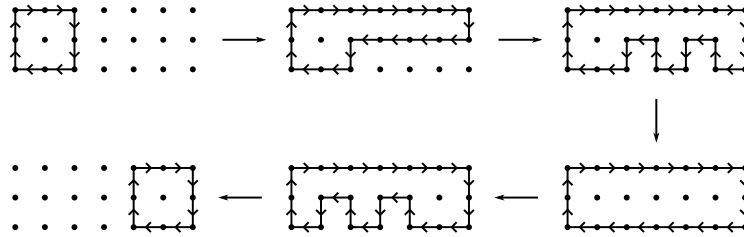


Figure 3.15: A boxed jewel with “free space” to the right. Starting from the first sock, we perform: four flip moves of type (a); two flip moves of type (a); two flip moves of type (a) to create a rectangle; two flip moves of type (a); and finally, the last sock is obtained by performing six flip moves of type (a) on the penultimate sock.

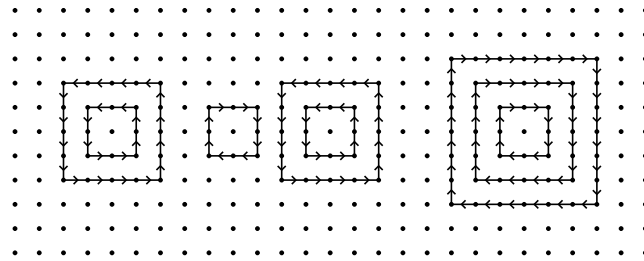


Figure 3.16: Example of an untangled sock.

each boxed jewel in an untangled sock moves very easily: it has free space both downwards and upwards.

Lemma 3.10. *Two untangled socks that have the same invariant are flip homotopic in \mathbb{Z}^2 .*

In this and in other proofs, we omit easy (but potentially tedious) details when we think the picture is sufficiently clear.

Proof. If the two socks consist of precisely the same boxed jewels but in a different order, then they are clearly flip homotopic, since we can easily move the jewels around and switch their positions as needed. We only need to check that boxed jewels that cancel out (that is, they refer to terms with the same exponent but opposite signs) can be “dissolved” by flip moves.

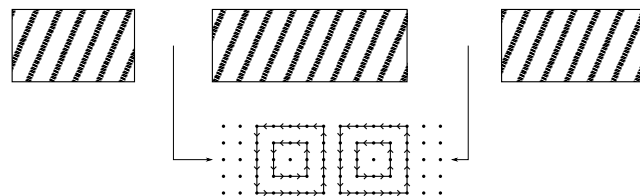


Figure 3.17: Illustration of how boxed jewels that cancel out can be brought close. The striped rectangles indicate areas where there may be other boxed jewels.

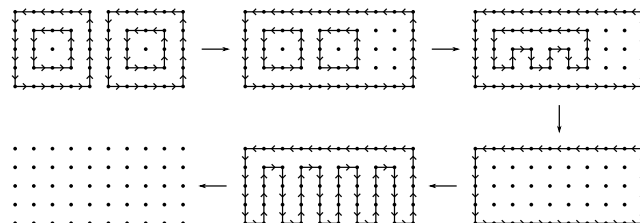


Figure 3.18: Some intermediate steps in the flip homotopy that “dissolves” a pair of cancelling boxed jewels

In order to see this, start by moving the boxed jewels that cancel out downwards, then toward each other until they are next to each other, as illustrated in Figure 3.17. Once they are next to each other, they can be eliminated by a sequence of flip moves. Figure 3.18 shows some of the steps involved in the flip homotopy that eliminates this pair of cancelling jewels.

□

If s is a sock, we define the *area* of s to be the sum of the areas enclosed by each cycle of s , thought of as a plane curve. The areas count as positive regardless of the orientation of the cycles. As an example, the boxed jewels shown in Figure 3.14 have areas 4 and 120, respectively, and the untangled sock in Figure 3.16 has area $20 + 4 + 20 + 56 = 100$. Naturally, the only sock with zero area is the empty sock (the sock with no cycles).

The following Lemma is the key step in the proof of Proposition 3.8:

Lemma 3.11. *Every sock is flip homotopic to an untangled sock in \mathbb{Z}^2 .*

Proof. Suppose, by contradiction, that there exists a sock which is not flip homotopic to an untangled sock. Of all the examples of such socks, pick one, s_0 , that has minimal area (which is greater than zero, because the empty sock is already untangled).

Among all the cycles in s_0 , consider the ones who have vertices that are furthest bottom. Among all these vertices, pick the rightmost one, which we will call v . In other words, assuming the axis are as in Figure 1.2: if

$m = \max\{n : (k, n) \text{ is a vertex of } s_0 \text{ for some } k \in \mathbb{Z}\}$ and $l = \max\{k : (k, m) \text{ is a vertex of } s_0\}$, then $v = (l, m)$.

Clearly v is the right end of a horizontal edge, and the bottom end of a vertical edge, as portrayed in Figure 3.19. We may assume without loss of generality that these edges are oriented as in the aforementioned Figure.

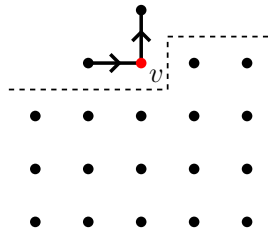


Figure 3.19: The rightmost bottommost vertex (v) in the nonempty sock s_0 . By definition, there can be no cycle parts in s_0 below the dotted line.

Consider the diagonal of the form $v - (n, n), n \geq 0, n \in \mathbb{Z}$, starting from v and pointing northwest, and let w be the first point (that is, the one with the smallest n) in this diagonal that is not the right end of a horizontal edge pointing to the right and the bottom end of a vertical edge pointing up (see Figure 3.20).

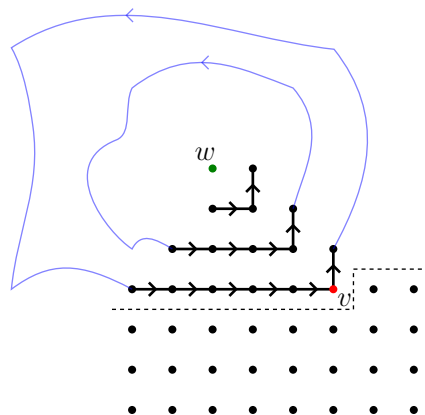


Figure 3.20: The vertices v and w ; w is the first vertex in the diagonal that does not follow the pattern (“edgewise”) of the other three. The curved blue segments represent (schematically) the relative positions of two of the cycles, which must be in this way because there can be no cycle parts below the dashed line.

We will now see that if w is not a jewel, then we can immediately reduce the area of s_0 with a single flip move. This leads to a contradiction, because the sock obtained after this flip move cannot be flip homotopic to an untangled sock, but has smaller area than s_0 .

Suppose w is not a jewel. With Figure 3.20 in mind, consider the vertex directly below w . It is either the bottom end of a vertical edge pointing

downward (case 1), or the right end of a horizontal edge pointing to the right. In case 1, a single flip move of type (a) will immediately reduce the area, as shown in the first drawing in Figure 3.21. The other three drawings handle all the possibilities for the other case (again, we omit the easy details): notice that in each case there is a flip move that reduces the area.

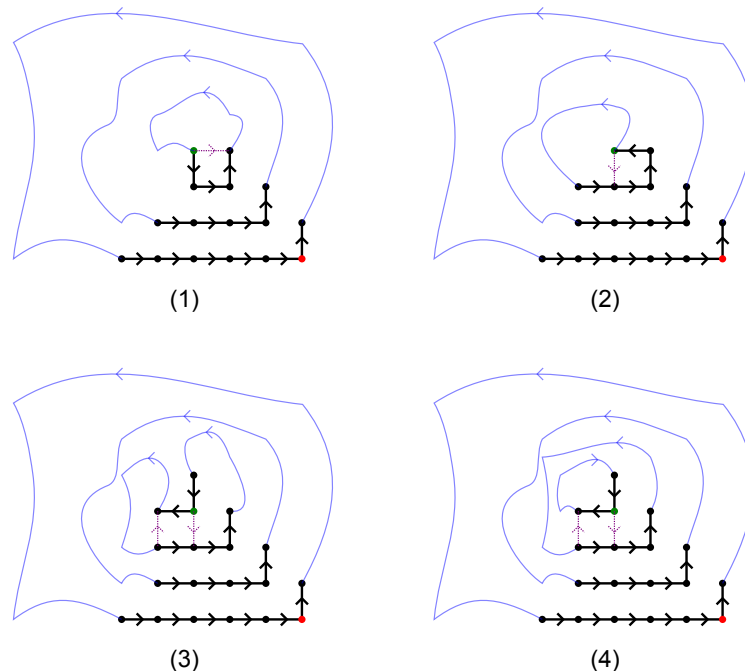


Figure 3.21: The four possibilities when w is not a jewel. Notice that, in each case, there is a flip move that reduces the area, which are indicated by the dotted purple lines.

The most interesting case is when w is a jewel. The key observation here is that the jewel may be then “extracted” from all the cycles as a boxed jewel, and what remains has smaller area. Figure 3.22 illustrates the steps involved in extracting a jewel.

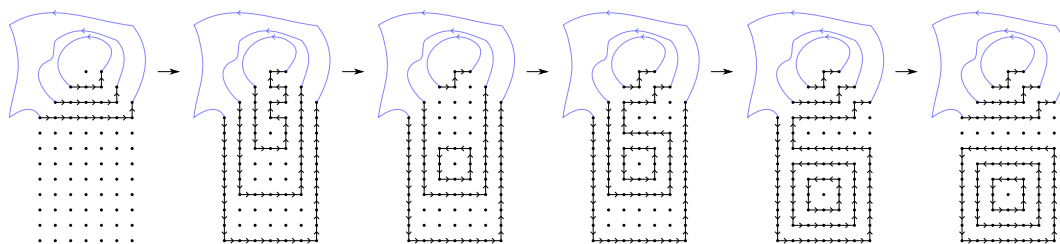


Figure 3.22: Some intermediate steps in the extraction of a jewel. Notice that this flip homotopy reduced the area of the cycles that previously enclosed the jewel.

Suppose w is a jewel. As in Figure 3.22, the jewel w can be extracted via flip moves. We first pull the cycles downward with flip moves of type (a) and then “cut” each cycle (innermost cycles first) with flip moves of type (b),

so that the jewel leaves the cycles as a boxed jewel (easy details are left to the reader). Let s_1 be the sock obtained at the end of this flip homotopy, and let $\tilde{s}_1 = \tilde{s}_2$ be the sock consisting of all the cycles of s_1 except the extracted boxed jewel. Clearly the area of \tilde{s}_2 is less than the area of s_0 , and since s_0 is a sock that has minimal area among those that are not flip homotopic to an untangled sock, it follows that there exists a flip homotopy, say $\tilde{s}_2, \tilde{s}_3, \dots, \tilde{s}_n$ such that \tilde{s}_n is an untangled sock.

Let $M = \max\{k : (l, k) \text{ is a vertex of } \tilde{s}_i \text{ for some } k \in \mathbb{Z}, 2 \leq i \leq n\}$. Recall that boxed jewels can move an arbitrary even distance if they have free space in some direction; by the definition of v , there can be no cycles or cycle parts below v in s_0 , so we can define s_2 (homotopic to s_1) by pulling the extracted jewel in s_1 down as much as we need, namely so that all vertices of the boxed jewel have y coordinate strictly larger than M . Notice that \tilde{s}_2 is obtained from s_2 by removing this boxed jewel. Clearly we can perform on s_2 all the flip moves that took \tilde{s}_2 to \tilde{s}_n , so that we obtain a flip homotopy s_2, s_3, \dots, s_n , where s_n consists of all the cycles in \tilde{s}_n plus a single boxed jewel down below. The other cycles in s_n are also boxed jewels whose centers have y coordinate equal to zero, because \tilde{s}_n is untangled; therefore, the boxed jewel down below can be brought up and sideways as needed, thus obtaining a flip homotopy from s_0 to an untangled sock s_{n+1} . This contradicts the initial hypothesis, and thus the proof is complete. \square

This proof also yields an algorithm for finding the flip homotopy from an arbitrary sock to an untangled sock, although probably not a very efficient one. Start with the initial sock, and find v and w as in the proof. If w is not a jewel, perform the flip move that reduces the area, and recursively untangle this new sock. If w is a jewel, extract the boxed jewel, recursively untangle the sock without the boxed jewel (which has smaller area), and calculate how much space you needed to solve it: this will tell how far down the boxed jewel needs to be pulled. The algorithm stops recursing when we reach a sock with zero area: all that's left to do then is to “organize” the boxed jewels.

Proof of Proposition 3.8. Let t_0 and t_1 be two tilings of a duplex region, and suppose $P_{t_0} = P_{t_1}$. Let s_0 and s_1 denote their corresponding socks in \mathbb{Z}^2 . Since $P_{s_0}(q) = P_{t_0}(q) - P_{t_0}(0) = P_{t_1}(q) - P_{t_1}(0) = P_{s_1}(q)$, it follows by Lemma 3.11 that s_0 and s_1 are flip homotopic to untangled socks \tilde{s}_0 and \tilde{s}_1 . By 3.10, \tilde{s}_0 and \tilde{s}_1 are flip homotopic in \mathbb{Z}^2 , and therefore so are s_0 and s_1 . Finally, by Lemma 3.9, there exists a two-floored box such that the embeddings \hat{t}_0 and \hat{t}_1 of t_0 and t_1 lie in the same flip connected component. \square

As a conclusion, the polynomial invariant here presented is, in a sense, complete: if two tilings have the same invariant and sufficient space is added to the region, then there is a sequence of flips taking one to the other.

3.6

Connectivity by flips and trits

In Section 3.4, we pointed out that the graph of flip connected components for Examples 3.6 and 3.7, shown in Figures 3.7 and 3.9, is connected in both cases. There, two components are joined if there exists a trit taking a tiling in one component to a tiling in the other. Hence, this graph is connected if and only if for any two tilings of the given region, we can reach one from the other using flips and trits.

A natural question is, therefore: for two-story regions, is it true that one can always reach a tiling from any other via flips and trits? The answer is, in general, no, as Figure 3.23 shows.

Nevertheless, this is true for duplex regions:

Proposition 3.12. *If \mathcal{R} is a duplex region and t_0, t_1 are two tilings of \mathcal{R} , there exists a sequence of flips and trits taking t_0 to t_1 .*

In order to prove this result, we'll once again make use of the concept of systems of cycles, or socks, that were introduced in Section 3.5.

Understanding the effect of a trit on a sock turns out to be quite easy: in fact, the effect of a trit can be captured to the world of socks via the insertion of a new move, which we will call the *trit move* (in addition to the three flip moves shown in Figure 3.12). The trit move is shown in Figure 3.24.

Another way to look at trit moves is that it either pulls a jewel out of a cycle or pushes one into a cycle. Two socks s_1 and s_2 are *flip and trit homotopic* in a graph G (which contains both s_1 and s_2) if there is a finite sequence of flip and/or trit moves taking s_1 to s_2 . Notice that, unlike in Section 3.5, where we were mainly interested in flip homotopies in \mathbb{Z}^2 , we are now interested in flip and trit homotopies in the finite graphs $G(\mathcal{R})$. Recall from Section 3.5

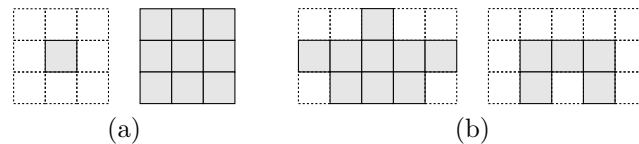


Figure 3.23: Two regions, each with two tilings where neither a flip nor a trit is possible.

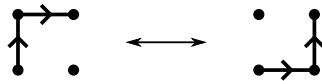


Figure 3.24: The trit move.

that if \mathcal{R} is a duplex region, $G(\mathcal{R})$ is the planar graph whose vertices are the centers of the squares in the associated drawing of \mathcal{R} , and where two vertices are joined by an edge if their Euclidean distance is exactly 1.

Again, for two tilings t_0, t_1 , there exists a sequence of flips and trits taking t_0 to t_1 if and only if their corresponding socks are flip and trit homotopic in $G(\mathcal{R})$.

Lemma 3.13. *If \mathcal{R} is duplex region, and s is a sock in $G(\mathcal{R})$, then s is flip and trit homotopic to the empty sock (the sock with no cycles) in $G(\mathcal{R})$.*

Proof. Suppose, by contradiction, that there exists a sock contained in $G(\mathcal{R})$ that is not flip and trit homotopic to the empty sock in $G(\mathcal{R})$. Of all the examples of such socks, let s be one with minimal area (the concept of area of a sock was defined in Section 3.5). We will show that there exists either a flip move or a trit move that reduces the area of s , which is a contradiction.

Let γ be a cycle of s such that there is no other cycle inside γ : hence, if there is any vertex enclosed by γ , it must be a jewel. Similar to the proof of Lemma 3.11, let v be the rightmost among the bottommost vertices of γ (notice that we are only considering the vertices of γ , and not all the vertices in s), or, in other words: if $m = \max\{n : (k, n) \text{ is a vertex of } \gamma \text{ for some } k \in \mathbb{Z}\}$ and $l = \max\{k : (k, m) \text{ is a vertex of } \gamma\}$, let $v = (l, m)$. Notice that v is the right end of a horizontal edge and the bottom end of a vertical edge: we may assume without loss of generality that this horizontal edge points to the right.

Notice that the vertex $w = v - (1, 1)$ is necessarily in the graph $G(\mathcal{R})$, because otherwise γ would have a hole inside, which contradicts the hypothesis that the (identical) floors of \mathcal{R} are simply connected. Suppose first that w is not a jewel. Since there are no cycles inside γ , it follows that w must be a vertex of γ . If w is the topmost end of a vertical edge pointing downward, we have the first case in Figure 3.25, where we clearly have a flip move that reduces the area. If this is not the case, it follows, in particular, that $u = v - (2, 0)$ must be in the graph $G(\mathcal{R})$: Cases (2) and (3) of Figure 3.25 show the two possibilities for the edges that are incident to w , and it is clear that there exists a flip move which reduces the area of s .

Finally, the case where w is a jewel is shown in case (4) of Figure 3.25: the available trit move clearly reduces the area. Hence, there is always a flip or

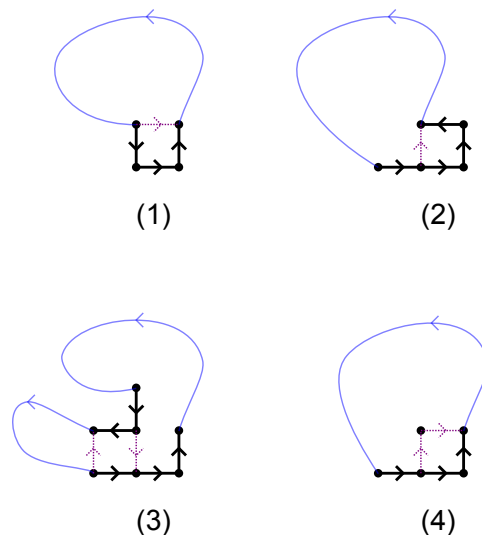


Figure 3.25: The four cases in the proof of Lemma 3.13, where the curved blue lines indicate schematically the position of the edges in γ that are not directly portrayed. The move that reduces the area is indicated by the dashed purple line: in the first three cases, it is a flip move; the last one is a trit move.

trit move that reduces the area of the sock, which contradicts the minimality of the area of s . \square

Therefore, we have established Proposition 3.12. Another observation is that the above proof also yields an algorithm for finding the flip and trit homotopy from a sock to the empty sock: while there is still some cycle in the sock, find one cycle that contains no other cycle. Then find v , as in the proof, and do the corresponding flip or trit move, depending on the case. Since each move reduces the area, it follows that we'll eventually reach the only sock with zero area, which is the empty sock.

3.7

The invariant when more floors are added

In this section, we'll discuss the fact that the invariant $P_t(q)$ is not preserved when the tilings are embedded in "big" regions with more than two floors.

As in Section 3.5, we'll consider duplex regions. Recall from that section that we defined the embedding of such a tiling in a two-floored box \mathcal{B} . Here, we'll extend this notion to embeddings in boxes with four floors in a rather straightforward manner.

If t is a tiling of a duplex region \mathcal{R} , and \mathcal{B} is a box with four floors such that \mathcal{R} is contained in the top two floors of \mathcal{B} , then the embedding \hat{t} of t in

\mathcal{B} is the tiling obtained by first embedding t in the top two floors of \mathcal{B} (as in Section 3.5), and then filling the bottom two floors with dominoes parallel to \vec{k} . This is illustrated in Figure 3.26.

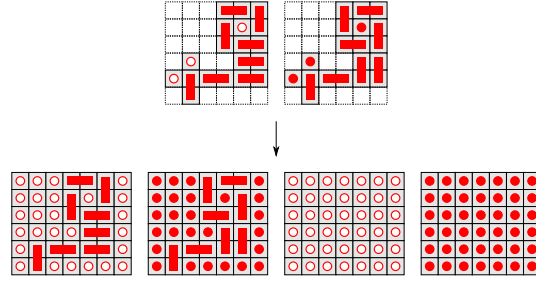


Figure 3.26: A tiling of a two-floored region and its embedding in a $7 \times 6 \times 4$ box.

Proposition 3.14. *If t_0 and t_1 are two tilings of a duplex region and $P'_{t_0}(1) = P'_{t_1}(1)$, then there exists a box with four floors \mathcal{B} such that the embeddings of t_0 and t_1 in \mathcal{B} lie in the same flip connected component.*

Proposition 3.14 is essentially stating that the invariant $P_t(q)$ no longer survives when more floors are added, although the twist $\text{Tw}(t)$ still does, as we will see in Chapter 4. The converse of Proposition 3.14, i.e., the fact that the twist is invariant by flips, follows from item (i) of Proposition 4.6.

Recall from Section 3.5 the definitions of boxed jewel and sock. The key fact in the proof of Proposition 3.14 is that a boxed jewel associated to a q^n term in $P_t(q)$ can be transformed into a number of smaller boxed jewels, their terms adding up to nq . In what follows, the *sign* of a boxed jewel is the sign of its contribution to P_t (i.e., 1 if the jewel is black, and -1 if it is white) and its *degree* is the number of cycles it contains, if all the cycles spin counterclockwise; it is minus this number if all the cycles are clockwise. In other words, if t is a tiling of a two-floored region whose sock is untangled and $\{b_i\}_i$ is the set of boxed jewels in this sock, then

$$P_t(q) = a_0 + \sum_i \text{sgn}(b_i) q^{\deg(b_i)},$$

where $a_0 = P_t(1) - \sum_i \text{sgn}(b_i)$, $\text{sgn}(b_i)$ is the sign of b_i and $\deg(b_i)$, its degree.

Lemma 3.15. *If t_0 and t_1 are tilings of a two-floored region such that their associated socks are both untangled (consist only of boxed jewels) and:*

- (i) *The associated sock of t_0 consists of a single boxed jewel of degree $n > 0$.*
- (ii) *The associated sock of t_1 consists of n boxed jewels of degree 1 and same sign as the boxed jewel in t_0 .*

Then there exists a box with four floors \mathcal{B} where their embeddings lie in the same connected components.

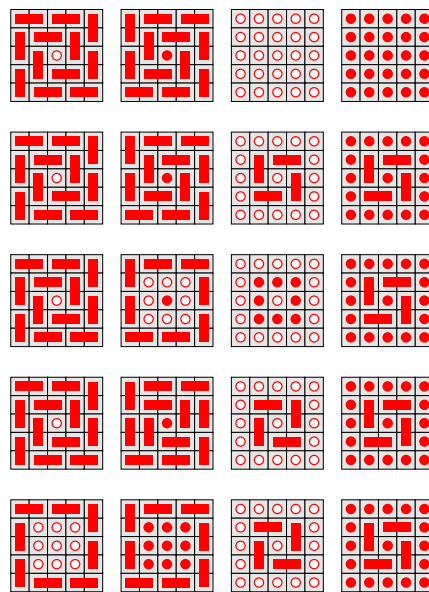


Figure 3.27: Five steps that bring a small boxed jewel from the top two floors to the bottom two floors, each consisting of four flips. In this case, a boxed jewel with degree 2 in the top two floors is transformed into a boxed jewel with degree 1 in the bottom two floors plus a cycle that can be easily flipped to a boxed jewel with degree 1 in the top two floors. Since the bottom jewel can move freely in the bottom floors, it can be brought back up in a different position.

Proof. We omit some easy details, but Figure 3.27 illustrates the key step in the proof: that the innermost boxed jewel can be transported to the bottom two floors via flips. If the box \mathcal{B} is big enough, the innermost boxed jewel can freely move in the bottom two floors, and can eventually be brought back up outside of any other cycles. Since after this maneuver the bottom two floors are back as they originally were, the result of this maneuver is the embedding of a tiling whose sock is flip homotopic to an untangled sock with two boxed jewels, one with degree $n - 1$ and another with degree 1 (but both have the same sign as the original boxed jewel). Proceeding by induction and using Proposition 3.8, we obtain the result. \square

Therefore, boxed jewels with degree $n > 0$ (resp. degree $-n < 0$) can be flipped into n boxed jewels with degree 1 (resp. -1). It only remains to see that boxed jewels with degrees 1 and -1 and same sign cancel out.

Lemma 3.16. *If t is a tiling of a duplex region whose sock is untangled and consists of two boxed jewels with degrees 1 and -1 but same sign, then there exists a box with four floors where the embedding of t is in the same flip*

connected component as the tiling consisting only of “jewels”, that is, the tiling containing only dominoes parallel to \vec{k} .

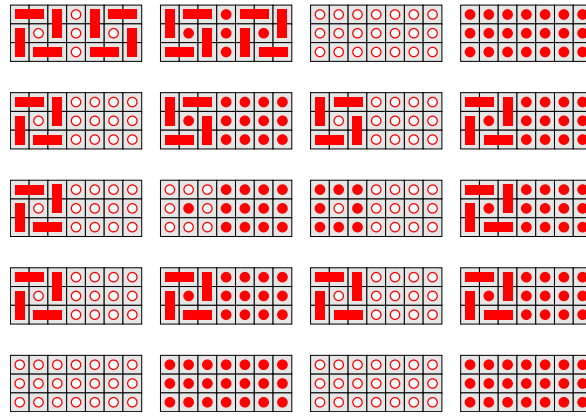


Figure 3.28: Illustration of how two boxed jewels with same sign but opposite degree cancel. One boxed jewel is transported to the bottom floor and there it moves so that it is exactly under the other boxed jewel (this is the first step). From then on, it is a relatively straightforward sequence of flips, and the three bottom drawings show some of the intermediate steps.

Proof. The basic procedure is illustrated in Figure 3.28. First, one jewel can be transported to the bottom floor using the procedure in Figure 3.27. There it can be moved so that it is right under the other boxed jewel, when they can easily be flipped into a tiling with all dominoes parallel to \vec{k} . \square

In short, what Lemmas 3.15 and 3.16 imply is that a tiling t whose sock is untangled and whose invariant is $P_t(q) = a_0 + \sum_{n \neq 0} a_n q^n$ can be embedded in a box with four floors in such a way that this embedding is in the same flip connected component as the embedding of another tiling \tilde{t} (of a duplex region) whose sock is untangled and whose invariant is $P_{\tilde{t}}(q) = \tilde{a}_0 + \left(\sum_{n \neq 0} n a_n\right) q = \tilde{a}_0 + P'_{\tilde{t}}(1)q$.

Proof of Proposition 3.14. Let t_0 and t_1 be two tilings of a duplex region such that $P'_{t_0}(1) = P'_{t_1}(1)$. By Lemmas 3.11 and 3.9, there exists a two-floored box $\tilde{\mathcal{B}}$ where the embeddings of t_0 and t_1 are in the same connected component, respectively, as \tilde{t}_0 and \tilde{t}_1 , two tilings whose sock is untangled. By Lemmas 3.15 and 3.16 and the previous paragraph, there exists a box with four floors \mathcal{B} where the embeddings of \tilde{t}_0 and \tilde{t}_1 lie in the same connected component, respectively, as the embeddings of \hat{t}_0 and \hat{t}_1 (of the same duplex region), with invariants $P_{\hat{t}_0}(q) = a_0 + P'_{t_0}(1)q$ and $P_{\hat{t}_1}(q) = a_1 + P'_{t_1}(1)q$. Since $P'_{t_0}(1) = P'_{t_1}(1)$, it follows that $a_0 = a_1$ and so $P_{\hat{t}_0}(q) = P_{\hat{t}_1}(q)$. By Proposition 3.8, the box \mathcal{B} can be chosen such that the embeddings of \hat{t}_0 and \hat{t}_1 lie in the same flip connected component; this concludes the proof. \square

4

The general case

Most of the material in this chapter is also covered in [18].

4.1

The twist for cylinders

For a domino d , define $\vec{v}(d) \in \Phi$ to be the center of the black cube contained in d minus the center of the white one. We sometimes draw $\vec{v}(d)$ as an arrow pointing from the center of the white cube to the center of the black one.

For a set $X \subset \mathbb{R}^3$ and $\vec{u} \in \Phi$, we define the (*open*) \vec{u} -shade of X as

$$\mathcal{S}^{\vec{u}}(X) = \text{int}((X + [0, \infty)\vec{u}) \setminus X) = \text{int}(\{x + s\vec{u} \in \mathbb{R}^3 | x \in X, s \in [0, \infty)\} \setminus X),$$

where $\text{int}(Y)$ denotes the interior of Y . The *closed* \vec{u} -shade $\bar{\mathcal{S}}^{\vec{u}}(X)$ is the closure of $\mathcal{S}^{\vec{u}}(X)$. We shall only refer to \vec{u} -shades of unions of basic cubes or basic squares, such as dominoes.

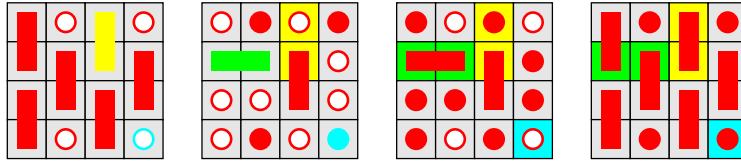


Figure 4.1: Tiling of a $4 \times 4 \times 4$ box, with three distinguished dominoes (painted yellow, green and cyan), whose \vec{k} -shades are highlighted in the same color as they are. Notice that the yellow shade intersects four dominoes, the green shade intersects three, and the cyan shade, only one.

Given two dominoes d_0 and d_1 of t , we define the *effect of d_0 on d_1 along \vec{u}* , as:

$$\tau^{\vec{u}}(d_0, d_1) = \begin{cases} \frac{1}{4} \det(\vec{v}(d_1), \vec{v}(d_0), \vec{u}), & d_1 \cap \mathcal{S}^{\vec{u}}(d_0) \neq \emptyset \\ 0, & \text{otherwise} \end{cases}$$

In other words, $\tau^{\vec{u}}(d_0, d_1)$ is zero unless the following three things happen: d_1 intersects the \vec{u} -shade of d_0 ; neither d_0 nor d_1 are parallel to \vec{u} ; and d_0 is not

parallel to d_1 . When $\tau^{\vec{u}}(d_0, d_1)$ is not zero, it's either $1/4$ or $-1/4$ depending on the orientations of $\vec{v}(d_0)$ and $\vec{v}(d_1)$.

For example, in Figure 4.1, for $\vec{u} = \vec{k}$, the yellow domino d_Y has no effect on any other domino: $\tau^{\vec{k}}(d_Y, d) = 0$ for every domino d in the tiling. The green domino d_G , however, affects the two dominoes in the rightmost floor which intersect its \vec{k} -shade, and $\tau^{\vec{i}}(d_G, d) = 1/4$ for both these dominoes.

If t is a tiling, we define the \vec{u} -pretwist as

$$T^{\vec{u}}(t) = \sum_{d_0, d_1 \in t} \tau^{\vec{u}}(d_0, d_1).$$

For example, the tiling on the left of Figure 1.4 has \vec{k} -pretwist equal to 1. To see this, notice that each of the four dominoes of the leftmost floor that are not parallel to \vec{k} has nonzero effect along \vec{k} on exactly one domino of the rightmost floor, and this effect is $1/4$ in each case. The reader may also check that the \vec{k} -pretwist of the tiling in Figure 4.1 is 0.

Lemma 4.1. *For any pair of dominoes d_0 and d_1 and any $\vec{u} \in \Phi$, $\tau^{\vec{u}}(d_0, d_1) = \tau^{-\vec{u}}(d_1, d_0)$. In particular, for a tiling t of a region we have $T^{-\vec{u}}(t) = T^{\vec{u}}(t)$.*

Proof. Just notice that $d_1 \cap \mathcal{S}^{\vec{u}}(d_0) \neq \emptyset$ if and only if $d_0 \cap \mathcal{S}^{-\vec{u}}(d_1) \neq \emptyset$, and $\det(\vec{v}(d_1), \vec{v}(d_0), \vec{u}) = \det(\vec{v}(d_0), \vec{v}(d_1), -\vec{u})$. \square

Translating both dominoes by a vector with integer coordinates clearly does not affect $\tau^{\vec{u}}(d_0, d_1)$, as $\det(\vec{v}(d_1), \vec{v}(d_0), \vec{u}) = \det(-\vec{v}(d_1), -\vec{v}(d_0), \vec{u})$. Therefore, if t is a tiling and $f(p) = p + b$, where $b \in \mathbb{Z}^3$, then $T^{\vec{u}}(f(t)) = T^{\vec{u}}(t)$.

Lemma 4.2. *Let \mathcal{R} be a region, and let $\vec{w} \in \Delta$. Consider the reflection $r = r_{\vec{w}} : \mathbb{R}^3 \rightarrow \mathbb{R}^3 : p \mapsto p - 2(p \cdot \vec{w})\vec{w}$; notice that $r(\mathcal{R})$ is a region. If t is a tiling of \mathcal{R} and $\vec{u} \in \Phi$, then the tiling $r(t) = \{r(d), d \in t\}$ of $r(\mathcal{R})$ satisfies $T^{\vec{u}}(r(t)) = -T^{\vec{u}}(t)$.*

Proof. Given a domino d of t , notice that $\vec{v}(r(d)) = -r(\vec{v}(d))$ and that $\mathcal{S}^{\vec{u}}(r(d)) = r(\mathcal{S}^{r(\vec{u})}(d))$. Therefore, $r(d_1) \cap \mathcal{S}^{\vec{u}}(r(d_0)) \neq \emptyset \Leftrightarrow d_1 \cap \mathcal{S}^{r(\vec{u})}(d_0) \neq \emptyset$ and

$$\begin{aligned} \det(\vec{v}(r(d_1)), \vec{v}(r(d_0)), \vec{u}) &= \det(-r(\vec{v}(d_1)), -r(\vec{v}(d_0)), \vec{u}) \\ &= \det(r(\vec{v}(d_1)), r(\vec{v}(d_0)), r(r(\vec{u}))) = -\det(\vec{v}(d_1), \vec{v}(d_0), r(\vec{u})). \end{aligned}$$

Therefore, $\tau^{\vec{u}}(r(d_0), r(d_1)) = -\tau^{r(\vec{u})}(d_0, d_1)$ and thus $T^{\vec{u}}(r(t)) = -T^{r(\vec{u})}(t)$. Since $r(\vec{u}) = \pm\vec{u}$, Lemma 4.1 implies that $T^{\vec{u}}(r(t)) = -T^{\vec{u}}(t)$, completing the proof. \square

A natural question at this point concerns how the choice of \vec{u} affects $T^{\vec{u}}$. It turns out that it will take us some preparation before we can tackle this question.

Proposition 4.3. *If \mathcal{R} is a cylinder and t is a tiling of \mathcal{R} ,*

$$T^{\vec{i}}(t) = T^{\vec{j}}(t) = T^{\vec{k}}(t) \in \mathbb{Z}.$$

Proof. Follows directly from Propositions 4.24 and 4.31 below. \square

This result doesn't hold in pseudocylinders or in more general simply connected regions; see Section 4.8 for counterexamples.

Definition 4.4. *For a tiling t of a cylinder \mathcal{R} , we define the twist $\text{Tw}(t)$ as*

$$\text{Tw}(t) = T^{\vec{i}}(t) = T^{\vec{j}}(t) = T^{\vec{k}}(t).$$

Until Section 4.4, we will not use Proposition 4.3, and will only refer to pretwists.

Let $\vec{u} \in \Delta$, and let $\beta = (\vec{\beta}_1, \vec{\beta}_2, \vec{\beta}_3) \in \mathbf{B}$ be such that $\vec{\beta}_3 = \vec{u}$. A region \mathcal{R} is said to be *fully balanced with respect to \vec{u}* if for each square $Q = p + [0, 2]\vec{\beta}_1 + [0, 2]\vec{\beta}_2$, where $p \in \mathbb{Z}^3$ and $Q \subset \mathcal{R}$, each of the two sets $\mathcal{A}^{\vec{u}} = \mathcal{R} \cap \bar{\mathcal{S}}^{\vec{u}}(Q)$ and $\mathcal{A}^{-\vec{u}} = \mathcal{R} \cap \bar{\mathcal{S}}^{-\vec{u}}(Q)$ contains as many black cubes as white ones. In other words,

$$\sum_{C \subset \mathcal{A}^{\vec{u}}} \text{color}(C) = \sum_{C \subset \mathcal{A}^{-\vec{u}}} \text{color}(C) = 0.$$

\mathcal{R} is *fully balanced* if it is fully balanced with respect to each $\vec{u} \in \Delta$.

Lemma 4.5. *Every pseudocylinder (in particular, every cylinder) is fully balanced.*

Proof. Let \mathcal{R} be a pseudocylinder with base \mathcal{D} and depth n , let $\vec{u} \in \Delta$ and let $Q = p_0 + [0, 2]\vec{\beta}_1 + [0, 2]\vec{\beta}_2 \subset \mathcal{R}$, where $\beta \in \mathbf{B}$ is such that $\vec{\beta}_3 = \vec{u}$ and $p_0 \in \mathbb{Z}^3$. Consider $\mathcal{A}^{\pm\vec{u}} = \mathcal{R} \cap \bar{\mathcal{S}}^{\pm\vec{u}}(Q)$.

If \vec{u} is the axis of the pseudocylinder, then $Q = Q' + k\vec{u}$, for some square $Q' \subset \mathcal{D}$ and some $0 \leq k \leq n$. Now $\mathcal{A}^{\vec{u}} = Q' + [k, n]\vec{u}$, which clearly contains $2(n - k)$ black cubes and $2(n - k)$ white ones; similarly, $\mathcal{A}^{-\vec{u}} = Q' + [0, k]\vec{u}$ contains $2k$ black cubes and $2k$ white ones.

If \vec{u} is perpendicular to the axis of the pseudocylinder, assume without loss of generality that $\vec{\beta}_1$ is the axis. Let Π denote the orthogonal projection on \mathcal{D} , and let $\mathcal{D}^\pm = \Pi(\bar{\mathcal{S}}^{\pm\vec{u}}(Q)) \cap \mathcal{D}$, which are planar regions, since they are unions of squares of \mathcal{D} . If $p_0 - \Pi(p_0) = k\vec{\beta}_1$, we have $\mathcal{A}^{\pm\vec{u}} = \mathcal{D}^\pm + [k, k+2]\vec{\beta}_1$, which clearly has the same number of black squares as white ones. \square

Proposition 4.6. *Let \mathcal{R} be a region that is fully balanced with respect to $\vec{u} \in \Phi$.*

- (i) *If a tiling t_1 of \mathcal{R} is reached from t_0 after a flip, then $T^{\vec{u}}(t_0) = T^{\vec{u}}(t_1)$*
- (ii) *If a tiling t_1 of \mathcal{R} is reached from t_0 after a single positive trit, then $T^{\vec{u}}(t_1) = T^{\vec{u}}(t_0) + 1$.*

Proof. In this proof, \vec{u} points towards the paper in all the drawings. We begin by proving (i). Suppose a flip takes the dominoes d_0 and \tilde{d}_0 in t_0 to d_1 and \tilde{d}_1 in t_1 . Notice that $\vec{v}(d_0) = -\vec{v}(\tilde{d}_0)$ and $\vec{v}(d_1) = -\vec{v}(\tilde{d}_1)$. For each domino $d \in t_0 \cap t_1$, define

$$E^{\pm\vec{u}}(d) = \tau^{\pm\vec{u}}(d, d_1) + \tau^{\pm\vec{u}}(d, \tilde{d}_1) - \tau^{\pm\vec{u}}(d, d_0) - \tau^{\pm\vec{u}}(d, \tilde{d}_0).$$

Notice that

$$T^{\vec{u}}(t_1) - T^{\vec{u}}(t_0) = \sum_{d \in t_0 \cap t_1} E^{\vec{u}}(d) + E^{-\vec{u}}(d).$$

Case 1. *Either d_0 or d_1 is parallel to \vec{u} .*

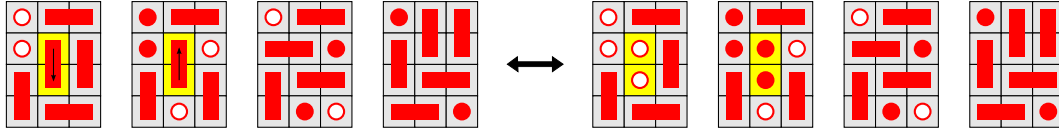


Figure 4.2: An example of Case 1, where the black arrows represent $\vec{v}(d_0)$ and $\vec{v}(\tilde{d}_0)$. It is clear that the effects of d_0 and \tilde{d}_0 cancel out.

Assume, without loss of generality, that d_1 (and thus also \tilde{d}_1) is parallel to \vec{u} . By definition, $\tau^{\pm\vec{u}}(d, d_1) = \tau^{\pm\vec{u}}(d, \tilde{d}_1) = 0$ for each domino d . Now notice that d_0 and \tilde{d}_0 are parallel and in adjacent floors (see Figure 4.2) : since $\vec{v}(d_0) = -\vec{v}(\tilde{d}_0)$, it follows that $\tau^{\pm\vec{u}}(d, d_0) + \tau^{\pm\vec{u}}(d, \tilde{d}_0) = 0$ for each domino d , so that $E^{\pm\vec{u}}(d) = 0$ and thus $T^{\vec{u}}(t_1) = T^{\vec{u}}(t_0)$.

Case 2. *Neither d_0 nor d_1 is parallel to \vec{u} .*

In this case, $d_0 \cup \tilde{d}_0 = d_1 \cup \tilde{d}_1 = Q + [0, 1]\vec{u} \subset \mathcal{R}$ for some square Q of side 2 and normal vector \vec{u} .

Notice that $\bar{\mathcal{S}}^{\vec{u}}(d_0) \cup \bar{\mathcal{S}}^{\vec{u}}(\tilde{d}_0) = \bar{\mathcal{S}}^{\vec{u}}(d_1) \cup \bar{\mathcal{S}}^{\vec{u}}(\tilde{d}_1) = \bar{\mathcal{S}}^{\vec{u}}(Q + \vec{u})$; let $\mathcal{A}^{\vec{u}} = \mathcal{R} \cap \bar{\mathcal{S}}^{\vec{u}}(Q + \vec{u})$.

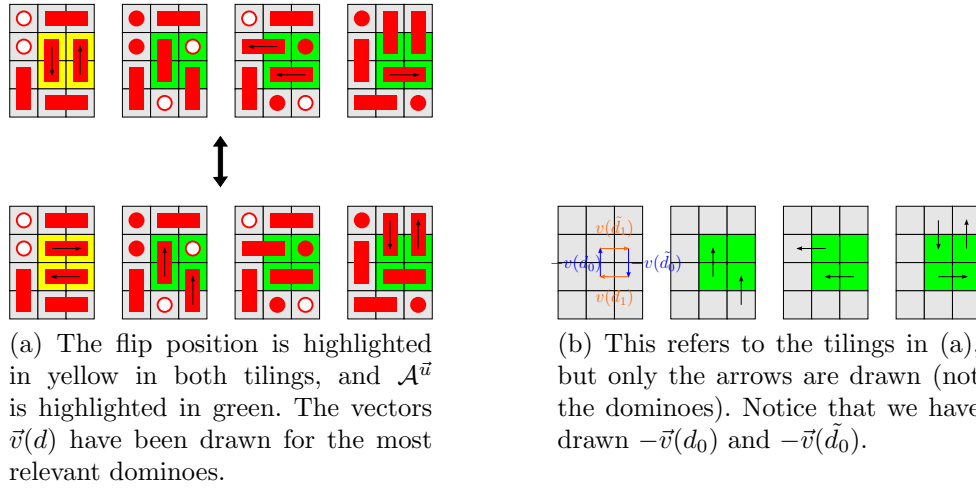


Figure 4.3: Example of a flip in Case 2, together with a schematic drawing portraying $\vec{v}(d)$ for the relevant dominoes.

Let d be a domino that is completely contained in $\mathcal{A}^{\vec{u}}$: we claim that $\tau(d_0, d) + \tau(\tilde{d}_0, d) = 0 = \tau(d_1, d) + \tau(\tilde{d}_1, d)$. This is obvious if d is parallel to \vec{u} ; if not, we can switch the roles of t_0 and t_1 if necessary and assume that d is parallel to d_0 , which implies that $\tau(d_0, d) = \tau(\tilde{d}_0, d) = 0$. Now notice that d is in the \vec{u} -shades of both d_1 and \tilde{d}_1 , so that $\tau(d_1, d) = -\tau(\tilde{d}_1, d)$. Hence, if $d \subset \mathcal{A}^{\vec{u}}$ (or if $d \cap \mathcal{A}^{\vec{u}} = \emptyset$), $E^{-\vec{u}}(d) = 0$.

For dominoes d that intersect $\mathcal{A}^{\vec{u}}$ but are not contained in it, first observe that by switching the roles of t_0 and t_1 and switching the colors of the cubes (i.e., translating) if necessary, we may assume that the vectors are as shown in Figure 4.3a. By looking at Figure 4.3b and working out the possible cases, we see that

$$E^{-\vec{u}}(d) = \begin{cases} -\frac{1}{4}, & \text{if } \vec{v}(d) \text{ points into } \mathcal{A}^{\vec{u}}; \\ \frac{1}{4}, & \text{if } \vec{v}(d) \text{ points away from } \mathcal{A}^{\vec{u}}. \end{cases}$$

Now for such dominoes, $\vec{v}(d)$ points away from the region if and only if d intersects a white cube of $\mathcal{A}^{\vec{u}}$, and points into the region if and only if d intersects a black cube in $\mathcal{A}^{\vec{u}}$: hence,

$$\sum_{d \in t_0 \cap t_1} E^{-\vec{u}}(d) = \sum_{C \subset \mathcal{A}^{\vec{u}}} (-\text{color}(C)) = 0,$$

because \mathcal{R} is fully balanced with respect to \vec{u} . A completely symmetrical argument shows that $\sum_{d \in t_0 \cap t_1} E^{\vec{u}}(d) = 0$, so we are done.

We now prove (ii). Suppose t_1 is reached from t_0 after a single positive trit. By rotating t_0 and t_1 in the plane $\vec{u}^\perp = \{\vec{w} | \vec{w} \cdot \vec{u} = 0\}$ (notice that this does not change $T^{\vec{u}}$), we may assume without loss of generality that the

dominoes involved in the positive trit are as shown in Figure 4.4a. Moreover, by translating if necessary, we may assume that the vectors $\vec{v}(d)$ are as shown in Figure 4.4.

A trit involves three dominoes, no two of them parallel. Since dominoes parallel to \vec{u} have no effect along \vec{u} , we consider only the four dominoes involved in the trit that are not parallel to \vec{u} : $d_0, \tilde{d}_0 \in t_0$, and $d_1, \tilde{d}_1 \in t_1$. Define $E^{\pm\vec{u}}$ with the same formulas as before.

By looking at Figure 2.1, the reader will see that $\tau(d_0, \tilde{d}_0) + \tau(\tilde{d}_0, d_0) = -1/4$ and $\tau(d_1, \tilde{d}_1) + \tau(\tilde{d}_1, d_1) = 1/4$.

Let $D = d_0 \cup \tilde{d}_0 \cup d_1 \cup \tilde{d}_1$: $\bar{\mathcal{S}}^{\vec{u}}(D)$ is shown in Figure 4.4. D contains a single square Q of side 2 and normal vector \vec{u} . Define $\mathcal{A}^{\vec{u}} = \bar{\mathcal{S}}^{\vec{u}}(D) \cap \mathcal{R}$, and notice that (see Figure 4.4) $\bar{\mathcal{S}}^{\vec{u}}(Q) \cap \mathcal{R} = \mathcal{A}^{\vec{u}} \cup C_1 \cup C_2 \cup C_3$, where C_i are three basic cubes: if we look at the arrows in Figure 4.4, we see that two of them are white and one is black. Since \mathcal{R} is fully balanced with respect to \vec{u} ,

$$\sum_{C \subset \mathcal{A}^{\vec{u}}} \text{color}(C) = \sum_{C \subset \bar{\mathcal{S}}^{\vec{u}}(Q) \cap \mathcal{R}} \text{color}(C) - \sum_{1 \leq i \leq 3} \text{color}(C_i) = 1.$$

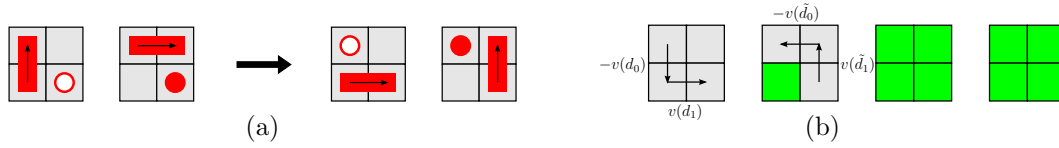


Figure 4.4: Illustration of a positive trit position. In (a), the dominoes and the corresponding vectors $\vec{v}(d)$ are shown, while in (b), the highlighted cubes represent $\bar{\mathcal{S}}^{\vec{u}}(D)$, and the vectors $-\vec{v}(d_0)$, $-\vec{v}(\tilde{d}_0)$, $\vec{v}(d_1)$ and $\vec{v}(\tilde{d}_1)$ are shown.

By looking at Figure 4.4, we see that we have a situation that is very similar to Figure 4.3b; for each $d \in t_0 \cap t_1$, we have

$$E^{-\vec{u}}(d) = \begin{cases} 0, & \text{if } d \subset \mathcal{A}^{\vec{u}} \text{ or } d \cap \mathcal{A}^{\vec{u}} = \emptyset; \\ \frac{1}{4}, & \text{if } \vec{v}(d) \text{ points into } \mathcal{A}^{\vec{u}}; \\ -\frac{1}{4}, & \text{if } \vec{v}(d) \text{ points away from } \mathcal{A}^{\vec{u}} \end{cases}$$

(when we say that $\vec{v}(d)$ points into or away from $\mathcal{A}^{\vec{u}}$, we are assuming that d intersects one cube of $\mathcal{A}^{\vec{u}}$). Hence,

$$\sum_{d \in t_0 \cap t_1} E^{-\vec{u}}(d) = \frac{1}{4} \sum_{C \subset \mathcal{A}^{\vec{u}}} \text{color}(C) = \frac{1}{4}.$$

A completely symmetrical argument shows that $\sum_{d \in t_0 \cap t_1} E^{\vec{u}}(d) = 1/4$, and hence

$$\begin{aligned} T^{\vec{u}}(t_1) - T^{\vec{u}}(t_0) &= (\tau(d_1, \tilde{d}_1) + \tau(\tilde{d}_1, d_1)) - (\tau(d_0, \tilde{d}_0) + \tau(\tilde{d}_0, d_0)) \\ &+ \sum_{d \in t_0 \cap t_1} E^{-\vec{u}}(d) + \sum_{d \in t_0 \cap t_1} E^{\vec{u}}(d) = \frac{1}{4} + \frac{1}{4} + \frac{1}{4} + \frac{1}{4} = 1, \end{aligned}$$

which completes the proof. \square

4.2

Topological groundwork for the twist

In this section, we develop a topological interpretation of tilings and twists. Dominoes are (temporarily) replaced by dimers, which, although formally different objects, are really just a different way of looking at dominoes. Although we will tend to work with dimers in this and the following section, we may in later sections switch back and forth between these two viewpoints.

We will now give some useful (but somewhat technical) definitions. The reader that is familiar with perfect matchings in graphs may find it easier to follow by recalling that domino tilings of a region can be seen as perfect matchings of a dual bipartite graph, and that the symmetric difference of two perfect matchings of the same graph is a disjoint set of cycles: we want to look at these cycles as oriented curves in \mathbb{R}^3 .

Let \mathcal{R} be a region. A *segment* ℓ of \mathcal{R} is a straight line of unit length connecting the centers of two cubes of \mathcal{R} ; in other words, $\ell : [0, 1] \rightarrow \mathbb{R}^3$ with $\ell(s) = p_0 + (p_1 - p_0)s$, where p_0 and p_1 are the centers of two cubes that share a face: this segment is a *dimer* if $p_0 = \ell(0)$ is the center of a white cube. We define $\vec{v}(\ell) = \ell(1) - \ell(0)$ (compare this with the definition of $\vec{v}(d)$ for a domino d). If ℓ is a segment, $(-\ell)$ denotes the segment $s \mapsto \ell(1 - s)$: notice that either ℓ or $-\ell$ is a dimer.

Two segments ℓ_0 and ℓ_1 are *adjacent* if $\ell_0 \cap \ell_1 \neq \emptyset$ (here we make the usual abuse of notation of identifying a curve with its image in \mathbb{R}^3); nonadjacent segments are *disjoint*. In particular, a segment is always adjacent to itself.

A *tiling* of \mathcal{R} by dimers is a set of pairwise disjoint dimers such that the center of each cube of \mathcal{R} belongs to exactly one dimer of t . If t is a tiling, $(-t)$ denotes the set of segments $\{-\ell | \ell \in t\}$.

Given a map $\gamma : [m, n] \rightarrow \mathbb{R}^3$, a segment ℓ and an integer $k \in [m, n - 1]$, we abuse notation by making the identification $\gamma|_{[k, k+1]} = \ell$ if $\gamma(s) = \ell(s - k)$ for each $s \in [k, k + 1]$. A *curve* of \mathcal{R} is a map $\gamma : [0, n] \rightarrow \mathbb{R}^3$ such that $\gamma|_{[k, k+1]}$

is (identified with) a segment of \mathcal{R} for $k = 0, 1, \dots, n-1$. We make yet another abuse of notation by also thinking of γ as a sequence or set of segments of \mathcal{R} , and we shall write $\ell \in \gamma$ to denote that $\ell = \gamma|_{[k, k+1]}$ for some k .

A curve $\gamma : [0, n] \rightarrow \mathbb{R}^3$ of \mathcal{R} is *closed* if $\gamma(0) = \gamma(n)$; it is *simple* if γ is injective in $[0, n)$. A closed curve $\gamma : [0, 2] \rightarrow \mathbb{R}^3$ of \mathcal{R} is called *trivial*: notice that, in this case, $\gamma|_{[0, 1]} = -(\gamma|_{[1, 2]})$ (when identified with their respective segments of \mathcal{R}). A *discrete rotation* on $[0, n]$ is a function $\rho : [0, n] \rightarrow [0, n]$ with $\rho(s) = (s + k) \bmod n$, for a fixed $k \in \mathbb{Z}$. If $\gamma_0 : [0, n] \rightarrow \mathbb{R}^3$ and $\gamma_1 : [0, m] \rightarrow \mathbb{R}^3$ are two closed curves, we say $\gamma_0 = \gamma_1$ if $n = m$ and $\gamma_1 = \gamma_0 \circ \rho$ for some discrete rotation ρ on $[0, n]$.

Given two tilings t_0 and t_1 , there exists a unique (up to discrete rotations) finite set of disjoint closed curves $\Gamma(t_0, t_1) = \{\gamma_i | 1 \leq i \leq m\}$ such that $t_0 \cup (-t_1) = \{\ell | \ell \in \gamma_i \text{ for some } i\}$ and such that every nontrivial γ_i is simple. Figure 4.7 shows an example. We define $\Gamma^*(t_0, t_1) := \{\gamma \in \Gamma(t_0, t_1) | \gamma \text{ nontrivial}\}$.

Translating effects from the world of dominoes to the world of dimers is relatively straightforward. For $\vec{u} \in \Phi$, $\Pi^{\vec{u}}$ will denote the orthogonal projection on the plane $\pi^{\vec{u}} = \vec{u}^\perp = \{\vec{w} \in \mathbb{R}^3 | \vec{w} \cdot \vec{u} = 0\}$. Given two segments ℓ_0 and ℓ_1 , we set:

$$\tau^{\vec{u}}(\ell_0, \ell_1) = \begin{cases} \frac{1}{4} \det(\vec{v}(\ell_1), \vec{v}(\ell_0), \vec{u}), & \Pi^{\vec{u}}(\ell_0) \cap \Pi^{\vec{u}}(\ell_1) \neq \emptyset, \ell_0(0) \cdot \vec{u} < \ell_1(0) \cdot \vec{u}; \\ 0, & \text{otherwise.} \end{cases}$$

Notice that this definition is analogous to the one given in Section 4.1 for dominoes.

The definition of $\tau^{\vec{u}}$ is given in terms of the orthogonal projection $\Pi^{\vec{u}}$. From a topological viewpoint, however, this projection is not ideal, because it gives rise to nontransversal intersections between projections of segments. In order to solve this problem, we consider small perturbations of these projections.

Recall that \mathbf{B} is the set of positively oriented basis $\beta = (\vec{\beta}_1, \vec{\beta}_2, \vec{\beta}_3)$ with vectors in Φ . If $\beta \in \mathbf{B}$ and $a, b \in \mathbb{R}$, $\Pi_{a,b}^\beta$ will be used to denote the projection on the plane $\pi^{\vec{\beta}_3} = \vec{\beta}_3^\perp = \{\vec{u} \in \mathbb{R}^3 | \vec{u} \cdot \vec{\beta}_3 = 0\}$ whose kernel is the subspace (line) generated by the vector $\vec{\beta}_3 + a\vec{\beta}_1 + b\vec{\beta}_2$. For instance, if $\beta = (\vec{i}, \vec{j}, \vec{k})$ is the canonical basis, $\Pi_{a,b}^\beta(x, y, z) = (x - az, y - bz, 0)$. Notice that $\Pi_{0,0}^\beta = \Pi^{\vec{\beta}_3}$ is the orthogonal projection on the plane $\pi^{\vec{\beta}_3}$, and, for small $(a, b) \neq (0, 0)$, $\Pi_{a,b}^\beta$ is a nonorthogonal projection on $\pi^{\vec{\beta}_3}$ which is a slight perturbation of $\Pi^{\vec{\beta}_3}$.

Given $\beta \in \mathbf{B}$, $\vec{u} = \vec{\beta}_3$ and small nonzero $a, b \in \mathbb{R}$, set the *slanted effect*

$$\tau_{a,b}^\beta(\ell_0, \ell_1) = \begin{cases} \det(\vec{v}(\ell_1), \vec{v}(\ell_0), \vec{u}), & \Pi_{a,b}^\beta(\ell_0) \cap \Pi_{a,b}^\beta(\ell_1) \neq \emptyset, \vec{u} \cdot \ell_0(0) < \vec{u} \cdot \ell_1(0); \\ 0, & \text{otherwise.} \end{cases}$$

Recall from knot theory the concept of crossing (see, e.g., [1, p.18]). Namely, if $\gamma_0 : I_0 \rightarrow \mathbb{R}^3$, $\gamma_1 : I_1 \rightarrow \mathbb{R}^3$ are two continuous curves, $s_j \in \text{int}(I_j)$ and Π is a projection from \mathbb{R}^3 to a plane, then $(\Pi, \gamma_0, s_0, \gamma_1, s_1)$ is a *crossing* if $\gamma_0(s_0) \neq \gamma_1(s_1)$ but $\Pi(\gamma_0(s_0)) = \Pi(\gamma_1(s_1))$. If, furthermore, γ_j is of class C^1 in s_j and the vectors $\gamma'_1(s_1)$, $\gamma'_0(s_0)$ and $\gamma_1(s_1) - \gamma_0(s_0)$ are linearly independent, then the crossing is *transversal*; its *sign* is the sign of $\det(\gamma'_1(s_1), \gamma'_0(s_0), \gamma_1(s_1) - \gamma_0(s_0))$. We are particularly interested in the case where the curves are segments of a region \mathcal{R} .

For a region \mathcal{R} and $\vec{u} \in \Phi$, we define the \vec{u} -length of \mathcal{R} as

$$N = \max_{p_0, p_1 \in \mathcal{R}} |\vec{u} \cdot (p_0 - p_1)|.$$

Lemma 4.7. *Let \mathcal{R} be a region, and fix $\beta \in \mathbf{B}$. Let N be the $\vec{\beta}_3$ -length of \mathcal{R} , and let $a, b \in \mathbb{R}$ with $0 < |a|, |b| < 1/N$. Then $\tau_{a,b}^\beta(\ell_0, \ell_1) + \tau_{a,b}^\beta(\ell_1, \ell_0) \neq 0$ if and only if there exist $s_0, s_1 \in [0, 1]$ such that $\ell_0(s_0) \neq \ell_1(s_1)$ but $\Pi_{a,b}^\beta(\ell_0(s_0)) = \Pi_{a,b}^\beta(\ell_1(s_1))$.*

Moreover, if the latter condition holds for s_0, s_1 , then $(\Pi_{a,b}^\beta, \ell_0, s_0, \ell_1, s_1)$ is a transversal crossing whose sign is given by $\tau_{a,b}^\beta(\ell_0, \ell_1) + \tau_{a,b}^\beta(\ell_1, \ell_0)$.

Proof. Suppose $\tau_{a,b}^\beta(\ell_0, \ell_1) + \tau_{a,b}^\beta(\ell_1, \ell_0) \neq 0$. We may without loss of generality assume $\tau_{a,b}^\beta(\ell_0, \ell_1) \neq 0$. By definition, we have $\Pi_{a,b}^\beta(\ell_0(s_0)) = \Pi_{a,b}^\beta(\ell_1(s_1))$ for some $s_0, s_1 \in [0, 1]$ and $\vec{\beta}_3 \cdot \ell_0(0) < \vec{\beta}_3 \cdot \ell_1(0)$. Since $\det(\vec{v}(\ell_1), \vec{v}(\ell_0), \vec{\beta}_3) \neq 0$, we have

$$\vec{\beta}_3 \cdot \ell_0(s_0) = \vec{\beta}_3 \cdot (\ell_0(0) + s_0 \vec{v}(\ell_0)) = \vec{\beta}_3 \cdot \ell_0(0) < \vec{\beta}_3 \cdot \ell_1(0) = \vec{\beta}_3 \cdot \ell_1(s_1),$$

and thus $\ell_0(s_0) \neq \ell_1(s_1)$.

Conversely, suppose $\ell_0(s_0) \neq \ell_1(s_1)$ but $\Pi_{a,b}^\beta(\ell_0(s_0)) = \Pi_{a,b}^\beta(\ell_1(s_1))$: this can be rephrased as

$$\ell_1(s_1) - \ell_0(s_0) = c(\vec{\beta}_3 + a\vec{\beta}_1 + b\vec{\beta}_2) \quad (4-1)$$

for some $c \neq 0$. Notice that $c = \vec{\beta}_3 \cdot (\ell_1(s_1) - \ell_0(s_0))$, so that $|c| \leq N$.

We now observe that $\det(\vec{v}(\ell_1), \vec{v}(\ell_0), \vec{\beta}_3) \neq 0$. Suppose, by contradiction, that $\det(\vec{v}(\ell_1), \vec{v}(\ell_0), \vec{\beta}_3) = 0$. Then, at least one of the following statements

must be true: $\vec{\beta}_1 \cdot \vec{v}(\ell_0) = \vec{\beta}_1 \cdot \vec{v}(\ell_1) = 0$; or $\vec{\beta}_2 \cdot \vec{v}(\ell_0) = \vec{\beta}_2 \cdot \vec{v}(\ell_1) = 0$. Assume that the first statement holds (i.e., $\vec{\beta}_1 \cdot \vec{v}(\ell_i) = 0$). By definition of segment, $\ell_i(s_i) = \ell_i(0) + s_i \vec{v}(\ell_i)$. By taking the inner product with $\vec{\beta}_1$ on both sides of (4-1), $ac = \vec{\beta}_1 \cdot (\ell_1(s_1) - \ell_0(s_0)) = \vec{\beta}_1 \cdot (\ell_1(0) - \ell_0(0))$. Now $\ell_0(0), \ell_1(0) \in (\mathbb{Z}^\sharp)^3$, so that $ac = \vec{\beta}_1 \cdot (\ell_1(0) - \ell_0(0)) \in \mathbb{Z}$. Since $|a| < 1/N$, $|ac| < 1$ and thus $c = 0$, which is a contradiction.

Finally, since $\vec{\beta}_3 \cdot \vec{v}(\ell_0) = \vec{\beta}_3 \cdot \vec{v}(\ell_1) = 0$, we have $\vec{\beta}_3 \cdot (\ell_1(0) - \ell_0(0)) = \vec{\beta}_3 \cdot (\ell_1(s_0) - \ell_0(s_1)) = c \neq 0$. From the definition of $\tau_{a,b}^\beta$, we see that $\tau_{a,b}^\beta(\ell_0, \ell_1) + \tau_{a,b}^\beta(\ell_1, \ell_0) \neq 0$.

To see the last claim, we first note that $s_i \in (0, 1)$: since $\vec{v}(\ell_i) \in \{\pm\vec{\beta}_1, \pm\vec{\beta}_2\}$, we may take the inner product with $\vec{v}(\ell_i)$ on both sides of (4-1) to get that s_i equals either $|ac|$ or $|bc|$, and hence $s_i \in (0, 1)$. Since $\vec{v}(\ell_0) \perp \vec{v}(\ell_1)$, this proves that $(\Pi_{a,b}^\beta, \ell_0, s_0, \ell_1, s_1)$ is a transversal crossing. If $\vec{w} = \vec{\beta}_3 + a\vec{\beta}_1 + b\vec{\beta}_2$, the sign of this crossing is given by the sign of $\det(\vec{v}(\ell_1), \vec{v}(\ell_0), c\vec{w})$. By switching the roles of ℓ_0 and ℓ_1 if necessary, we may assume that $c > 0$, so that this sign equals $\det(\vec{v}(\ell_1), \vec{v}(\ell_0), \vec{w}) = \det(\vec{v}(\ell_1), \vec{v}(\ell_0), \vec{\beta}_3) = \tau_{a,b}(\ell_0, \ell_1)$, completing the proof. \square

Lemma 4.8. *Let \mathcal{R} be a region, and let $\beta \in \mathbf{B}$. Let N denote the $\vec{\beta}_3$ -length of \mathcal{R} , and suppose $0 < \epsilon < 1/N$. Given two segments ℓ_0 and ℓ_1 ,*

$$\tau^{\vec{\beta}_3}(\ell_0, \ell_1) = \frac{1}{4} \sum_{i,j \in \{-1,1\}} \tau_{i\epsilon, j\epsilon}^\beta(\ell_0, \ell_1).$$

Proof. We may assume that $\vec{\beta}_3 \cdot \ell_0(0) < \vec{\beta}_3 \cdot \ell_1(0)$ and that $\det(\vec{v}(\ell_1), \vec{v}(\ell_0), \vec{\beta}_3) \neq 0$ (otherwise both sides would be zero). Since rotations in the $\vec{\beta}_3^\perp$ plane leave both sides unchanged, we may assume that $\vec{v}(\ell_1) = \pm\vec{\beta}_1$, $\vec{v}(\ell_0) = \pm\vec{\beta}_2$ (see Figure 4.5).

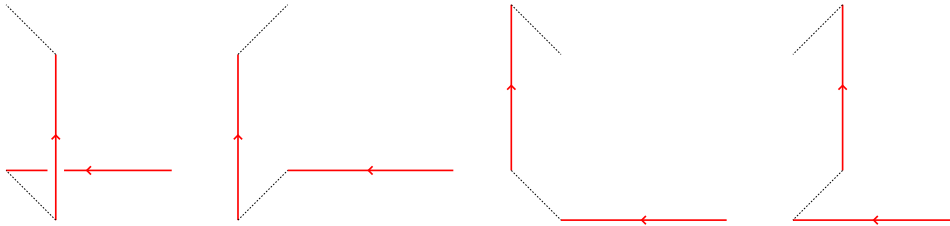


Figure 4.5: Illustrations of the four different projections $\Pi_{\pm\epsilon, \pm\epsilon}^\beta$ of two segments ℓ_0, ℓ_1 with $\tau^{\vec{\beta}_3}(\ell_0, \ell_1) = 1/4$. The dotted lines represent the projection of lines which are parallel to $\vec{\beta}_3$, in each of the four cases. Notice that the segments are involved in a crossing for exactly one of the projections, and this crossing is positive.

Our strategy is to show these two facts:

- (i) If $\tau_{i\epsilon, j\epsilon}^\beta(\ell_0, \ell_1) \neq 0$ for some $(i, j) \in \{-1, 1\}^2$, then $\tau^{\vec{\beta}_3}(\ell_0, \ell_1) \neq 0$.
- (ii) If $\tau^{\vec{\beta}_3}(\ell_0, \ell_1) \neq 0$, then there exists a unique $(i, j) \in \{-1, 1\}^2$ such that $\tau_{i\epsilon, j\epsilon}^\beta(\ell_0, \ell_1) \neq 0$.

Once we prove (i) and (ii), we get the result.

Let $c = \vec{\beta}_3 \cdot (\ell_1(0) - \ell_0(0))$, and consider the closed sets

$$A_{ij} = \left\{ \delta \in [0, \epsilon] \mid \exists s_0, s_1 \in [0, 1], \ell_1(s_1) - \ell_0(s_0) = c(\vec{\beta}_3 + i\delta\vec{\beta}_1 + j\delta\vec{\beta}_2) \right\}.$$

Notice that $\epsilon \in A_{ij}$ if and only if $\tau_{i\epsilon, j\epsilon}^\beta(\ell_0, \ell_1) \neq 0$, and $0 \in A_{ij}$ if and only if $\tau^{\vec{\beta}_3}(\ell_0, \ell_1) \neq 0$.

Suppose $\epsilon \in A_{ij}$ for some $(i, j) \in \{-1, 1\}^2$, and let $\delta = \min A_{ij}$. If $\delta > 0$, $\ell_1(s_1) - \ell_0(s_0) = c(\vec{\beta}_3 + i\delta\vec{\beta}_1 + j\delta\vec{\beta}_2)$ implies, by Lemma 4.7, that $s_0, s_1 \in (0, 1)$. Hence, there must exist $\delta' < \delta$ such that $\delta' \in A_{ij}$, a contradiction. Therefore, we must have $\delta = 0$, so that $0 \in A_{ij}$. We have proved (i).

Now suppose $\tau^{\vec{\beta}_3}(\ell_0, \ell_1) \neq 0$, that is, $\ell_1(k_1) - \ell_0(k_0) = c\vec{\beta}_3$ for some $k_0, k_1 \in [0, 1]$. Clearly $k_0, k_1 \in \{0, 1\}$; for simplicity, assume that $k_0 = k_1 = 0$ (the other cases are analogous). Now for any $s_0, s_1 \in [0, 1]$, $\ell_1(s_1) - \ell_0(s_0) = c\vec{\beta}_3 - s_0\vec{v}(\ell_0) + s_1\vec{v}(\ell_1)$. Thus, given $(i, j) \in \{-1, 1\}^2$,

$$\epsilon \in A_{ij} \Leftrightarrow \exists s_0, s_1 \in [0, 1] : \quad s_1(\vec{v}(\ell_1) \cdot \vec{\beta}_1) = i\epsilon c, \quad -s_0(\vec{v}(\ell_0) \cdot \vec{\beta}_2) = j\epsilon c,$$

which occurs if and only if $i\epsilon c(\vec{v}(\ell_1) \cdot \vec{\beta}_1) > 0$ and $j\epsilon c(\vec{v}(\ell_0) \cdot \vec{\beta}_2) < 0$: this determines a unique $(i, j) \in \{-1, 1\}^2$, so we have proved (ii). \square

If A_0 and A_1 are two sets of segments (curves are also seen as sets of segments), $\vec{u} \in \Phi, \beta \in \mathbf{B}$, define

$$T^{\vec{u}}(A_0, A_1) = \sum_{\substack{\ell_0 \in A_0 \\ \ell_1 \in A_1}} \tau^{\vec{u}}(\ell_0, \ell_1), \quad T_{a,b}^\beta(A_0, A_1) = \sum_{\substack{\ell_0 \in A_0 \\ \ell_1 \in A_1}} \tau_{a,b}^\beta(\ell_0, \ell_1).$$

For shortness, $T^{\vec{u}}(A) = T^{\vec{u}}(A, A)$ and $T_{a,b}^\beta(A) = T_{a,b}^\beta(A, A)$.

Consider two disjoint simple closed curves γ_0, γ_1 and a projection Π from \mathbb{R}^3 to some plane. Assume there exists finitely many crossings $(\Pi, \gamma_0, s_0, \gamma_1, s_1)$, all transversal. Recall from knot theory (see, e.g., [1, pp. 18–19]) that the *linking number* $\text{Link}(\gamma_0, \gamma_1)$ equals half the sum of the signs of all these crossings.

Lemma 4.9. *Let γ_0 and γ_1 be two disjoint simple closed curves of a region \mathcal{R} . Fix $\beta \in \mathbf{B}$, and let N denote the $\vec{\beta}_3$ -length of \mathcal{R} . Then*

- (i) If $0 < |a|, |b| < 1/N$, $T_{a,b}^{\vec{\beta}}(\gamma_0, \gamma_1) + T_{a,b}^{\vec{\beta}}(\gamma_1, \gamma_0) = 2 \text{Link}(\gamma_0, \gamma_1)$.
- (ii) $T^{\vec{\beta}_3}(\gamma_0, \gamma_1) + T^{\vec{\beta}_3}(\gamma_1, \gamma_0) = 2 \text{Link}(\gamma_0, \gamma_1)$.

Proof. By Lemma 4.7, the sum of signs of the crossings is given by $T_{a,b}^{\beta}(\gamma_0, \gamma_1) + T_{a,b}^{\beta}(\gamma_1, \gamma_0)$, which establishes (i). Also, (ii) follows from (i) and Lemma 4.8. \square

Lemma 4.10. *Let ℓ_0 and ℓ_1 be two segments of \mathcal{R} , and let $\vec{u} \in \mathbb{R}^3$ be a vector such that $\|\vec{u}\| < 1$. Then these two statements are equivalent:*

- (i) *There exist $s_0, s_1 \in [0, 1]$ such that $\ell_0(s_0) - \ell_1(s_1) = \vec{u}$.*
- (ii) *There exist $(i, j) \in \{0, 1\}^2$ and $a_0, a_1 \in (-1, 1)$ such that $\ell_0(i) = \ell_1(j)$ and $\vec{u} = a_0 \vec{v}(\ell_0) + a_1 \vec{v}(\ell_1)$ with $(-1)^i a_0 \geq 0$ and $(-1)^j a_1 \leq 0$.*

Proof. First, suppose (i) holds. If ℓ_0 and ℓ_1 are not adjacent, then $\text{dist}(\ell_0, \ell_1) \geq 1 > \|\vec{u}\|$, which is a contradiction. Thus, ℓ_0 and ℓ_1 are adjacent, and thus $\ell_0(i) = \ell_1(j)$ for some $(i, j) \in \{0, 1\}^2$: then

$$\begin{aligned} \vec{u} = \ell_0(s_0) - \ell_1(s_1) &= [\ell_0(i) + (s_0 - i)\vec{v}(\ell_0)] - [\ell_1(j) + (s_1 - j)\vec{v}(\ell_1)] \\ &= (s_0 - i)\vec{v}(\ell_0) + (j - s_1)\vec{v}(\ell_1), \end{aligned}$$

that is, $\vec{u} = a_0 \vec{v}(\ell_0) + a_1 \vec{v}(\ell_1)$ with $(i + a_0), (j - a_1) \in [0, 1]$, which implies that $(-1)^i a_0 \geq 0$ and $(-1)^j a_1 \leq 0$. Also, since $\|\vec{u}\| < 1$, we can take $a_0, a_1 \in (-1, 1)$.

For the other direction, suppose (ii) holds, so that $\ell_0(i) = \ell_1(j)$ for some $(i, j) \in \{0, 1\}^2$. Then setting $s_0 = (i + a_0)$ and $s_1 = (j - a_1)$, we have $s_0, s_1 \in [0, 1]$ and $\ell_0(i + a_0) - \ell_1(j - a_1) = [\ell_0(i) + a_0 \vec{v}(\ell_0)] - [\ell_1(j) - a_1 \vec{v}(\ell_1)] = \vec{u}$. \square

For a map $\gamma : [0, n] \rightarrow \mathbb{R}^3$ and a vector $\vec{u} \in \mathbb{R}^3$, let $(\gamma + \vec{u}) : [0, 1] \rightarrow \mathbb{R}^3 : s \mapsto \gamma(s) + \vec{u}$ denote the translation of γ by \vec{u} .

Lemma 4.11. *Let γ be a curve of \mathcal{R} , let $\beta \in \mathbf{B}$, and let $\vec{u} = a\vec{\beta}_1 + b\vec{\beta}_2 + c\vec{\beta}_3 \in \mathbb{R}^3$. If $\|\vec{u}\| < 1$ and $abc \neq 0$, then the curves γ and $\gamma + \vec{u}$ are disjoint.*

Notice that $\gamma + \vec{u}$ is not a curve of \mathcal{R} .

Proof. Suppose, by contradiction, that there exist $s_0, s_1 \in [0, n]$ (the domain of γ) such that $\gamma(s_0) = \gamma(s_1) + \vec{u}$. Let $k_0, k_1 \in \mathbb{Z}$ be such that $k_i \leq s_i \leq k_i + 1 \leq n$, and set $\tilde{s}_i = s_i - k_i$. Since γ is a curve of \mathcal{R} , $\ell_i = \gamma|_{[k_i, k_i+1]}$ are segments of \mathcal{R} such that $\ell_0(\tilde{s}_0) - \ell_1(\tilde{s}_1) = \gamma(s_0) - \gamma(s_1) = \vec{u}$. By Lemma 4.10, $\vec{u} = a_0 \vec{v}(\ell_0) + a_1 \vec{v}(\ell_1)$, which means that at least one of the three coordinates of \vec{u} is zero: this contradicts the fact that $abc \neq 0$. \square

Consider a simple closed curve $\gamma : I \rightarrow \mathbb{R}^3$ and a vector $\vec{u} \in \mathbb{R}^3$, $\vec{u} \neq 0$. Assume that there exists $\delta > 0$ such that for each $s \in (0, \delta]$, the curves γ and $\gamma + s\vec{u}$ are disjoint. Then define the *directional writhing number* in the direction \vec{u} by $\text{Wr}(\gamma, \vec{u}) = \text{Link}(\gamma, \gamma + \delta\vec{u})$ (see [9, §3]). Since Link is symmetric and invariant by translations, $\text{Wr}(\gamma, \vec{u}) = \text{Wr}(\gamma, -\vec{u})$.

Lemma 4.12. *Fix $\beta \in \mathbf{B}$, and let γ be a simple closed curve of \mathcal{R} . If $0 < |a|, |b| < 1/N$, where N is the $\vec{\beta}_3$ -length of \mathcal{R} , then $\text{Wr}(\gamma, \vec{\beta}_3 + a\vec{\beta}_1 + b\vec{\beta}_2) = T_{a,b}^\beta(\gamma)$.*

Proof. We would like to use the fact that the sums of the signs of the crossings of the orthogonal projection of a smooth curve in the direction of a vector \vec{u} equals its directional writhing number (in the direction of \vec{u}): this is essentially what we're trying to prove for our curve, except that $\Pi_{a,b}^\beta$ is not the orthogonal projection and that γ is not a smooth curve. However, these difficulties can be avoided, as the following paragraphs show.

The orthogonality of the projection makes no real difference, because the orthogonal projection in the direction of $(a, b, 1)$ has the same kernel as $\Pi_{a,b}^\beta$, so the crossings occur in the same positions (and clearly have the same signs). Therefore, by Lemma 4.7, $T_{a,b}^\beta(\gamma)$ equals the sums of the signs of the crossings of the aforementioned orthogonal projection.

For the smoothness of the curve, there is a finite number of points where γ is not smooth: precisely, the set of $k \in \mathbb{Z}$ such that the two segments of γ that intersect at $\gamma(k)$ are not parallel. To simplify notation, let $[0, n]$ be the domain of γ , and for $k = 0, 1, \dots, n-1$ let ℓ_k be the segment of γ such that $\ell_k(0) = \gamma(k)$ (notice that $\ell_k(1) = \gamma(k+1)$). It is also convenient to set $\ell_{-1} := \ell_{n-1}$, so that $\ell_{-1}(1) = \ell_{n-1}(1) = \gamma(n) = \gamma(0)$.

Recall from Lemma 4.7 that every crossing in the projections occur in the interiors of the segments: since the number of segments is finite, we can pick $0 < \epsilon < 1/2$ sufficiently small so that $\Pi_{a,b}^\beta(\gamma(U_\epsilon))$ contains no crossings, where $U_\epsilon = [0, n] \cap \left(\bigcup_{k \in \mathbb{Z}} [k - \epsilon, k + \epsilon]\right)$.

Let $\phi_1 : \mathbb{R} \rightarrow \mathbb{R}$ be a nondecreasing C^∞ function such that $\phi_1(t) = 0$ whenever $t \leq -\epsilon$ and $\phi_1(t) = t$ whenever $t \geq \epsilon$. Let $\phi_0(t) = t + \epsilon - \phi_1(t)$. Consider the smooth simple closed curve of \mathbb{R}^3 , $\tilde{\gamma} : [0, n] \rightarrow \mathbb{R}^3$, given by

$$\tilde{\gamma}(s) = \begin{cases} \gamma(k - \epsilon) + \phi_0(s - k)\vec{v}(\ell_{k-1}) + \phi_1(s - k)\vec{v}(\ell_k), & s \in (k - \epsilon, k + \epsilon); \\ \gamma(s), & s \notin U_\epsilon. \end{cases}$$

To simplify notation, write $\vec{w} = \vec{\beta}_3 + a\vec{\beta}_1 + b\vec{\beta}_2$ and fix $\delta < 1/\sqrt{1+a^2+b^2}$, so that $\|\delta\vec{w}\| < 1$. By Lemma 4.11, γ and $\gamma + s\vec{w}$ are disjoint whenever $s \in (0, \delta]$.

Clearly, the sums of the signs of the crossings in the orthogonal projection of $\tilde{\gamma}$ equals that of γ ; moreover, $\text{Link}(\tilde{\gamma}, \tilde{\gamma} + s\vec{w}) = \text{Link}(\gamma, \gamma + s\vec{w})$ for sufficiently small $s > 0$. Since $\tilde{\gamma}$ is smooth, $T_{a,b}^\beta(\gamma) = \text{Wr}(\tilde{\gamma}, \vec{w}) = \text{Link}(\gamma, \gamma + s\vec{w}) = \text{Wr}(\gamma, \vec{w})$. \square

The following rather technical Lemma will be used in the proof of Lemma 4.14:

Lemma 4.13. *Let $\beta \in \mathbf{B}$, and let ℓ_0 and ℓ_1 be two segments of a region \mathcal{R} whose $\vec{\beta}_3$ -length is N . Let $\vec{u} = b\vec{\beta}_2 + c\vec{\beta}_3$ with $bc \neq 0$ and $b^2 + c^2 < 1$. Let $0 < \epsilon < \min\left(\frac{|b|}{N+|c|}, \frac{1-|b|}{N+|c|}\right)$.*

If, for some $s_0, s_1 \in [0, 1]$, $\Pi_{\epsilon, \epsilon}^\beta(\ell_0(s_0) - \ell_1(s_1) - \vec{u}) = 0$, then ℓ_0 and ℓ_1 are not parallel, and $s_0, s_1 \in (0, 1)$.

Proof. Suppose $\Pi_{\epsilon, \epsilon}^\beta(\ell_0(s_0) - \ell_1(s_1) - \vec{u}) = 0$. Let $\alpha_i = \vec{\beta}_i \cdot (\ell_0(s_0) - \ell_1(s_1))$, $i = 1, 2, 3$, so that $\alpha_1 = \epsilon(\alpha_3 - c)$, $\alpha_2 - b = \epsilon(\alpha_3 - c)$.

Suppose, by contradiction, that at least one of these things occurs:

- (i) ℓ_0 and ℓ_1 are parallel;
- (ii) $s_0 \in \{0, 1\}$ or $s_1 \in \{0, 1\}$.

We claim that at least two of the three α_i 's are integers. To see this, suppose first (i), so that $\vec{v}(\ell_0), \vec{v}(\ell_1) \parallel \vec{\beta}_i$, so that for $j \neq i$, $\alpha_j = \vec{\beta}_j \cdot (\ell_0(s_0) - \ell_1(s_1)) \in \mathbb{Z}$. On the other hand, if (ii) holds, say $s_1 \in \{0, 1\}$, then $\ell_1(s_1) \in \mathbb{Z}^\#$ and $\vec{v}(\ell_0) \parallel \vec{\beta}_i$, so that, again, for $j \neq i$, $\alpha_j \in \mathbb{Z}$.

We claim that $\alpha_2 \notin \mathbb{Z}$. In fact, if $\alpha_2 \in \mathbb{Z}$ then we would have $|\alpha_2| = |b + \epsilon(\alpha_3 - c)| < |b| + \frac{1-|b|}{N+|c|}(N+|c|) = 1$, so that $\alpha_2 = 0$ and $|b| = \epsilon|\alpha_3 - c| < \frac{|b|}{N+|c|}(N+|c|)$, which is a contradiction.

Therefore, we must have $\alpha_1, \alpha_3 \in \mathbb{Z}$. Then $|\alpha_1| = |\epsilon(\alpha_3 - c)| < |b| < 1$, so $\alpha_1 = 0 = \alpha_3 - c$. Thus $c = \alpha_3 \in \mathbb{Z}$ but $|c| \in (0, 1)$, which is a contradiction. \square

The following definition is specific for Lemmas 4.14 and 4.18. Let $\gamma : [0, n] \rightarrow \mathbb{R}^3$ be a simple closed curve of a region \mathcal{R} and $\beta \in \mathbf{B}$. For $k = 0, 1, \dots, n-1$, set $\ell_k = \gamma|_{[k, k+1]}$, and set also $\ell_n = \ell_0$. Finally, we define

$$\eta_\gamma^\beta(k) = \begin{cases} 1, & (\vec{v}(\ell_k), \vec{v}(\ell_{k+1})) = (\vec{\beta}_2, \vec{\beta}_3) \text{ or } (-\vec{\beta}_3, -\vec{\beta}_2); \\ -1, & (\vec{v}(\ell_k), \vec{v}(\ell_{k+1})) = (-\vec{\beta}_2, -\vec{\beta}_3) \text{ or } (\vec{\beta}_3, \vec{\beta}_2); \\ 0, & \text{otherwise.} \end{cases}$$

Lemma 4.14. Let $\gamma : [0, n] \rightarrow \mathbb{R}^3$ be a simple closed curve of a region \mathcal{R} . For $k = 0, 1, \dots, n-1$, set $\ell_k = \gamma|_{[k, k+1]}$, and set also $\ell_n = \ell_0$; for shortness, write $\vec{v}_k = \vec{v}(\ell_k)$. Then if $\beta \in \mathbf{B}$ and $a, b, c > 0$, then

$$\text{Wr}(\gamma, a\vec{\beta}_1 + b\vec{\beta}_2 + c\vec{\beta}_3) - \text{Wr}(\gamma, -a\vec{\beta}_1 + b\vec{\beta}_2 + c\vec{\beta}_3) = \sum_{0 \leq k < n} \eta_\gamma^\beta(k).$$

Proof. We may assume that $a^2 + b^2 + c^2 < 1$. Let $0 < \epsilon < \min\left(\frac{|b|}{N+|c|}, \frac{1-|b|}{N+|c|}\right)$, and set $\vec{u}(s) = s\vec{\beta}_1 + b\vec{\beta}_2 + c\vec{\beta}_3$. By Lemma 4.11, $\text{Link}(\gamma, \gamma + \vec{u}(a))$ depends only on the signs of a, b and c . Therefore, we may, without loss of generality, assume that $a > 0$ is sufficiently small such that for every $s \in [-a, a]$ and every $i, j \in \{0, 1, \dots, n\}$,

$$\Pi_{\epsilon, \epsilon}^\beta(\ell_i) \cap \Pi_{\epsilon, \epsilon}^\beta(\ell_j + \vec{u}(s)) \neq \emptyset \Leftrightarrow \Pi_{\epsilon, \epsilon}^\beta(\ell_i) \cap \Pi_{\epsilon, \epsilon}^\beta(\ell_j + \vec{u}(0)) \neq \emptyset$$

(this is possible by Lemma 4.13). Therefore, clearly $\text{Link}(\gamma, \gamma + \vec{u}(a)) - \text{Link}(\gamma, \gamma + \vec{u}(-a))$ equals the number of pairs of segments ℓ_i, ℓ_j such that $\Pi_{\epsilon, \epsilon}^\beta(\ell_i) \cap \Pi_{\epsilon, \epsilon}^\beta(\ell_j + \vec{u}(s)) \neq \emptyset$ for every $s \in [-a, a]$ and such that the crossing changes its sign as s goes from $-a$ to a . Now a crossing may only change its sign if $\ell_i \cap (\ell_j + \vec{u}(s)) \neq \emptyset$ for some s : by Lemma 4.11, this can only happen if $s = 0$.

By Lemma 4.10, $\ell_i \cap (\ell_j + \vec{u}(0)) \neq \emptyset$ if and only if for some $m_i, m_j \in \{0, 1\}$, $\ell_i(m_i) = \ell_j(m_j)$ and $\vec{u}(0) = b\vec{\beta}_2 + c\vec{\beta}_3 = a_i\vec{v}(\ell_i) + a_j\vec{v}(\ell_j)$, with $(-1)^{m_i}a_i \geq 0$, $(-1)^{m_j}a_j \leq 0$. Since ℓ_i and ℓ_j are segments of the simple curve γ , they can only be adjacent if, for some k , $\{\ell_i, \ell_j\} = \{\ell_k, \ell_{k+1}\}$. Now, $\ell_{k+1}(0) = \ell_k(1)$, so that $(0, b, c) = a_0\vec{v}(\ell_{k+1}) - a_1\vec{v}(\ell_k)$ with either $a_0, a_1 \geq 0$ or $a_0, a_1 \leq 0$ (depending on which is ℓ_i and which is ℓ_j). Since $b, c > 0$, this implies that $\{\vec{v}(\ell_k), \vec{v}(\ell_{k+1})\} = \{\vec{\beta}_2, \vec{\beta}_3\}$ or $\{-\vec{\beta}_2, -\vec{\beta}_3\}$ and, therefore, $\eta_\gamma^\beta(k) = \pm 1$.

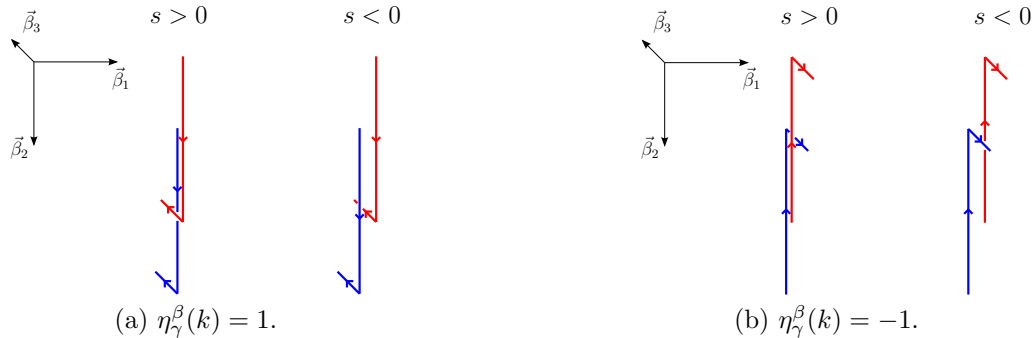


Figure 4.6: Illustration of the crossings $\Pi_{\epsilon, \epsilon}^\beta(\gamma) \cap \Pi_{\epsilon, \epsilon}^\beta(\gamma + s\vec{\beta}_1 + b\vec{\beta}_2 + c\vec{\beta}_3)$ for $s \in [-a, a]$. Notice that simultaneously switching the orientations of both segments does not change the signs of the crossings.

We now analyze each of the four possible cases for $(\vec{v}(\ell_k), \vec{v}(\ell_{k+1}))$ (as an ordered pair). When $(\vec{v}(\ell_k), \vec{v}(\ell_{k+1})) = (\vec{\beta}_2, \vec{\beta}_3)$ or $(-\vec{\beta}_3, -\vec{\beta}_2)$, so that $\eta_\gamma^\beta(k) = 1$, we see a situation as illustrated in Figure 4.6a (perhaps with both orientations reversed): when $s > 0$, we have a positive crossing; when $s < 0$, we have a negative crossing. Figure 4.6b illustrates (up to orientation) the case $(\vec{v}(\ell_k), \vec{v}(\ell_{k+1})) = (-\vec{\beta}_2, -\vec{\beta}_3)$ or $(\vec{\beta}_3, \vec{\beta}_2)$ ($\eta_\gamma^\beta(k) = -1$): negative crossing for $s > 0$, and positive crossing for $s < 0$. These observations yield the result. \square

4.3

Writhe formula for the twist

Now that the groundwork is done, we set out to obtain a new formula for the twist of pseudocylinders of even depth (we work with pseudocylinders because the hypothesis of simple connectivity will not play any role). Pseudocylinders of even depth have the advantage of always admitting a tiling such that all dimers are parallel to its axis: for a \vec{w} -pseudocylinder \mathcal{R} ($\vec{w} \in \Delta$) with even depth, let $t_{\vec{w}} = t_{\vec{w}}(\mathcal{R})$ denote the tiling such that every dimer is parallel to \vec{w} (see Figure 4.7). Not only does this tiling trivially satisfy $T^{\vec{w}}(t_{\vec{w}}) = 0$, but also for any segment ℓ of \mathcal{R} and any dimer $\ell_0 \in t_{\vec{w}}$ we have $\tau^{\vec{w}}(\ell_0, \ell) = \tau^{\vec{w}}(\ell, \ell_0) = 0$. This allows for a direct interpretation of the twist via a set of curves, which, in particular, allows us to show that it is an integer.

Lemma 4.15. *Given $\vec{w} \in \Delta$, let t be a tiling of a \vec{w} -pseudocylinder of even depth \mathcal{R} , and let $t_{\vec{w}} = t_{\vec{w}}(\mathcal{R})$. If $\Gamma^*(t, t_{\vec{w}}) = \{\gamma_i \mid 1 \leq i \leq m\}$, then*

$$T^{\vec{w}}(t) = \sum_{1 \leq i \leq m} T^{\vec{w}}(\gamma_i) + 2 \sum_{1 \leq i < j \leq m} \text{Link}(\gamma_i, \gamma_j).$$

Proof. Clearly,

$$T^{\vec{w}}(t) = T^{\vec{w}}(t \sqcup (-t_{\vec{w}})) = \sum_{i,j} T^{\vec{w}}(\gamma_i, \gamma_j) = \sum_i T^{\vec{w}}(\gamma_i) + 2 \sum_{i < j} \text{Link}(\gamma_i, \gamma_j),$$

the last equality holding by Lemma 4.9. \square

For Lemmas 4.16 and 4.17, assume $\vec{w} \in \Delta$, t is a tiling of a \vec{w} -pseudocylinder with even depth \mathcal{R} , and $t_{\vec{w}} = t_{\vec{w}}(\mathcal{R})$.

Lemma 4.16. *Fix $\beta \in \mathbf{B}$ such that $\vec{\beta}_3 = \vec{w}$. If γ is a curve of $\Gamma^*(t, t_{\vec{w}})$ and $a^2 + b^2 + c^2 < 1$ and $ab \neq 0$, then $(\gamma + a\vec{\beta}_1 + b\vec{\beta}_2 + c\vec{\beta}_3) \cap \gamma = \emptyset$.*

Notice that the case $c \neq 0$ follows from Lemma 4.11.

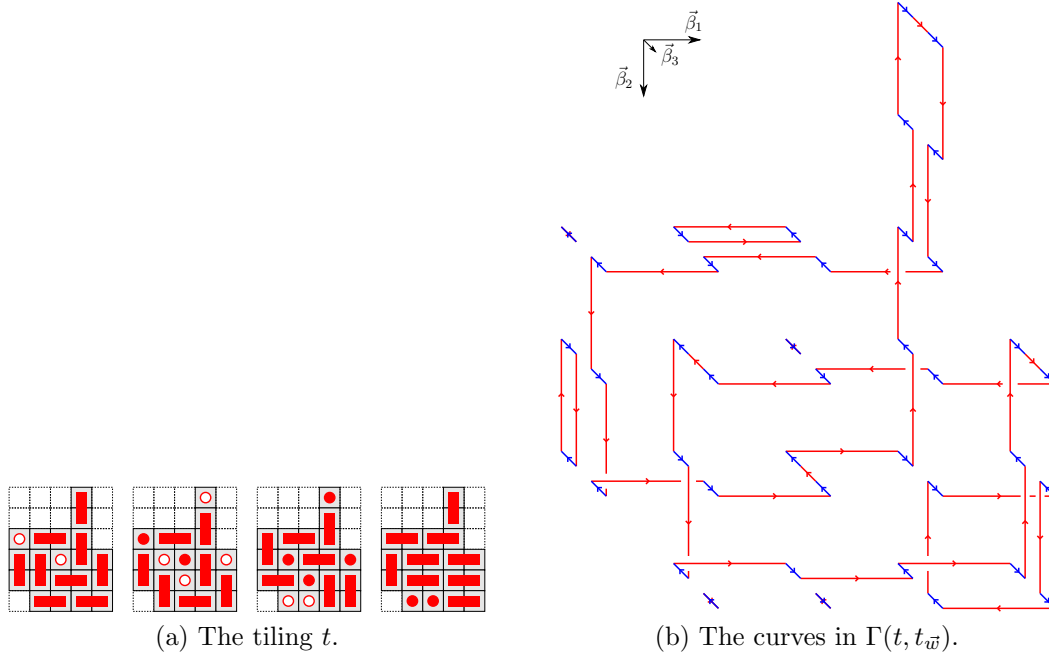


Figure 4.7: A tiling t of a \vec{w} -cylinder with depth 4, and $\Gamma(t, t_{\vec{w}})$, where $t_{\vec{w}}$ is the tiling such that every dimer is parallel to \vec{w} . The dimers of t are the red segments, and the blue segments are the ones in $(-t_{\vec{w}})$. We chose a basis $\beta \in \mathbf{B}$ with $\vec{w} = \vec{\beta}_3$; \vec{w} points “towards the paper”. $\Gamma(t, t_{\vec{w}})$ consists of nine curves, four of which are trivial; the five nontrivial curves form $\Gamma^*(t, t_{\vec{w}})$.

Proof. Let $\vec{u} = a\vec{\beta}_1 + b\vec{\beta}_2 + c\vec{\beta}_3$. Suppose, by contradiction, that γ and $\gamma + \vec{u}$ are not disjoint, and let ℓ_0 and ℓ_1 be two segments of γ such that $\ell_0(s_0) = \ell_1(s_1) + \vec{u}$ for some $s_0, s_1 \in [0, 1]$. By Lemma 4.10, ℓ_0 and ℓ_1 must be adjacent, so that at least one of these two segments is in $(-t_{\vec{w}})$, hence parallel to \vec{u} . Lemma 4.10 also implies that $\vec{u} = a\vec{\beta}_1 + b\vec{\beta}_2 + c\vec{\beta}_3 = a_0\vec{v}(\ell_0) + a_1\vec{v}(\ell_1)$. Since at least one of $\vec{v}(\ell_0), \vec{v}(\ell_1)$ is parallel to $\vec{w} = \vec{\beta}_3$, it follows that $a = 0$ or $b = 0$, which contradicts the hypothesis. \square

By Lemma 4.16, if $\gamma \in \Gamma^*(t, t_{\vec{w}})$, $\text{Wr}(\gamma, a\vec{\beta}_1 + b\vec{\beta}_2 + c\vec{\beta}_3)$ is defined whenever $ab \neq 0$. Set

$$\text{Wr}^+(\gamma) = \text{Wr}(\gamma, \vec{\beta}_1 + \vec{\beta}_2), \quad \text{Wr}^-(\gamma) = \text{Wr}(\gamma, \vec{\beta}_1 - \vec{\beta}_2).$$

Clearly,

$$\text{Wr}(\gamma, a\vec{\beta}_1 + b\vec{\beta}_2 + c\vec{\beta}_3) = \begin{cases} \text{Wr}^+(\gamma), & ab > 0; \\ \text{Wr}^-(\gamma), & ab < 0. \end{cases} \quad (4-2)$$

Lemma 4.17. *If γ is a curve of $\Gamma^*(t, t_{\vec{w}})$, then*

$$T^{\vec{w}}(\gamma) = \frac{\text{Wr}^+(\gamma) + \text{Wr}^-(\gamma)}{2}.$$

Proof. Fix $\beta \in \mathbf{B}$ with $\vec{\beta}_3 = \vec{w}$, and let N denote the \vec{w} -length of the pseudocylinder (which is equal to its depth). By Lemmas 4.8 and 4.12, given $0 < \epsilon < 1/N$,

$$T^{\vec{w}}(\gamma) = \frac{1}{4} \sum_{i,j \in \{-1,1\}} T_{i\epsilon, j\epsilon}^{\beta}(\gamma) = \frac{1}{4} \sum_{i,j \in \{-1,1\}} \text{Wr}(\gamma, i\epsilon\vec{\beta}_1 + j\epsilon\vec{\beta}_2 + \vec{\beta}_3);$$

Equation (4-2) completes the proof. \square

Lemma 4.18. *Let $\vec{w} \in \Delta$, and let t be a tiling of a \vec{w} -pseudocylinder with even depth. If γ is a curve of $\Gamma^*(t, t_{\vec{w}})$, then $(\text{Wr}^+(\gamma) + \text{Wr}^-(\gamma))/2 \in \mathbb{Z}$.*

Proof. Pick $\beta \in \mathbf{B}$ with $\vec{\beta}_3 = \vec{w}$. Assume without loss of generality that $\mathcal{R} = \mathcal{D} + [0, 2N]\vec{\beta}_3$, $\mathcal{D} \subset \vec{\beta}_3^\perp$. If $\gamma : [0, n] \rightarrow \mathbb{R}^3$, set $\ell_k = \gamma|_{[k, k+1]}$ for $k = 0, 1, \dots, n-1$, and set $\ell_n = \ell_0$.

By definition and using Lemma 4.14, $\text{Wr}^+(\gamma) - \text{Wr}^-(\gamma) = \sum_k \eta_\gamma^\beta(k)$. We need to look at k such that $\eta_\gamma^\beta(k) \neq 0$, i.e., $\{\vec{v}(\ell_k), \vec{v}(\ell_{k+1})\} = \{\vec{\beta}_2, \vec{\beta}_3\}$ or $\{-\vec{\beta}_2, -\vec{\beta}_3\}$. Since every segment of $-t_{\vec{w}}$ is parallel to $\vec{\beta}_3$, we need to look at every segment of t that is parallel to $\vec{\beta}_2$.

For each segment ℓ_k of t with $\vec{v}(\ell_k) = \pm\vec{\beta}_2$, let $z_k^\sharp = \vec{\beta}_3 \cdot \ell_k(0)$, so that $z_k \in \mathbb{Z}$. If z_k is odd, then, by definition of $t_{\vec{w}}$, $\vec{v}(\ell_{k-1}) = \vec{\beta}_3 = -\vec{v}(\ell_{k+1})$, so that either $(\vec{v}(\ell_{k-1}), \vec{v}(\ell_k)) = (\vec{\beta}_3, \vec{\beta}_2)$ or $(\vec{v}(\ell_k), \vec{v}(\ell_{k+1})) = (-\vec{\beta}_2, -\vec{\beta}_3)$. Making a similar analysis for z_k even, we see that $\eta_\gamma^\beta(k-1) + \eta_\gamma^\beta(k) = (-1)^{z_k}$. Working with congruence modulo 2,

$$\text{Wr}^+(\gamma) + \text{Wr}^-(\gamma) \equiv \text{Wr}^+(\gamma) - \text{Wr}^-(\gamma) = \sum_{\vec{v}(\ell_k) = \pm\vec{\beta}_2} (-1)^{z_k} \equiv \sum_k (\vec{v}(\ell_k) \cdot \vec{\beta}_2) = 0,$$

which completes the proof. \square

Proposition 4.19. *If $\vec{w} \in \Delta$, \mathcal{R} is a \vec{w} -pseudocylinder with even depth, t is a tiling of \mathcal{R} , $t_{\vec{w}} = t_{\vec{w}}(\mathcal{R})$ and $\Gamma^*(t, t_{\vec{w}}) = \{\gamma_i \mid 1 \leq i \leq m\}$, then*

$$T^{\vec{w}}(t) = \sum_{1 \leq i \leq m} \frac{\text{Wr}^+(\gamma_i) + \text{Wr}^-(\gamma_i)}{2} + 2 \sum_{1 \leq i < j \leq m} \text{Link}(\gamma_i, \gamma_j) \in \mathbb{Z}.$$

Proof. Follows directly from Lemmas 4.15, 4.17 and 4.18. \square

4.4

Different directions of projection

Our goal for this section is to prove Proposition 4.3, that is, that all pretwists coincide for a cylinder.

Lemma 4.20. *Let $\vec{w} \in \Delta$, and let \mathcal{R} be a \vec{w} -pseudocylinder with even depth. Let t be a tiling of \mathcal{R} , and let $t_{\vec{w}}$ be the tiling such that every dimer is parallel to \vec{w} . If $\vec{u} \in \Phi$, then $T^{\vec{u}}(t \sqcup (-t_{\vec{w}})) = T^{\vec{w}}(t)$.*

Proof. Suppose $\Gamma^*(t, t_{\vec{w}}) = \{\gamma_i \mid 1 \leq i \leq m\}$. Clearly,

$$T^{\vec{u}}(t \sqcup (-t_{\vec{w}})) = \sum_{i,j} T^{\vec{u}}(\gamma_i, \gamma_j) = \sum_i T^{\vec{u}}(\gamma_i) + 2 \sum_{i < j} \text{Link}(\gamma_i, \gamma_j).$$

Let L be the \vec{u} -length of \mathcal{R} and $0 < \epsilon < 1/L$. Let $\beta \in \mathbf{B}$ such that $\vec{\beta}_3 = \vec{u}$. Then, by Lemmas 4.8 and 4.12,

$$T^{\vec{u}}(\gamma_i) = \frac{1}{4} \sum_{k,l \in \{-1,1\}} T_{k\epsilon, l\epsilon}^{\beta}(\gamma_i) = \frac{1}{4} \sum_{k,l \in \{-1,1\}} \text{Wr}(\gamma_i, k\epsilon\vec{\beta}_1 + l\epsilon\vec{\beta}_2 + \vec{\beta}_3).$$

By Equation (4-2) and Proposition 4.19,

$$T^{\vec{u}}(t \sqcup (-t_{\vec{w}})) = \sum_i \frac{\text{Wr}^+(\gamma_i) + \text{Wr}^-(\gamma_i)}{2} + 2 \sum_{i < j} \text{Link}(\gamma_i, \gamma_j) = T^{\vec{w}}(t).$$

□

Lemma 4.21. *Let $\mathcal{B} = [0, L] \times [0, M] \times [0, N]$ be a box that has at least one even dimension, and let t be a tiling of \mathcal{B} . Then $T^{\vec{i}}(t) = T^{\vec{j}}(t) = T^{\vec{k}}(t)$.*

Proof. By rotating, we may assume that N is even, so that \mathcal{B} is a \vec{k} -cylinder with even depth; let $\vec{u} \in \Phi$, $\vec{u} \perp \vec{k}$. We want to show that $T^{\vec{u}}(t) = T^{\vec{k}}(t)$.

By Lemma 4.20, $T^{\vec{k}}(t) = T^{\vec{u}}(t \sqcup (-t_{\vec{k}}))$. Now,

$$T^{\vec{u}}(t \sqcup (-t_{\vec{k}})) = T^{\vec{u}}(t) + T^{\vec{u}}(-t_{\vec{k}}) + T^{\vec{u}}(t, -t_{\vec{k}}) + T^{\vec{u}}(-t_{\vec{k}}, t).$$

$T^{\vec{u}}(-t_{\vec{k}}) = 0$ because all segments of $(-t_{\vec{k}})$ are parallel. It remains to show that $T^{\vec{u}}(t, -t_{\vec{k}}) = T^{\vec{u}}(-t_{\vec{k}}, t) = 0$, which yields the result.

Let $\vec{w} = \vec{u} \times \vec{k}$. Given $\ell_0 \in t$, we now want to show that $\sum_{\ell \in t_{\vec{k}}} \tau^{\vec{u}}(\ell, \ell_0) = \sum_{\ell \in t_{\vec{k}}} \tau^{\vec{u}}(\ell_0, \ell) = 0$. This is obvious if ℓ_0 is not parallel to \vec{w} . Otherwise, effects cancel out, as illustrated in Figure 4.8. □

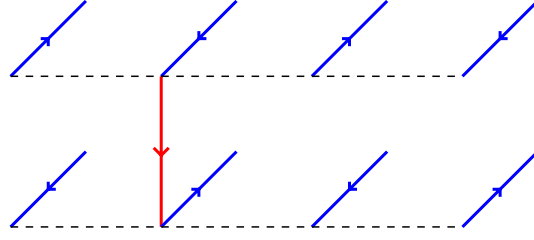


Figure 4.8: A dimer ℓ_0 parallel to \vec{w} , portrayed in red, and the pairs of segments (blue) of $t_{\vec{k}}$ affected by it: \vec{u} -effects cancel.

If $Q \subset \pi$ is a basic square and $\vec{w} \in \Delta$ is a normal vector for π , define the color of Q to be the same as the color of the basic cube $Q - [0, 1]\vec{w}$; and

$$\text{color}(Q) = \begin{cases} 1, & \text{if } Q \text{ is black;} \\ -1, & \text{if } Q \text{ is white.} \end{cases}$$

Recall the definition of \vec{u} -shade from Section 4.1. If A is a set of segments or a set of dominoes, $\vec{u} \in \Phi$ and Q is a basic square with normal $\vec{w} \in \Delta$, we set

$$S(A, \vec{u}, Q, n) = \{\ell \in A \mid \ell \cap \mathcal{S}^{\vec{u}}(Q + [0, n]\vec{w}) \neq \emptyset\}.$$

Lemma 4.22. *Let \mathcal{R} be a \vec{w} -cylinder ($\vec{w} \in \Delta$) with base $\mathcal{D} \subset \pi$ and even depth N . Let $Q \subset \pi$ be a basic square, $Q \not\subset \mathcal{D}$, let t be a tiling of \mathcal{R} and let $\vec{u} \in \Phi$. Then*

$$\sum_{d \in S(t, \vec{u}, Q, N)} \det(\vec{v}(d), \vec{w}, \vec{u}) = 0.$$

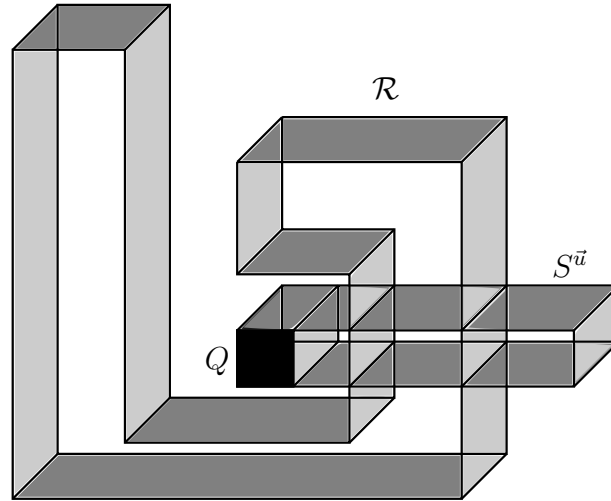


Figure 4.9: A cylinder \mathcal{R} with base $\mathcal{D} \subset \pi$ and depth N , a basic square $Q \subset \pi$, $Q \not\subset \mathcal{D}$ and the shade $\mathcal{S}^{\vec{u}}(Q + [0, N]\vec{w})$.

Proof. The reader may want to follow by looking at Figure 4.9. Let $t_{\vec{w}} = t_{\vec{w}}(\mathcal{R})$, $S_t = S(t, \vec{u}, Q, N)$, and for each $\gamma \in \Gamma^*(t, t_{\vec{w}})$, let S_γ denote $S(\gamma, \vec{u}, Q, N)$.

Clearly,

$$\sum_{d \in S_t} \det(\vec{v}(d), \vec{w}, \vec{u}) = \sum_{\substack{\gamma \in \Gamma^*(t, t_{\vec{w}}) \\ \ell \in S_\gamma}} \det(\vec{v}(\ell), \vec{w}, \vec{u}).$$

Let p_Q be the center of the square Q , and let Π denote the orthogonal projection on π . For each $\gamma \in \Gamma^*(t, t_{\vec{w}})$, $\Pi \circ \gamma$ is a polygonal curve, so that the winding number of γ around p_Q equals (see, e.g., [2] for an algorithmic discussion of winding numbers)

$$\begin{aligned} \text{wind}(\Pi \circ \gamma, p_Q) &= \frac{1}{2} (\#\{\ell \in S_\gamma \mid \vec{v}(\ell) = \vec{w} \times \vec{u}\} - \#\{\ell \in S_\gamma \mid \vec{v}(\ell) = -\vec{w} \times \vec{u}\}) \\ &= \frac{1}{2} \sum_{\ell \in S_\gamma} \det(\vec{v}(\ell), \vec{w}, \vec{u}). \end{aligned}$$

But $\text{wind}(\Pi \circ \gamma, p_Q) = 0$ ($p_Q \notin \mathcal{D}$ and \mathcal{D} is simply connected), so we get the result. \square

Remark 4.23. *The fact that*

$$\sum_{d \in S(t, \vec{u}, Q, N)} \det(\vec{v}(d), \vec{w}, \vec{u}) = \sum_{\gamma \in \Gamma^*(t, t_{\vec{w}})} \text{wind}(\Pi \circ \gamma, p_Q)$$

(using the notation in the proof of Lemma 4.22) also holds in pseudocylinders, as the hypothesis of simply connected is only needed in the last step of the proof. In fact, if we define the flux $\phi(t) = \sum_{Q, \gamma} \text{color}(Q) \text{wind}(\Pi \circ \gamma, p_Q)$ (Q runs through all the basic squares not contained in \mathcal{D} , γ runs through all the curves in $\Gamma^*(t, t_{\vec{w}})$), then a modification in the proof of Proposition 4.24 yields that $T^{\vec{i}}(t) = T^{\vec{j}}(t) = T^{\vec{k}}(t) + \phi(t)$ (in particular, since $\phi(t) \in \mathbb{Z}$, the three pretwists are integers).

Proposition 4.24. *Let $N \in \mathbb{N}$ be even, and suppose \mathcal{R} is a cylinder with depth N . If t is a tiling of \mathcal{R} , then $T^{\vec{i}}(t) = T^{\vec{j}}(t) = T^{\vec{k}}(t) \in \mathbb{Z}$.*

Proof. Suppose $\mathcal{R} = \mathcal{D} + [0, N]\vec{w}$, where $\mathcal{D} \subset \pi$ is simply connected and $\vec{w} \in \Delta$ is the axis of the cylinder. Let $\mathcal{A} \subset \pi$ be a rectangle with vertices in \mathbb{Z}^3 such that $\mathcal{D} \subset \mathcal{A}$: this implies that the box $\mathcal{B} = \mathcal{A} + [0, N]\vec{w} \supset \mathcal{R}$. Let $\vec{u} \in \Phi$, $\vec{u} \perp \vec{w}$. We want to show that $T^{\vec{u}}(t) = T^{\vec{w}}(t)$.

Let t be a tiling of \mathcal{R} , and let t_* be the tiling of $\mathcal{B} \setminus \mathcal{R}$ such that every dimer is parallel to \vec{w} . Applying Lemma 4.21 to the box \mathcal{B} , we see that $T^{\vec{u}}(t \sqcup t_*) = T^{\vec{w}}(t)$: it remains to show that $T^{\vec{u}}(t \sqcup t_*) - T^{\vec{w}}(t) = 0$.

Let $t_{\vec{w}}$ be the tiling of \mathcal{R} such that every domino is parallel to \vec{w} , and let $Q \subset \pi$ be a basic square such that $\text{int}(Q) \subset \mathcal{A} \setminus \mathcal{D}$. Let t_Q be the set of $N/2$

dominoes of t_* contained in $Q + [0, N]\vec{w}$: we have

$$T^{\vec{u}}(t \sqcup t_*) - T^{\vec{u}}(t) = T^{\vec{u}}(t, t_*) + T^{\vec{u}}(t_*, t) = \sum_{\text{int}(Q) \subset \mathcal{A} \setminus \mathcal{D}} T^{\vec{u}}(t_Q, t) + T^{\vec{u}}(t, t_Q).$$

Notice that, for every domino $d \in t_Q$, $\vec{v}(d) = \text{color}(Q)\vec{w}$. Moreover, the dominoes in $S_{t, \vec{u}} = S(t, \vec{u}, Q, N)$ are precisely the ones that intersect the \vec{u} -shade of at least one domino of t_Q , so that

$$T^{\vec{u}}(t_Q, t) = \frac{1}{4} \sum_{d \in S_{t, \vec{u}}} \det(\vec{v}(d), \text{color}(Q)\vec{w}, \vec{u}) = \frac{\text{color}(Q)}{4} \sum_{d \in S_{t, \vec{u}}} \det(\vec{v}(d), \vec{w}, \vec{u}),$$

which equals 0 by Lemma 4.22. Analogously (the first equality below uses Lemma 4.1),

$$T^{\vec{u}}(t, t_Q) = T^{-\vec{u}}(t_Q, t) = \frac{\text{color}(Q)}{4} \sum_{d \in S(t, -\vec{u}, Q, n)} \det(\vec{v}(d), \vec{w}, -\vec{u}) = 0.$$

Since $T^{\vec{w}}(t) \in \mathbb{Z}$ (by Proposition 4.19), we have completed the proof. \square

Lemma 4.25. *Let $N \in \mathbb{Z}$ be odd, and let \mathcal{R} be a cylinder with depth N that admits a tiling t . Then $T^{\vec{i}}(t) = T^{\vec{j}}(t) = T^{\vec{k}}(t) \in \frac{1}{2}\mathbb{Z}$.*

In fact, we prove in Proposition 4.31 that $T^{\vec{i}}(t) = T^{\vec{j}}(t) = T^{\vec{k}}(t) \in \mathbb{Z}$, but for our proof this first step is needed. Also, it is not clear when a cylinder with odd depth N is tileable: see Lemma 4.28 for a related result.

Proof. Suppose \mathcal{R} has base \mathcal{D} and axis $\vec{w} \in \Delta$, so that $\mathcal{R} = \mathcal{D} + [0, N]\vec{w}$, and let $\vec{u} \in \Phi$, $\vec{u} \perp \vec{w}$. Let t be a tiling of \mathcal{R} . We want to show that $T^{\vec{u}}(t) = T^{\vec{w}}(t)$.

Consider $\mathcal{R}' = \mathcal{D} + [0, 2N]\vec{w}$, and the tiling $\hat{t} = t_0 \sqcup t_1$ of \mathcal{R}' which consists of two copies t_0 and t_1 of t , where t_0 tiles the subregion $\mathcal{D} + [0, N]\vec{w}$ and t_1 tiles the subregion $\mathcal{D} + [N, 2N]\vec{w}$.

By Proposition 4.24, $T^{\vec{u}}(\hat{t}) = T^{\vec{w}}(\hat{t}) \in \mathbb{Z}$. Now clearly $T^{\vec{u}}(\hat{t}) = 2T^{\vec{u}}(t)$, because the \vec{u} -shades of dimers of t_0 do not intersect dimers of t_1 (and vice-versa). We need to prove that $T^{\vec{w}}(\hat{t}) = 2T^{\vec{w}}(t)$.

Notice that $T^{\vec{w}}(\hat{t}) = T^{\vec{w}}(t_0) + T^{\vec{w}}(t_1) + T^{\vec{w}}(t_0, t_1) = 2T^{\vec{w}}(t) + T^{\vec{w}}(t_0, t_1)$. Let $d_0 \in t_0$, $d_1 \in t_1$ be dominoes, and let \tilde{d}_0 and \tilde{d}_1 be the dominoes of t that they “refer to”. If $\tilde{d}_0 \neq \tilde{d}_1$, then clearly

$$d_1 \cap \mathcal{S}^{\vec{w}}(d_0) \neq \emptyset \Leftrightarrow \tilde{d}_1 \cap (\mathcal{S}^{\vec{w}}(\tilde{d}_0) \cup \mathcal{S}^{-\vec{w}}(\tilde{d}_0)) \neq \emptyset$$

and $\tau^{\vec{w}}(d_0, d_1) = \frac{1}{4} \det(\vec{v}(d_1), \vec{v}(d_0), \vec{w}) = -\frac{1}{4} \det(\vec{v}(\tilde{d}_1), \vec{v}(\tilde{d}_0), \vec{w}) = \tau^{-\vec{w}}(\tilde{d}_0, \tilde{d}_1) - \tau^{\vec{w}}(\tilde{d}_0, \tilde{d}_1)$. Therefore, $T^{\vec{w}}(t_0, t_1) = \sum_{d, d' \in t} \tau^{-\vec{w}}(d, d') - \tau^{\vec{w}}(d, d') = 0$. Consequently, $T^{\vec{w}}(\hat{t}) = 2T^{\vec{w}}(t)$ and thus $T^{\vec{u}}(t) = T^{\vec{w}}(t)$.

Moreover, since $T^{\vec{w}}(t) = T^{\vec{w}}(\hat{t})/2$ and $T^{\vec{w}}(\hat{t}) \in \mathbb{Z}$, it follows that $T^{\vec{w}}(t) \in \frac{1}{2}\mathbb{Z}$, which completes the proof. \square

Remark 4.26. *The statement of Lemma 4.25 (and also of Proposition 4.3) also holds for pseudocylinders with odd depth. The key observation is that if \hat{t} is the tiling obtained by stacking two copies of t , one above the other, then $\phi(\hat{t}) = 0$ (see Remark 4.23 for the definition of the flux ϕ).*

Lemma 4.27. *Let $\mathcal{D} \subset \pi$ be a planar region, and let $\vec{w} \in \Delta$ be the normal vector for π . For each $k \in \mathbb{N}$, write $\mathcal{R}_k = \mathcal{D} + [0, 2k+1]\vec{w}$. If $k_1, k_2 \in \mathbb{N}$, then for each $\vec{u} \in \Phi$ and every pair of tilings t_1 of \mathcal{R}_{k_1} , t_2 of \mathcal{R}_{k_2} , $T^{\vec{u}}(t_1) - T^{\vec{u}}(t_2) \in \mathbb{Z}$.*

Should \mathcal{R}_{k_1} or \mathcal{R}_{k_2} not be tileable, the statement is vacuously true.

Proof. By Lemma 4.25, it suffices to show the result for $\vec{u} \perp \vec{w}$. Let t_1 and t_2 be tilings of \mathcal{R}_{k_1} and \mathcal{R}_{k_2} , respectively. Consider the cylinder with even depth $\mathcal{R} = \mathcal{D} + [0, 2k_1+2k_2+2]\vec{w}$, and let \tilde{t}_2 denote the tiling of $\mathcal{D} + [2k_1+1, 2k_1+1+2k_2+1]\vec{w}$ which is a copy of t_2 . If $t = t_1 \sqcup \tilde{t}_2$, then $T^{\vec{u}}(t) \in \mathbb{Z}$, by Proposition 4.24. Also, since $\vec{u} \perp \vec{w}$, $T^{\vec{u}}(t) = T^{\vec{u}}(t_1) + T^{\vec{u}}(\tilde{t}_2) = T^{\vec{u}}(t_1) + T^{\vec{u}}(t_2)$, so that

$$T^{\vec{u}}(t_1) - T^{\vec{u}}(t_2) = T^{\vec{u}}(t_1) + T^{\vec{u}}(t_2) - 2T^{\vec{u}}(t_2) = T^{\vec{u}}(t) - 2T^{\vec{u}}(t_2).$$

Since, by Lemma 4.25, $2T^{\vec{u}}(t_2) \in \mathbb{Z}$, we're done. \square

Lemma 4.28. *Let π be a basic plane with normal $\vec{w} \in \Delta$, and let $\mathcal{D} \subset \pi$ be a planar region with connected interior such that*

$$\#(\text{black squares in } \mathcal{D}) = \#(\text{white squares in } \mathcal{D}) = n.$$

Then there exists a tiling t_0 of $\mathcal{D} + [0, 2n-1]\vec{w}$ such that $T^{\vec{w}}(t_0) \in \mathbb{Z}$.

Notice that, with Lemma 4.28, the proof of Proposition 4.3 is complete. However, we need some preparation before we can prove Lemma 4.28.

It is a well-known fact that domino tilings of a region can be seen as perfect matchings of a related graph: in fact, if we consider the graph whose vertices are centers of the cubes (squares in the planar case) of the region, and where two vertices are joined if their Euclidean distance is 1, then a domino tiling can be directly translated as a perfect matching in this graph. This graph is called the *associated graph* of a region \mathcal{R} (planar or spatial), and denoted

$G(\mathcal{R})$. Since the proof of Lemma 4.28 will come more naturally in the setting of matchings in associated graphs, we shall revert to this viewpoint for what follows.

A *bicoloring* of a graph G is a coloring of each vertex of G as black or white, in such a way that no two adjacent vertices have the same color. Associated graphs for a region \mathcal{R} are always bicolored: each vertex inherits the color of the cube (or square) it refers to. For what follows, we shall assume that all graphs are already bicolored. Moreover, any subgraph of a bicolored graph G (for instance, the one obtained after deleting a vertex) shall inherit the bicoloring of G .

Lemma 4.29. *Let T be a bicolored tree. If all leaves are white, then the number of white vertices in T is strictly larger than the number of black vertices in T .*

By definition, a tree is connected and, therefore, nonempty.

Proof. We proceed by induction on the number of vertices. The result is clearly true if T has three or fewer vertices. Suppose, by induction, that the result holds for balanced trees with m vertices for any $m < n$. Let T be a tree with n vertices such that all leaves are white.

Let $w \in T$ be a (white) leaf, and let $v \in T$ be the only neighbor of w . Let F be the forest obtained by deleting w and v : F is nonempty, otherwise v would have to be a black leaf, which contradicts the hypothesis. Now for each connected component T' of F , T' is a tree with less than n vertices such that all leaves are white: therefore, by induction, F has more white vertices than black vertices. However, the vertices of T are those of F plus one black vertex (v) and one white vertex (w), so that the number of white vertices in T is greater than that of black ones. By induction, we get the result. \square

A connected bicolored graph G is *balanced* if the number of white vertices equals the number of black ones. By Lemma 4.29, a balanced tree must have at least one white leaf and one black leaf.

A *perfect matching* of a bipartite graph G is a set of pairwise disjoint edges of G , such that every vertex is adjacent to (exactly) one of the edges in the matching. Clearly, a necessary condition for the existence of a perfect matching is that G is balanced.

Let $G = (V, E)$ be a bicolored graph (in this notation, V is the vertex set of G , and E is its edge set), and let $I_n = \{0, 1, \dots, n-1\}$. Let $G \times I_n = (V \times I_n, E_n)$, where E_n consists of all edges connecting (v, j) and $(v, j+1)$, for each $v \in V$ and $j \in I_{n-1}$, plus the edges connecting (v_1, j) and

(v_2, j) for each $j \in I_n$ whenever the edge $v_1 v_2 \in E$. The color of a vertex $(v, j) \in G \times I_n$ equals the color of v if and only if j is even. Naturally, if $\mathcal{D} \subset \pi$ is a planar region with normal \vec{w} , then $G(\mathcal{D}) \times I_n \approx G(\mathcal{D} + [0, n]\vec{w})$.

Let G be a (nonempty) balanced connected bicolored graph with $2n$ vertices. Algorithm 1 finds a perfect matching M of $G \times I_{2n-1}$.

Algorithm 1 Algorithm for finding a perfect matching M of $G \times I_{2n-1}$.

Pick a spanning tree T for G . $\triangleright T$ is a balanced tree
 $M_0 \leftarrow \emptyset$
 $T_0 \leftarrow T$
 $k \leftarrow 0$
while $T_k \neq \emptyset$ **do**
 Pick a white leaf v_w and a black leaf v_b of T_k
 \triangleright Lemma 4.29 ensures that a balanced tree has at least one white leaf and one black leaf
 Pick a path $P_k = v_{k,1} v_{k,2} \dots v_{k,m_k}$ in T_k from v_w to v_b
 \triangleright i.e., $v_{k,1} = v_w, v_{k,m_k} = v_b$; notice that m_k is necessarily even
 $D_k \leftarrow \{(v, 2k-1)(v, 2k) \mid v \in T \setminus T_k\} \sqcup \{(v, 2k)(v, 2k+1) \mid v \in T_k \setminus P_k\}$
 $E_k \leftarrow \{(v_{k,2i-1} v_{k,2i}, 2k) \mid 1 \leq i \leq \frac{m_k}{2}\} \sqcup \{(v_{k,2i} v_{k,2i+1}, 2k+1) \mid 1 \leq i < \frac{m_k}{2}\}$
 \triangleright Here (vw, l) means the edge $(v, l)(w, l)$, i.e., the edge between the vertices (v, l) and (w, l)
 $M_{k+1} \leftarrow M_k \sqcup D_k \sqcup E_k$
 $T_{k+1} \leftarrow T_k \setminus \{v_w, v_b\}$
 \triangleright Notice that T_{k+1} is still a balanced tree (except in the last iteration, when it is empty)
 $k \leftarrow k + 1$
end while
 $M \leftarrow M_k$

Lemma 4.30. *If G is a connected bicolored balanced graph with $2n$ vertices, then the set of edges M generated by running Algorithm 1 on G is a perfect matching of $G \times I_{2n-1}$.*

Proof. To see that $M \subset E(G \times I_{2n-1})$, notice that any spanning tree has $2n$ vertices, and exactly two vertices are deleted in each iteration, so that the last iteration where $T_k \neq \emptyset$ occurs when $k = n - 1$. In all other iterations (i.e., $0 \leq k < n - 1$), clearly any edge created is contained in $E(G \times I_{2n-1})$. When $k = n - 1$, T_k is a balanced tree with two vertices, so $P_k = v_w v_b$ and only the edges $\{(v, 2n-3)(v, 2n-2) \mid v \in T \setminus T_k\}$ plus the edge $(v_w, 2n-2)(v_b, 2n-2)$ are created. Now these edges are contained in $E(G \times I_{2n-1})$, so we're done.

This proves that M is a subset of the edgeset of $G \times I_{2n-1}$. The reader will easily convince himself that it is a perfect matching (i.e., that every vertex (v, j) of $G \times I_{2n-1}$ is adjacent to exactly one edge of M). \square

Next we shall prove Lemma 4.28. In order to make the explanation clearer, we shall first introduce a few concepts. Let G be a bicolored connected balanced graph, and consider the perfect matching M of $G \times I_{2n-1}$ obtained by running Algorithm 1 on G , as well as the intermediate objects that were created, such as E_k and P_k .

Given an edge $e = (vw, j)$ of E_k , we say e is adjacent to v and to w (even though it is not an edge of G). For $v \in G$ and $0 \leq k \leq 2n-1$, we write $E(v, k) = \{e \in E_k \mid e \text{ adjacent to } v\}$.

Consider the paths $P_k = v_{k,1}v_{k,2} \dots v_{k,m_k}$ chosen in each step of the algorithm (we shall also use this notation in the proof). If $j > k$, we say that a path P_j *meets* P_k at $v \in G$ if $v = v_{j,i} \in P_k$ for some $i > 1$, but $v_{j,i-1} \notin P_k$. Analogously, P_j *leaves* P_k at v if $v = v_{j,i} \in P_k$ for some $i < m_j$, but $v_{j,i+1} \notin P_k$. Notice that a path P_j can meet and leave P_k at the same vertex v . Also, notice that P_j can only meet (resp. leave) P_k at most once (i.e., at no more than one vertex).

Proof of Lemma 4.28. Consider the graph $G = G(\mathcal{D})$ associated with the planar region \mathcal{D} . Clearly G is balanced; since \mathcal{D} has connected interior, it follows that G is also connected. Let M be the perfect matching obtained after running Algorithm 1 on G , and let t be the tiling of $\mathcal{D} + [0, 2n-1]\vec{w}$ associated with M .

If $e_0, e_1 \in M$, we will abuse notation and write $\tau^{\vec{w}}(e_0, e_1) = \tau^{\vec{w}}(d_0, d_1)$, where $d_i \in t$ is the domino associated with $e_i \in M$: we also say that two edges are parallel if their associated dominoes are parallel.

Notice that the only dominoes that are not parallel to \vec{w} are those associated with the edges of E_k for each k : therefore,

$$T^{\vec{w}}(t) = \sum_{i \leq j} T^{\vec{w}}(E_i, E_j) = \sum_{\substack{i \leq j \\ e \in E_i, e' \in E_j}} \tau^{\vec{w}}(e, e').$$

Fix $0 \leq k \leq n-1$. We want to show that $\sum_{j \geq k} T^{\vec{w}}(E_k, E_j) \in \mathbb{Z}$. First, write

$$\sum_{j \geq k} T^{\vec{w}}(E_k, E_j) = \sum_{\substack{1 \leq i \leq m_k \\ j \geq k}} T^{\vec{w}}(E(v_{k,i}, k), E(v_{k,i}, j));$$

we may ignore $v_{k,1}$ and v_{k,m_k} because they are deleted from the tree in step k , so that $E(v_{k,1}, j) = E(v_{k,m_k}, j) = \emptyset$ for each $j > k$ (for $j = k$, it contains only one edge, so there is also no effect).

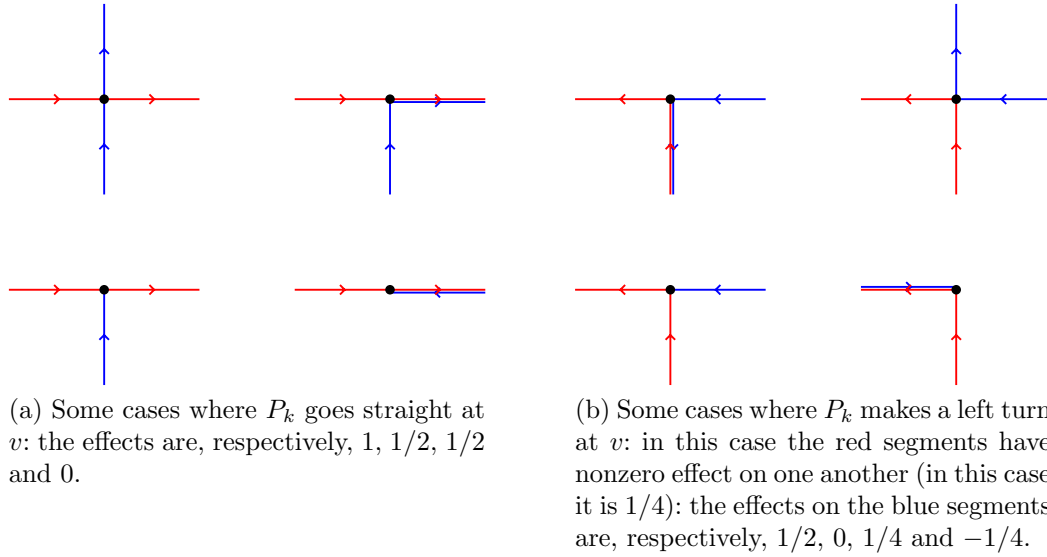


Figure 4.10: Edges of E_k (red) and E_j (blue) for some $j > k$, portrayed as edges of G . The edges are oriented as $\vec{v}(d)$, where d is the associated domino. The portrayed vertex is v , which we assume here to be black: notice that v is one of the endpoints of P_j in the bottom two cases of each figure.

For $v = v_{k,i}$, $1 < i < m_k$, we claim that, modulo 1, $\sum_{j \geq k} T^{\vec{w}}(E(v, k), E(v, j))$ equals

$$\frac{1}{2} (\#\{j > k \mid P_j \text{ meets } P_k \text{ at } v\} + \#\{j > k \mid P_j \text{ leaves } P_k \text{ at } v\})$$

(in other words, their difference is an integer).

If the two edges in $E(v, k)$ are parallel (i.e., P_k goes straight at v), then $T^{\vec{w}}(E(v, k), E(v, k)) = 0$. By checking a number of cases (see Figure 4.10a) we see that the following holds for each $j > k$:

$$T^{\vec{w}}(E(v, k), E(v, j)) = \begin{cases} \pm 1, & P_j \text{ meets and leaves } P_k \text{ at } v; \\ \pm 1/2, & P_j \text{ either meets or leaves } P_k \text{ at } v; \\ 0, & \text{otherwise.} \end{cases} \quad (4-3)$$

If the two edges in $E(v, k)$ are not parallel (i.e., P_k makes a turn at v), we proceed as follows: assume that the path P_k makes a left turn and that v is a black vertex (the other cases are analogous). Let k' be the step where v is chosen as the black leaf to be deleted (so that $v = v_{k', m_{k'}}$): again, inspection of a few possible cases (some of which are shown in Figure 4.10b) shows that (4-3) holds for $k < j < k'$ (and for $j > k'$, obviously $T^{\vec{w}}(E(v, k), E(v, j)) = 0$). Also, $T^{\vec{w}}(E(v, k), E(v, k)) = 1/4$ (because it is a left turn and v is black), and

(see the last two examples in Figure 4.10b)

$$T^{\vec{w}}((E(v, k), E(v, k'))) = \begin{cases} 1/4, & P_{k'} \text{ meets } P_k \text{ at } v; \\ -1/4, & \text{otherwise;} \end{cases}$$

so that $T^{\vec{w}}(E(v, k), E(v, k)) + T^{\vec{w}}((E(v, k), E(v, k'))) = 1/2$ if and only if $P_{k'}$ meets P_j at v (and 0 otherwise), so that we get the result.

Now let $N(v) = \#\{j > k \mid P_j \text{ meets } P_k \text{ at } v\} + \#\{j > k \mid P_j \text{ leaves } P_k \text{ at } v\}$. To finish the proof, we need to show that

$$N = \sum_{1 \leq i \leq m_k} N(v_{k,i}) = \#\{j > k \mid P_j \text{ meets } P_k\} + \#\{j > k \mid P_j \text{ leaves } P_k\}$$

is even. Because all P_j 's are paths in a tree T_k , it follows that each path meets (or leaves) P_k at most once. Therefore, each $j > k$ may contribute 0 (if it never meets nor leaves P_k), 1 (if it either meets or leaves P_k , but not both) or 2 (if it meets and leaves P_k) to the above sum. This contribution is 0 if $v_{j,1}, v_{j,m_j} \in P_k$; it is 0 or 2 if $v_{j,1}, v_{j,m_j} \notin P_k$. If exactly one of the two is in P_k , the contribution is 1; however, since $\#\{j > k \mid v_{j,1} \in P_k, v_{j,m_j} \notin P_k\} = \#\{j > k \mid v_{j,1} \notin P_k, v_{j,m_j} \in P_k\}$, it follows that N is even, so that $T^{\vec{w}}(t) = \sum_{j \geq k} T^{\vec{w}}(E_k, E_j) \equiv N/2 \pmod{1}$ is an integer. \square

We sum up our main results in the following proposition:

Proposition 4.31. *Let $\mathcal{D} \subset \pi$ be a planar region with normal vector \vec{w} and connected interior such that*

$$\#(\text{black squares in } \mathcal{D}) = \#(\text{white squares in } \mathcal{D}) = n.$$

Then $\mathcal{D} + [0, 2n - 1]\vec{w}$ is tileable. Moreover, for each $k \in \mathbb{N}$ such that $\mathcal{D} + [0, 2k - 1]\vec{w}$ is tileable (in particular, for each $k \geq n$), every tiling t of $\mathcal{D} + [0, 2k - 1]\vec{w}$ satisfies $T^{\vec{i}}(t) = T^{\vec{j}}(t) = T^{\vec{k}}(t) \in \mathbb{Z}$.

Proof. Follows directly from Lemmas 4.25, 4.27 and 4.28. \square

Now that we have seen that the twist, as in Definition 4.4, is well-defined for cylinders, we may adopt the notation $\text{Tw}(t)$ when t is a tiling of a cylinder.

4.5

Additive properties and proof of Theorem 3

The goal for this section is to discuss some additive properties of the twist and to complete the proof of Theorem 3.

Lemma 4.32. *Let \mathcal{R}_0 and \mathcal{R}_1 be two regions whose interiors are disjoint. Let $t_{\mathcal{R}_0,0}$ and $t_{\mathcal{R}_0,1}$ be two tilings of \mathcal{R}_0 and $t_{\mathcal{R}_1,0}$ and $t_{\mathcal{R}_1,1}$ be two tilings of \mathcal{R}_1 . For each $(i,j) \in \{0,1\}^2$, set $t_{ij} = t_{\mathcal{R}_0,i} \sqcup t_{\mathcal{R}_1,j}$, which is a tiling of $\mathcal{R} = \mathcal{R}_0 \cup \mathcal{R}_1$. Let $\Gamma_i^* = \Gamma^*(t_{\mathcal{R}_i,0}, t_{\mathcal{R}_i,1})$, $i = 0, 1$. Then, for each $\vec{u} \in \Phi$,*

$$T^{\vec{u}}(t_{00}) - T^{\vec{u}}(t_{01}) - T^{\vec{u}}(t_{10}) + T^{\vec{u}}(t_{11}) = 2 \sum_{\gamma_0 \in \Gamma_0^*, \gamma_1 \in \Gamma_1^*} \text{Link}(\gamma_0, \gamma_1).$$

In particular, if \mathcal{R}_0 or \mathcal{R}_1 is simply connected, then $T^{\vec{u}}(t_{00}) - T^{\vec{u}}(t_{01}) - T^{\vec{u}}(t_{10}) + T^{\vec{u}}(t_{11}) = 0$.

Proof. For shortness, given two sets of segments A_0 and A_1 , we shall in this proof write $T_{\text{sym}}^{\vec{u}}(A_0, A_1) = T^{\vec{u}}(A_0, A_1) + T^{\vec{u}}(A_1, A_0)$.

For each $(i,j) \in \{0,1\}^2$, we have

$$T^{\vec{u}}(t_{ij}) = T^{\vec{u}}(t_{\mathcal{R}_0,i} \sqcup t_{\mathcal{R}_1,j}) = T^{\vec{u}}(t_{\mathcal{R}_0,i}) + T^{\vec{u}}(t_{\mathcal{R}_1,j}) + T_{\text{sym}}^{\vec{u}}(t_{\mathcal{R}_0,i}, t_{\mathcal{R}_1,j}).$$

Notice that the last term is the only one that depends on both i and j , so that it is the only one that does not cancel out in the sum $\sum_{i,j \in \{0,1\}} (-1)^{i+j} \text{Tw}(t_{ij})$. Therefore, we have

$$\begin{aligned} \sum_{i,j \in \{0,1\}} (-1)^{i+j} T^{\vec{u}}(t_{ij}) &= \sum_{i,j \in \{0,1\}} (-1)^{i+j} T_{\text{sym}}^{\vec{u}}(t_{\mathcal{R}_0,i}, t_{\mathcal{R}_1,j}) = \\ &= T_{\text{sym}}^{\vec{u}}(t_{\mathcal{R}_0,0} \sqcup (-t_{\mathcal{R}_0,1}), t_{\mathcal{R}_1,0} \sqcup (-t_{\mathcal{R}_1,1})) = \sum_{\gamma_0 \in \Gamma_0^*, \gamma_1 \in \Gamma_1^*} T_{\text{sym}}^{\vec{u}}(\gamma_0, \gamma_1). \end{aligned}$$

Since for each pair γ_0, γ_1 in the sum we have $\gamma_i \subset \text{int}(\mathcal{R}_i)$, it follows that $\gamma_0 \cap \gamma_1 = \emptyset$. Hence, by Lemma 4.9, $T_{\text{sym}}^{\vec{u}}(\gamma_0, \gamma_1) = 2 \text{Link}(\gamma_0, \gamma_1)$, which yields the result. \square

Corollary 4.33. *Let \mathcal{R} be a simply connected region, and suppose that there exists a box $\mathcal{B} \supset \mathcal{R}$ such that $\mathcal{B} \setminus \mathcal{R}$ is tileable. If t_0, t_1 are two tilings of \mathcal{R} and t_a, t_b are two tilings of $\mathcal{B} \setminus \mathcal{R}$, then*

$$\text{Tw}(t_0 \sqcup t_a) - \text{Tw}(t_1 \sqcup t_a) = \text{Tw}(t_0 \sqcup t_b) - \text{Tw}(t_1 \sqcup t_b).$$

Proof. Use Lemma 4.32 with $\mathcal{R}_0 = \mathcal{R}$, $\mathcal{R}_1 = \mathcal{B} \setminus \mathcal{R}$. \square

Lemma 4.34. *Suppose L, M, N are even positive integers, and let $\mathcal{B} = [0, L] \times [0, M] \times [0, N]$. If $\mathcal{R} \subset \mathcal{B}$ is a cylinder with even depth, then there exists a tiling t_* of $\mathcal{B} \setminus \mathcal{R}$ such that $\text{Tw}(t \sqcup t_*) = \text{Tw}(t)$ for each tiling t of \mathcal{R} .*

Corollary 4.33 and Lemma 4.34 imply that for any tiling \tilde{t}_* of $\mathcal{B} \setminus \mathcal{R}$, there exists a constant K such that, for any tiling t of \mathcal{R} , $\text{Tw}(t \sqcup \tilde{t}_*) = \text{Tw}(t) + K$.

Proof. We may without loss of generality assume that the axis of \mathcal{R} is \vec{k} , so that $\mathcal{R} = \mathcal{D} + [E, F]\vec{k}$, where $\mathcal{D} \subset [0, L] \times [0, M] \times \{0\}$ and $F - E$ is even.

Let $\mathcal{B}_1 = [0, L] \times [0, M] \times [E, F]$. Clearly there exists a tiling $t_{1,*}$ of $\mathcal{B}_1 \setminus \mathcal{R}$ such that every domino is parallel to \vec{k} : hence, $\text{Tw}(t \sqcup t_{1,*}) = T^{\vec{k}}(t \sqcup t_{1,*}) = T^{\vec{k}}(t) = \text{Tw}(t)$ for each tiling t of \mathcal{R} . On the other hand, since L is even, there exists a tiling $t_{2,*}$ of $\mathcal{B} \setminus \mathcal{B}_1$ such that every dimer is parallel to \vec{i} , so that $\text{Tw}(t \sqcup t_{2,*}) = T^{\vec{i}}(t \sqcup t_{2,*}) = T^{\vec{i}}(t) = \text{Tw}(t)$ for each tiling t of \mathcal{B}_1 . Setting $t_* = t_{1,*} \sqcup t_{2,*}$ we get the result. \square

Lemma 4.35. *Let \mathcal{R} be a tileable cylinder with base \mathcal{D} , axis $\vec{w} \in \Delta$ and depth n . Let $\mathcal{R}' = \mathcal{D} + [0, 2n]\vec{w}$ be a cylinder with even depth formed by two copies of \mathcal{R} ; let $\mathcal{B} \supset \mathcal{R}'$ be a box with all dimensions even. Then there exist a tiling t_* of $\mathcal{B} \setminus \mathcal{R}$ and a constant K such that, for each tiling t of \mathcal{R} , $\text{Tw}(t \sqcup t_*) = \text{Tw}(t) + K$.*

Proof. By Lemma 4.34, there exists a tiling \tilde{t} of $\mathcal{B} \setminus \mathcal{R}'$ such that $\text{Tw}(t \sqcup \tilde{t}) = \text{Tw}(t)$ for each tiling t of \mathcal{R}' . Fix a tiling t_0 of $\mathcal{D} + [n, 2n]\vec{w}$ (which is tileable because \mathcal{R} is tileable). If we set $t_* = t_0 \sqcup \tilde{t}$ and $K = \text{Tw}(t_0)$, then for every tiling t of \mathcal{R} ,

$$\text{Tw}(t \sqcup t_*) = \text{Tw}(t \sqcup t_0 \sqcup \tilde{t}) = \text{Tw}(t \sqcup t_0) = \text{Tw}(t) + \text{Tw}(t_0);$$

the last equality holding by fixing $\vec{u} \in \Phi$, $\vec{u} \perp \vec{w}$ and writing $\text{Tw}(t \sqcup t_0) = T^{\vec{u}}(t \sqcup t_0) = T^{\vec{u}}(t) + T^{\vec{u}}(t_0)$. \square

Proof of Theorem 3. The twist is constructed in Definition 4.4 and its integrality follows from Proposition 4.3. Lemma 4.5 and Proposition 4.6 yield items (i) and (ii). To see item (iii), let \mathcal{R} be a duplex region with axis \vec{w} , and consider the tiling $t_{\vec{w}}$ such that all dominoes are parallel to \vec{w} : clearly $\text{Tw}(t_{\vec{w}}) = P'_{t_{\vec{w}}}(1) = 0$ (we assume that the reader is familiar with the notation from Chapter 3). Since the space of domino tilings of \mathcal{R} is connected by flips and trits (by Theorem 1), Proposition 4.6, together with Theorems 1 and 2, implies that for each tiling t of \mathcal{R} , $\text{Tw}(t) = P'_t(1)$ (for a more direct proof of item (iii), see Section 4.7).

We're left with proving item (iv). Let \mathcal{R} be a cylinder, and suppose $\mathcal{R} = \bigcup_{1 \leq j \leq m} \mathcal{R}_j$, where each \mathcal{R}_j is a cylinder (they need not have the same axis) and $\text{int}(\mathcal{R}_i) \cap \text{int}(\mathcal{R}_j) = \emptyset$ if $i \neq j$. Suppose the bases, axes and depths are respectively, \mathcal{D}, \vec{w}, n and $\mathcal{D}_j, \vec{w}_j, n_j$.

Let $t_{j,0}$ and $t_{j,1}$ be two tilings of \mathcal{R}_j . It suffices to show that

$$\text{Tw} \left(\bigsqcup_{1 \leq j \leq m} t_{j,1} \right) - \text{Tw} \left(\bigsqcup_{1 \leq j \leq m} t_{j,0} \right) = \sum_{1 \leq j \leq m} (\text{Tw}(t_{j,1}) - \text{Tw}(t_{j,0})).$$

For $0 \leq j \leq m$, let $t_j = \bigsqcup_{1 \leq i \leq j} t_{i,1} \sqcup \bigsqcup_{j < i \leq m} t_{i,0}$. We want to show that $\text{Tw}(t_m) - \text{Tw}(t_0) = \sum_{1 \leq j \leq m} (\text{Tw}(t_{j,1}) - \text{Tw}(t_{j,0}))$.

Let \mathcal{B} be a box with all dimensions even such that $\mathcal{D} + [0, 2n]\vec{w} \subset \mathcal{B}$ and $\mathcal{D}_j + [0, 2n_j]\vec{w}_j \subset \mathcal{B}$ for $j = 1, \dots, m$. By Lemma 4.35, there exist: a tiling t_* of $\mathcal{B} \setminus \mathcal{R}$ and a constant K ; and for each j , a tiling $t_{j,*}$ of $\mathcal{B} \setminus \mathcal{R}_j$ and a constant K_j such that $\text{Tw}(t \sqcup t_*) = \text{Tw}(t) + K$ for each tiling t of \mathcal{R} , and $\text{Tw}(t \sqcup t_{j,*}) = \text{Tw}(t) + K_j$ for each tiling t of \mathcal{R}_j .

Write $\hat{t}_j = t_* \sqcup \bigsqcup_{1 \leq i < j} t_{i,1} \sqcup \bigsqcup_{j < i \leq m} t_{i,0}$ for each j , so that \hat{t}_j is a tiling of $\mathcal{B} \setminus \mathcal{R}_j$. Notice that, for $1 \leq j \leq m$, $t_j \sqcup t_* = t_{j,1} \sqcup \hat{t}_j$ and $t_{j-1} \sqcup t_* = t_{j,0} \sqcup \hat{t}_j$. Therefore, we have

$$\begin{aligned} \text{Tw}(t_m) - \text{Tw}(t_0) &= \sum_{1 \leq j \leq m} (\text{Tw}(t_j) - \text{Tw}(t_{j-1})) \\ &= \sum_{1 \leq j \leq m} ((\text{Tw}(t_j \sqcup t_*) - K) - (\text{Tw}(t_{j-1} \sqcup t_*) - K)) \\ &= \sum_{1 \leq j \leq m} (\text{Tw}(t_{j,1} \sqcup \hat{t}_j) - \text{Tw}(t_{j,0} \sqcup \hat{t}_j)) \stackrel{\dagger}{=} \sum_{1 \leq j \leq m} (\text{Tw}(t_{j,1} \sqcup t_{j,*}) - \text{Tw}(t_{j,0} \sqcup t_{j,*})) \\ &= \sum_{1 \leq j \leq m} ((\text{Tw}(t_{j,1}) + K_j) - (\text{Tw}(t_{j,0}) + K_j)) = \sum_{1 \leq j \leq m} (\text{Tw}(t_{j,1}) - \text{Tw}(t_{j,0})). \end{aligned}$$

Equality \dagger holds by Corollary 4.33, because \hat{t}_j and $t_{j,*}$ are two tilings of $\mathcal{B} \setminus \mathcal{R}_j$. \square

4.6

Embeddable regions

We shall now describe a simple generalization of the twist to a wider class of simply connected regions. An *embedding* of a region \mathcal{R} is a triple $(\mathcal{R}, \mathcal{B}, t_*)$, where $\mathcal{B} \supset \mathcal{R}$ is a box and t_* is a tiling of $\mathcal{B} \setminus \mathcal{R}$. A region \mathcal{R} is said to be *embeddable* if it admits an embedding.

Lemma 4.36. *Let \mathcal{R} be a simply connected region and suppose $(\mathcal{R}, \mathcal{B}_0, t_0)$ and $(\mathcal{R}, \mathcal{B}_1, t_1)$ are two embeddings of \mathcal{R} . If t, t' are two tilings of \mathcal{R} , then*

$$\text{Tw}(t \sqcup t_0) - \text{Tw}(t' \sqcup t_0) = \text{Tw}(t \sqcup t_1) - \text{Tw}(t' \sqcup t_1).$$

Proof. Let \mathcal{B} be a box containing \mathcal{B}_0 and \mathcal{B}_1 such that all its dimensions are even. Since \mathcal{B}_0 and \mathcal{B}_1 are tileable boxes, at least one of their dimensions is even: by Lemma 4.34, there exist tilings $t_{0,*}$ of $\mathcal{B} \setminus \mathcal{B}_0$ and $t_{1,*}$ of $\mathcal{B} \setminus \mathcal{B}_1$ such that $\text{Tw}(t_{\mathcal{B}_0} \sqcup t_{0,*}) = \text{Tw}(t_{\mathcal{B}_0})$ and $\text{Tw}(t_{\mathcal{B}_1} \sqcup t_{1,*}) = \text{Tw}(t_{\mathcal{B}_1})$ for every tiling $t_{\mathcal{B}_0}$ of \mathcal{B}_0 and $t_{\mathcal{B}_1}$ of \mathcal{B}_1 . Therefore,

$$\text{Tw}(t \sqcup t_0) - \text{Tw}(t' \sqcup t_0) = \text{Tw}(t \sqcup t_0 \sqcup t_{0,*}) - \text{Tw}(t' \sqcup t_0 \sqcup t_{0,*}).$$

Notice that $t_0 \sqcup t_{0,*}$ and $t_1 \sqcup t_{1,*}$ are two tilings of $\mathcal{B} \setminus \mathcal{R}$. By Corollary 4.33,

$$\text{Tw}(t \sqcup t_0 \sqcup t_{0,*}) - \text{Tw}(t' \sqcup t_0 \sqcup t_{0,*}) = \text{Tw}(t \sqcup t_1 \sqcup t_{1,*}) - \text{Tw}(t' \sqcup t_1 \sqcup t_{1,*}),$$

and hence $\text{Tw}(t \sqcup t_0) - \text{Tw}(t' \sqcup t_0) = \text{Tw}(t \sqcup t_1) - \text{Tw}(t' \sqcup t_1)$. \square

Given a simply connected embeddable region \mathcal{R} and two tilings t_0, t_1 , define the *relative twist* $\text{TW}(t_0, t_1) = \text{Tw}(t_0 \sqcup t_*) - \text{Tw}(t_1 \sqcup t_*)$, where $(\mathcal{R}, \mathcal{B}, t_*)$ is any embedding of \mathcal{R} . Moreover, if we fix a base tiling t_0 , then the function $t \mapsto \text{TW}(t, t_0)$ is an invariant with the same properties as the twist in cylinders (for instance, items (i), (ii) and (iv) in Theorem 3); and different choices of base tiling alter this function by an additive constant.

Example 4.37 (Cylinders). *If \mathcal{R} is a cylinder, then $\text{TW}(t, t') = \text{Tw}(t) - \text{Tw}(t')$ for any two tilings of \mathcal{R} (this follows directly from Lemma 4.35).*

A natural question at this point is: “how large” is the class of tileable embeddable simply connected regions? Since the box $\mathcal{B} \supset \mathcal{R}$ can be chosen to be as large as needed, it is clear that embeddable regions are, in fact, very common: for instance, if the complement of \mathcal{R} does not contain any narrow areas (where space is limited), \mathcal{R} will almost certainly be embeddable. However, there exist simply connected (and even contractible) regions that are not embeddable: Figure 4.11 shows an example. Notice that the complement of \mathcal{R} contains a narrow area where cubes of one color happen in much larger number.

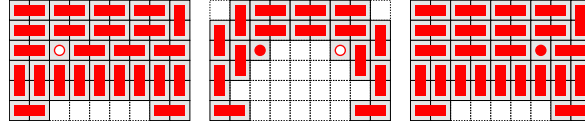


Figure 4.11: A tileable contractible region that is not embeddable. Notice the narrow area in the middle floor, which contains a large surplus of cubes of one color, while only a few of them are connected to the “outer space”. Adding more space in the complement of \mathcal{R} clearly does not help, so \mathcal{R} is not embeddable.

4.7

The twist for duplex regions

In this section, we provide an alternative proof for the following fact:

Proposition 4.38. *If \mathcal{R} is a duplex region, then, for any tiling t of \mathcal{R} ,*

$$P'_t(1) = T^{\vec{\mathbf{i}}}(t) = T^{\vec{\mathbf{j}}}(t) = T^{\vec{\mathbf{k}}}(t).$$

The equality $T^{\vec{\mathbf{i}}}(t) = T^{\vec{\mathbf{j}}}(t) = T^{\vec{\mathbf{k}}}(t)$ above is a special case of Proposition 4.3. We shall now give an independent proof of this equality in the particular case of duplex regions.

Let \mathcal{R} be a duplex region. Let t be a tiling of \mathcal{R} , and let s be its corresponding sock in G . For $p \in \mathbb{R}^2$ and a cycle γ of s , let $\text{wind}(\gamma, p)$ be the winding number of γ , thought of as a curve in \mathbb{R}^2 , around p . Clearly we can write our invariant $P_t(q)$ as

$$P_t(q) = \sum_{v \in G} \text{color}(v) q^{\sum_{\gamma, v \notin \gamma} \text{wind}(\gamma, v)}, \quad (4-4)$$

where the sum in the exponent of q is taken over all the cycles in s that do not contain v . Notice that

$$P'_t(1) = \sum_{v \in G, \gamma \text{ cycle}} \text{color}(v) \text{wind}(\gamma, v) = \sum_{v \in \mathbb{Z}^2, \gamma \text{ cycle}} \text{color}(v) \text{wind}(\gamma, v).$$

Lemma 4.39. *If \mathcal{R} is a $\vec{\mathbf{k}}$ -duplex region with associated graph G , $\vec{u} \in \{\pm \vec{\mathbf{i}}, \pm \vec{\mathbf{j}}\}$ and t is a tiling of \mathcal{R} with corresponding sock s , then $T^{\vec{u}}(t) = P'_t(1)$.*

Proof. Two dominoes that are not parallel to $\vec{\mathbf{k}}$ have no effect along \vec{u} on one another. Therefore, we only consider pairs of dominoes where one is parallel to $\vec{\mathbf{k}}$, that is, refers to a jewel of s .

If γ is a cycle of s and v is a jewel, one way of computing $\text{wind}(\gamma, v)$ is to count (with signs) the intersections of γ with the half-line $v + [0, \infty)\vec{u}$. Thus, if

d_v denotes the domino containing v and $d \in \gamma$ means that d refers to an edge of γ , then $\text{color}(v) \text{wind}(\gamma, v) = 2 \sum_{d \in \gamma} \tau^{\vec{u}}(d, d_v) = 2 \sum_{d \in \gamma} \tau^{\vec{u}}(d_v, d)$. Thus,

$$P'_t(1) = \sum_{\gamma, v} \text{color}(v) \text{wind}(\gamma, v) = \sum_{\substack{\gamma, v \\ d \in \gamma}} (\tau^{\vec{u}}(d, d_v) + \tau^{\vec{u}}(d_v, d)) = T^{\vec{u}}(t),$$

completing the proof. \square

We now consider $T^{\vec{k}}$. Again, let t be a tiling of a duplex region with corresponding sock s . Let the *charge enclosed* by a cycle γ of s be

$$\text{charge}_{\text{int}}(\gamma) = \sum_{v \notin \gamma} \text{color}(v) \text{wind}(\gamma, v),$$

so that $P'_t(1) = \sum_{\gamma \text{ cycle of } s} \text{charge}_{\text{int}}(\gamma)$. Charges can be looked at from a point of view that is more interesting for our purposes. Given $v \in \mathbb{R}^2$, consider the set of four points $\mathcal{N}_v = \{v + (\frac{k}{2}, \frac{l}{2}) | k, l \in \{-1, 1\}\}$, i.e., the set of points of the form $v + (\pm\frac{1}{2}, \pm\frac{1}{2})$. The *metric weight* of a vertex $v \in \mathbb{Z}^2$ with respect to a cycle γ of s is given by

$$w_{\text{metric}}(\gamma, v) = \frac{1}{4} \sum_{u \in \mathcal{N}_v} \text{wind}(\gamma, u),$$

while the *topological weight* $w_{\text{top}}(\gamma, v)$ of v is the (arithmetic) average of the set $\text{wind}(\gamma, \mathcal{N}_v) = \{\text{wind}(\gamma, u) | u \in \mathcal{N}_v\}$ (see Figure 4.12).

Lemma 4.40.

$$\text{charge}_{\text{int}}(\gamma) = \sum_{v \in \mathbb{Z}^2} \text{color}(v) w_{\text{top}}(\gamma, v).$$

Proof. Notice that

$$w_{\text{top}}(\gamma, v) = \begin{cases} \text{wind}(\gamma, v), & \text{if } v \notin \gamma, \\ \frac{1}{2}, & \text{if } v \in \gamma \text{ and } \gamma \text{ is counterclockwise oriented,} \\ -\frac{1}{2}, & \text{if } v \in \gamma \text{ and } \gamma \text{ is clockwise oriented.} \end{cases}$$

In particular, $\sum_{v \in \gamma} w_{\text{top}}(\gamma, v) \text{color}(v) = \pm\frac{1}{2} \sum_{v \in \gamma} \text{color}(v) = 0$. Hence,

$$\text{charge}_{\text{int}}(\gamma) = \sum_{v \in \mathbb{Z}^2} \text{color}(v) w_{\text{top}}(\gamma, v).$$

\square

If s is the corresponding sock of a tiling t and γ is a cycle of s , then the angle $\angle(\gamma, v)$ of a vertex $v \in \gamma$ is the difference between the angle of

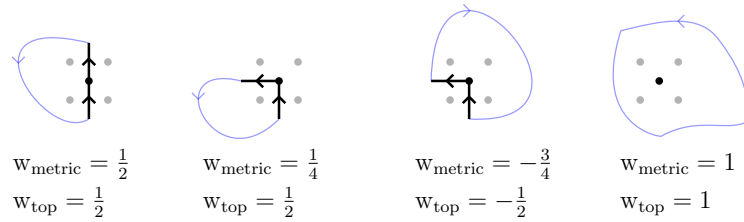


Figure 4.12: Illustration of topological and metric weights. The points in \mathcal{N}_v are in grey.

the edge of γ leaving v and the angle of the edge of γ entering v , counted in counterclockwise laps. In other words, a vertex v where the curve goes straight has angle 0, whereas a vertex where a left (resp. right) turn occurs has angle $1/4$ (resp. $-1/4$), as shown in Figure 4.13.

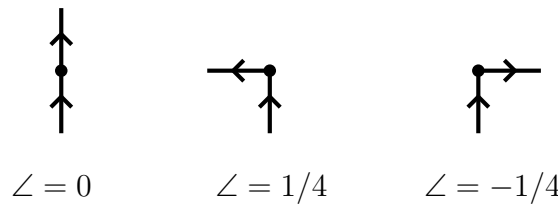


Figure 4.13: Illustration of the angle of a vertex.

The *boundary charge* of a curve γ is $\text{charge}_{\partial}(\gamma) = \sum_{v \in \gamma} \angle(\gamma, v) \text{color}(v)$. Notice that

$$T^{\vec{\mathbf{k}}}(t) = \sum_{\gamma \text{ cycle of } s} \text{charge}_{\partial}(\gamma). \quad (4-5)$$

We now set out to prove that, for each γ , $\text{charge}_{\partial}(\gamma) = \text{charge}_{\text{int}}(\gamma)$, which will complete the proof of Proposition 4.38.

Lemma 4.41. *For each cycle γ of s ,*

$$\sum_{v \in \mathbb{Z}^2} w_{\text{metric}}(\gamma, v) \text{color}(v) = 0.$$

Proof.

$$\sum_{v \in \mathbb{Z}^2} w_{\text{metric}}(\gamma, v) \text{color}(v) = \sum_{u \in \mathbb{Z}^2 + (\frac{1}{2}, \frac{1}{2})} \left(\frac{1}{4} \text{wind}(\gamma, u) \sum_{v \in \mathcal{N}_u} \text{color}(v) \right) = 0.$$

□

Lemma 4.42. *If $v \in \mathbb{Z}^2$,*

$$w_{\text{top}}(\gamma, v) - w_{\text{metric}}(\gamma, v) = \begin{cases} \angle(\gamma, v), & \text{if } v \in \gamma, \\ 0, & \text{otherwise.} \end{cases}$$

Proof. Figure 4.12 illustrates most of the elements needed in this proof. If $v \notin \gamma$, then $\text{wind}(\gamma, u) = \text{wind}(\gamma, v)$ for each $u \in \mathcal{N}_v$, so $w_{\text{metric}}(\gamma, v) = w_{\text{top}}(\gamma, v) = \text{wind}(\gamma, v)$.

If $v \in \gamma$ and the curve goes straight at v , then, for some k , two points in \mathcal{N}_v have winding number k and the other two have winding number $k + 1$, so $w_{\text{metric}}(\gamma, v) = \frac{1}{4}(k + k + (k + 1) + (k + 1)) = \frac{1}{2}(k + (k + 1)) = w_{\text{top}}(\gamma, v)$.

If $v \in \gamma$ and the curve turns left at v , then the winding numbers are $k, k, k, k + 1$, so $w_{\text{top}}(\gamma, v) - w_{\text{metric}}(\gamma, v) = 1/4 = \angle(\gamma, v)$. Analogously, $w_{\text{top}}(\gamma, v) - w_{\text{metric}}(\gamma, v) = -1/4 = \angle(\gamma, v)$ if γ turns right at v . \square

Lemma 4.43. *For each cycle γ of s , $\text{charge}_{\partial}(\gamma) = \text{charge}_{\text{int}}(\gamma)$.*

Proof. By Lemma 4.42, the boundary charge of γ can also be written as

$$\begin{aligned} \text{charge}_{\partial}(\gamma) &= \sum_{v \in \gamma} \angle(\gamma, v) \text{color}(v) \\ &= \sum_{v \in \mathbb{Z}^2} (w_{\text{top}}(\gamma, v) - w_{\text{metric}}(\gamma, v)) \text{color}(v) \\ &= \sum_{v \in \mathbb{Z}^2} w_{\text{top}}(\gamma, v) \text{color}(v) - \sum_{v \in \mathbb{Z}^2} w_{\text{metric}}(\gamma, v) \text{color}(v) \\ &= \sum_{v \in \mathbb{Z}^2} w_{\text{top}}(\gamma, v) \text{color}(v) = \text{charge}_{\text{int}}(\gamma), \end{aligned}$$

the fourth equality holding because of Lemma 4.41; the last equality is Lemma 4.40. \square

Proof of Proposition 4.38. Lemma 4.43 and Equation (4-5) imply that $P'_t(1) = T^{\vec{k}}(t)$. Together with Lemma 4.39, this proves the result. \square

4.8

Examples and counterexamples

In this short section, we give a few examples and counterexamples that help motivate the theory and some of the results obtained.

For instance, when looking at Proposition 4.3, one might wonder whether the pretwists are always integers or if they always coincide, at least for, say, simply connected or contractible regions. This turns out not to be the case, as Figure 4.14a shows: for the tiling t portrayed there, $T^{\vec{i}}(t) = T^{\vec{j}}(t) = 0$ but $T^{\vec{k}}(t) = 1/4$.

One might ask whether the pretwists coincide in a pseudocylinder (i.e., if the base is not necessarily simply connected): the tiling t portrayed in Figure

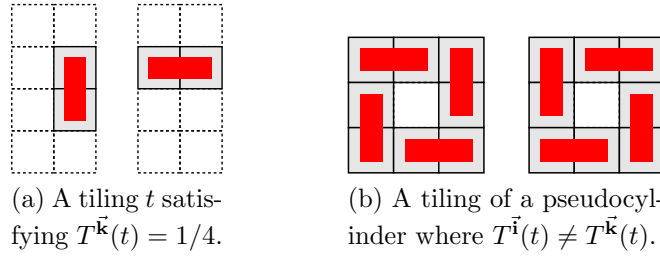


Figure 4.14: Two examples of tilings: \vec{k} is chosen to point towards the paper.

4.14b satisfies $T^{\vec{i}}(t) = T^{\vec{j}}(t) = 0$ and $T^{\vec{k}}(t) = 1$ (see Remarks 4.23 and 4.26 for an idea of what can be shown for pseudocylinders in this respect).

Example 4.44 (The $4 \times 4 \times 4$ box). *A particularly interesting example is the $4 \times 4 \times 4$ box, which has 5051532105 tilings, divided into 93 flip connected components. The number associated to each component is completely arbitrary, it has to do with the order in which our computer program found each one. Table 4.1 shows the components in decreasing order of size, whereas Figure 4.15 contains a graph whose vertices are the connected components: it shows which components are connected via trits.*

The reader will find more information in [16]. There, he will find details about each connected component (e.g., pictures of a sample tiling in each of the components), as well as other examples and the source code for the C[#] program used to generate them.

Connected Component	Number of tilings	Tw
0	4412646453	0
1	310185960	1
2	310185960	-1
8	8237514	2
7	8237514	-2
3	718308	2
5	718308	-2
4,6	283044	0
27,36,58	2576	3
28,35,57	2576	-3
9,13,22,23,29,32,37,43,49,55,76,80	618	3
12,16,21,25,30,31,39,45,51,56,75,77	618	-3
10,15,24,34,38,42,47,52,54,59,78,82	236	1
11,14,26,33,40,41,44,50,53,60,79,81	236	-1
48,61,83	4	4
46,62,84	4	-4
17,63,67,72,85,92	1	4
18,19,64,65,68,70,71,73,86,87,90,91	1	0
20,66,69,74,88,89	1	-4

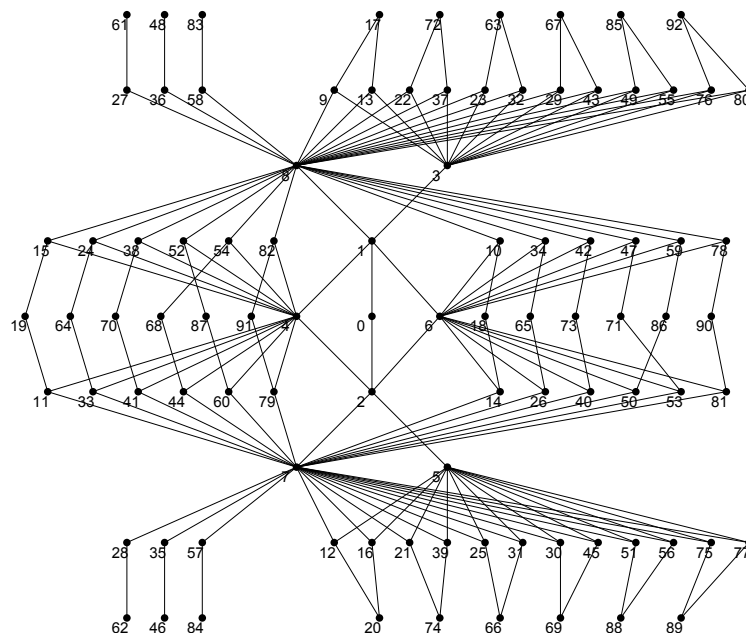
Table 4.1: Flip connected components of a $4 \times 4 \times 4$ box

Figure 4.15: Graph with 93 vertices, each one representing a flip connected component of the $4 \times 4 \times 4$ box. Two components are joined by an edge if there exists a trit taking a tiling in one component to a tiling of the other. Components that are below have a lower twist: hence, edges going up always refer to positive trits (and edges going down always refer to negative trits).

5

Possible values of the twist

Now that we have established (in Proposition 4.19) that the twist of a cylinder is always an integer, we wish to take a closer look at the set of values that can be the twist of some tiling of a given box. If \mathcal{B} is a box, define $\text{Tw}(\mathcal{B}) = \{\text{Tw}(t) | t \text{ is a tiling of } \mathcal{B}\} \subset \mathbb{Z}$. An easy observation, that follows directly from Lemma 4.2, is that $\text{Tw}(\mathcal{B})$ is symmetric with respect to zero, i.e., $k \in \text{Tw}(\mathcal{B}) \Leftrightarrow -k \in \text{Tw}(\mathcal{B})$. In this chapter, our main concern is to provide bounds for the value $\text{Tw}_{\max}(L, M, N) = \max \text{Tw}([0, L] \times [0, M] \times [0, N])$.

Lemma 5.1. *Let L, M, N be integers, at least one of them even, with $N \leq M \leq L$. Then*

$$\text{Tw}_{\max}(L, M, N) \leq \frac{LM \lceil N/2 \rceil \lfloor N/2 \rfloor}{4} \leq \frac{LMN^2}{16}.$$

Proof. Suppose, without loss of generality, that $N \leq L, M$, and let t be a tiling of \mathcal{B} . For each $(x, y) \in \mathbb{Z}^2$, $0 \leq x \leq L-1$, $0 \leq y \leq M-1$, let, for $\vec{u} \in \{\vec{\mathbf{i}}, \vec{\mathbf{j}}\}$, $d_{\vec{u}}(x, y) = \{d \in t | \vec{v}(d) = \pm \vec{u}, C(x^\sharp, y^\sharp, z^\sharp) \subset d \text{ for some } z \in \mathbb{Z}\}$, and let $n_{\vec{u}}(x, y)$ be the number of elements of $d_{\vec{u}}(x, y)$. Notice that there is a one-to-one correspondence between pairs (d_0, d_1) such that $d_0 \in d_{\vec{\mathbf{i}}}(x, y)$, $d_1 \in d_{\vec{\mathbf{j}}}(x, y)$, and pairs (d_0, d_1) such that $\tau(d_0, d_1) + \tau(d_1, d_0) \neq 0$; also, the latter condition implies that $\tau(d_0, d_1) + \tau(d_1, d_0) = \pm 1/4$. For fixed x, y , the number of such pairs is $n_{\vec{\mathbf{i}}}(x, y)n_{\vec{\mathbf{j}}}(x, y)$. Therefore,

$$|\text{Tw}(t)| \leq \frac{1}{4} \sum_{x=0}^{L-1} \sum_{y=0}^{M-1} n_{\vec{\mathbf{i}}}(x, y)n_{\vec{\mathbf{j}}}(x, y).$$

Since $n_{\vec{\mathbf{i}}}(x, y) + n_{\vec{\mathbf{j}}}(x, y) \leq N$, it follows that $n_{\vec{\mathbf{i}}}(x, y)n_{\vec{\mathbf{j}}}(x, y) \leq \lceil N/2 \rceil \lfloor N/2 \rfloor$, so that

$$|\text{Tw}(t)| \leq \frac{1}{4} \sum_{x=0}^{L-1} \sum_{y=0}^{M-1} \lceil N/2 \rceil \lfloor N/2 \rfloor = \frac{LM \lceil N/2 \rceil \lfloor N/2 \rfloor}{4}.$$

□

In Lemma 5.6 below, we use a similar (but more refined) analysis to find a slightly better upper bound.

5.1

Asymptotic lower bounds

We will now describe some constructions that yield asymptotic lower bounds for $\text{Tw}_{\max}(L, M, N)$. We begin with an exact description for the asymptotic behavior in boxes with two floors (Lemma 5.3). First, however, we need an auxiliary construction.

Recall from Section 3.5 the definition of a sock. The *eel* of *thickness* m and *length* n is a sock in \mathbb{Z}^2 that consists of m cycles, with the same orientation, such that each cycle surrounds a set of n consecutive jewels in a diagonal (and those are the only jewels each cycle surrounds): Figures 5.1 and 5.2 show examples of eels of different thicknesses and lengths. Notice that an eel of length 1 is a boxed jewel. If e is an eel of thickness m and length n such that the n jewels are black and the cycles spin counterclockwise, then $P_e(q) = nq^m$, so that $P'_e(1) = mn$.

Lemma 5.2. *For $n \geq 0$, let $f(n) = \text{Tw}_{\max}(n, n, 2)$. Then*

$$\lim_{n \rightarrow \infty} \frac{f(n)}{4n^2} = \frac{1}{16}.$$

Proof. Let $\mathcal{B}_n = [0, n] \times [0, n] \times [0, 2]$. By Lemma 5.1, we only need to show that $\lim_{n \rightarrow \infty} f(n)/(4n^2) \geq 1/16$. Also, let $\mathcal{P}_n = \mathcal{D}_n \times [0, 2]$, where $\mathcal{D}_n \subset \mathbb{R}^2$ consists of all the basic squares completely contained in the set $\{(x, y) \mid x, y \geq 0, x + y \leq n + 1\}$ (see Figure 5.2). Let, for $n \geq 0$, $g(n) = \max \text{Tw}(\mathcal{P}_n)$. We claim that f and g satisfy the following inequalities:

$$f(n) \geq \max_{0 \leq k \leq (n-1)/2} k(n-2k) + 2g(n-2k-1), \quad (5-1)$$

$$g(n) \geq \max_{0 \leq k \leq (n-1)/4} k(n-4k) + g(n-4k-1) + 2g(2k), \quad (5-2)$$

with $f(0) = g(0) = 0$.

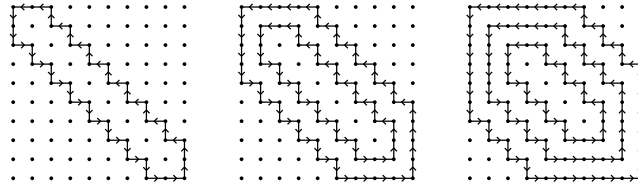


Figure 5.1: Socks for the eels of thickness 1, 2 and 3 in \mathcal{B}_{10} .

Figure 5.1 illustrates that we can fit an eel e_k of thickness k and length $n - 2k$ in \mathcal{B}_n whenever $0 \leq k \leq (n - 1)/2$. Notice that the jewels not in the eel form two copies of \mathcal{P}_{n-2k-1} . Since $\text{Tw}(t) = P'_t(1)$ for tilings of duplex regions, it follows that $\max \text{Tw}(\mathcal{B}_n) \geq P'_{e_k}(1) + 2 \max \text{Tw}(\mathcal{P}_{n-2k-1})$, which implies (5-1).

For Equation (5-2), notice that, whenever $0 \leq k \leq (n - 1)/4$, we can fit an eel of thickness k and length $n - 4k$ in \mathcal{P}_n , as illustrated in Figure 5.2. The remaining jewels form three regions: two copies of \mathcal{P}_{2k} and one copy of \mathcal{P}_{n-4k-1} , thus $g(n) \geq k(n - 4k) + g(n - 4k - 1) + 2g(2k)$.

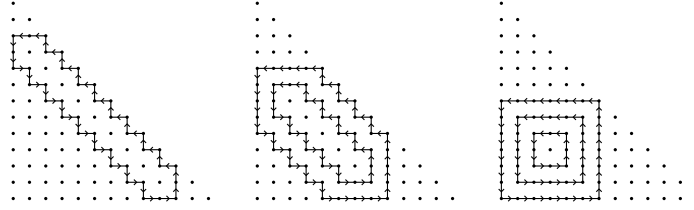


Figure 5.2: Socks for the constructions of eels of thickness 1, 2 and 3 in \mathcal{P}_{13} .

Now let $g^*(n) = n(n + 1)/2 - 4g(n)$. We claim that, for all $n \in \mathbb{N}$, $g^*(n) < 2n^{3/2}$. By (5-2),

$$g^*(n) \leq \min_{0 \leq k \leq (n-1)/4} 4k^2 + n - 4k + g^*(n - 4k - 1) + 2g^*(2k). \quad (5-3)$$

Now for $0 \leq n \leq 100$, we check (with a computer) that $g^*(n) \leq 2n^{3/2}$ by recursively calculating upper bounds for $g^*(n)$ via (5-3).

Let $n > 100$, and assume, by induction, that $g^*(n_0) \leq 2n_0^{2/3}$ whenever $n_0 < n$. Let $k = \lfloor \sqrt{n}/2 \rfloor \geq 5$. Using the induction hypothesis on $n - 4k - 1$ and on $2k$, we get

$$2n^{3/2} - g^*(n) \geq 2(n^{3/2} - (n - 4k - 1)^{3/2}) - (4k^2 + 4(2k)^{3/2} - 4k + n).$$

Since $h(x) = x^{3/2}$ is convex and $h'(x) = (3/2)x^{1/2}$, we have

$$2n^{3/2} - g^*(n) \geq 3(n - 4k - 1)^{1/2}(4k + 1) - 4k^2 - 4(2k)^{3/2} + 4k - n.$$

Since $\sqrt{n}/2 - 1 \leq k \leq \sqrt{n}/2$, we have $4k^2 \leq n \leq 4k^2 + 8k + 4$. Thus,

$$2n^{3/2} - g^*(n) \geq 3(4k^2 - 4k - 1)^{1/2}(4k + 1) - 8k^2 - 4(2k)^{3/2} - 4k - 4.$$

Consider the function $u(x) = 3(4x^2 - 4x - 1)^{1/2}(4x + 1) - 8x^2 - 4(2x)^{3/2} - 4x - 4$, defined on $[2, \infty)$. It is a simple exercise to prove that $u'(x) > 0$ for $x \geq 2$. Also, $u(5) \approx 209.465 > 0$ and hence $2n^{3/2} - g^*(n) \geq u(k) \geq u(5) > 0$, establishing the claim.

By (5-1), $0 \leq n^2 - 4f(n) \leq 4k^2 + n - 2k + 2g^*(n - 2k - 1)$ for each $0 \leq k \leq (n - 1)/2$, and thus $0 \leq n^2 - 4f(n) \leq 2n^{3/2} + n$. Multiplying by $1/(16n^2)$ and taking the limit, we complete the proof. \square

Lemma 5.3. *The following holds:*

$$\lim_{L, M \rightarrow \infty} \frac{\text{Tw}_{\max}(L, M, 2)}{4LM} = \frac{1}{16}.$$

Proof. Let $B_{L,M} = [0, L] \times [0, M] \times [0, 2]$, and let $f(n) = \text{Tw}_{\max}(n, n, 2)$. Fix $k \in \mathbb{N}$. Notice that we can place $\lfloor L/k \rfloor \lfloor M/k \rfloor$ copies of $\mathcal{B}_{k,k}$ inside $\mathcal{B}_{L,M}$, so that $\text{Tw}_{\max}(L, M, 2) \geq \lfloor L/k \rfloor \lfloor M/k \rfloor f(k) \geq (L/k - 1)(M/k - 1)f(k)$. Therefore,

$$\liminf_{L, M \rightarrow \infty} \frac{\text{Tw}_{\max}(L, M, 2)}{4LM} \geq \frac{f(k)}{4k^2}.$$

Since this inequality holds for any fixed k , we may take the limit as $k \rightarrow \infty$ to get, by Lemma 5.2, that

$$\frac{1}{16} \leq \liminf_{L, M \rightarrow \infty} \frac{\text{Tw}_{\max}(L, M, 2)}{4LM} \leq \limsup_{m, n \rightarrow \infty} \frac{\text{Tw}_{\max}(L, M, 2)}{4LM} \leq \frac{1}{16},$$

yielding the result. \square

Lemma 5.4. *The following holds:*

(i) *If $N \geq 2$ is fixed, then*

$$\lim_{L, M \rightarrow \infty} \frac{\text{Tw}_{\max}(L, M, N)}{LMN^2} = \frac{\lceil N/2 \rceil \lfloor N/2 \rfloor}{4N^2}.$$

(ii)

$$\lim_{\substack{N, \mu, \lambda \rightarrow \infty \\ L = \lfloor \lambda N \rfloor, M = \lfloor \mu N \rfloor}} \frac{\text{Tw}_{\max}(L, M, N)}{LMN^2} = \frac{1}{16},$$

where the limit is taken over values $N \in \mathbb{Z}$ and $\mu, \lambda \in \mathbb{R}$ such that at least one of L, M, N is even.

Proof. Given L, M, N , take any even positive integer K such that $L, M \geq 2K$. We shall describe a tiling $t_{K,L,M,N}$ of the box $\mathcal{B} = [0, L] \times [0, M] \times [0, N]$, which is hinted at in Figure 5.3. Let $q_1 = \lceil N/2 \rceil$, $q_2 = \lfloor N/2 \rfloor$, $q = 2 \lceil N/4 \rceil = 2 \lceil q_1/2 \rceil$,

$$n_1 = 2 \left\lfloor \frac{L - 2K + q}{2(K + q)} \right\rfloor, n_2 = 2 \left\lfloor \frac{M - 2K + q}{2(K + q)} \right\rfloor.$$

Divide the box \mathcal{B} into the following parts (see Figure 5.3):

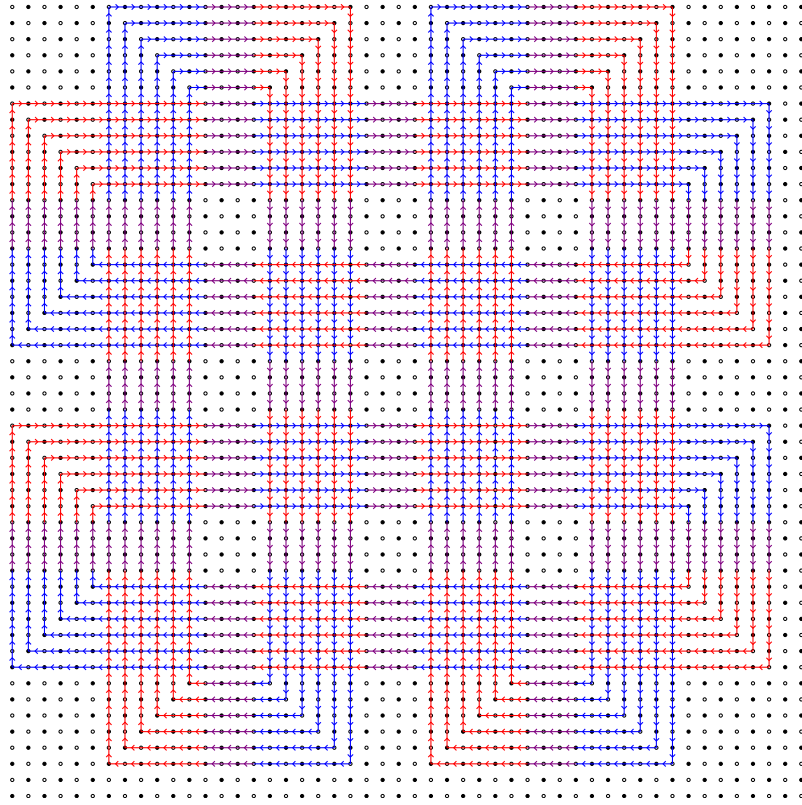


Figure 5.3: Schematic representation of a tiling of $\mathcal{B} = [0, 50] \times [0, 50] \times [0, 8]$, illustrating the construction with $K = 6$, so that $q_1 = q_2 = q = 4$ and $n_1 = n_2 = 4$. This representation works more or less like a sock, but the red arrows indicate that in the top four (in general q_1 or q_2 , depending on the cycle) floors, all the dominoes are in the given direction and with the given orientation (taking cube colors into account); blue arrows are similar, but with respect to the bottom four (again, q_1 or q_2) floors; finally, the purple arrows indicates that dominoes that are parallel to the arrow point in the given direction (but some dominoes are not parallel to it: see Figures 5.4 and 5.5).

- The *exterior padding area*, which is the area in the complement of $[K, 2K + (n_1 - 1)(K + q)] \times [K, 2K + (n_2 - 1)(K + q)] \times [0, N]$ where the curves make turns.
- The *crossing zones*, formed by the subregions $[K + i(K + q), 2K + i(K + q)] \times [K + j(K + q), 2K + j(K + q)] \times [0, N]$, $0 \leq i < n_1$, $0 \leq j < n_2$, where red and blue arrows cross.
- The *transition zones*, formed by the areas where purple arrows occur: each of these areas form a $q \times K \times N$ or $K \times q \times N$ subregion.
- The *filler*, which is the remainder of the box.

The idea for the tiling is as follows: each subregion $[0, L] \times [j, j + 1] \times [0, N]$, where $0 \leq j - K - n(K + q) < K$ for some n , is tiled in a similar fashion as Figure 5.4: the part that “flows horizontally” is formed by q_1 simple paths

that move up and down together such that all horizontal dominoes d have $\vec{v}(d)$ parallel to the corresponding arrow in Figure 5.3 (which are also horizontal in that figure). Similarly, subregions of the form $[i, i + 1] \times [0, M] \times [0, N]$, where $0 \leq i - K - n(K + q) < K$ for some n , are tiled similarly to Figure 5.5: one clearly sees q_2 paths flowing horizontally, which correspond to vertical arrows in Figure 5.3.

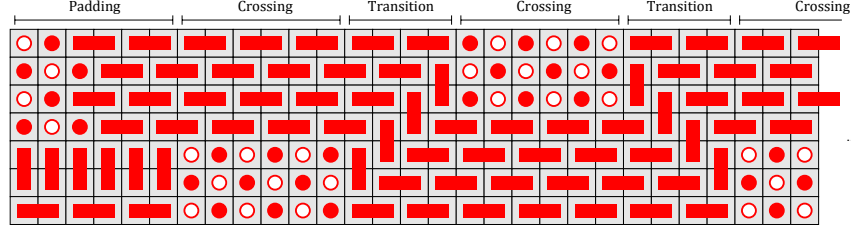


Figure 5.4: Lateral view on the construction, with $K = 6$ and $N = 7$, so that $q = q_1 = 4$ and $q_2 = 3$: this represents part of the subregion $[0, L] \times [K + 2, K + 3] \times [0, N]$ (see also Figure 5.3).

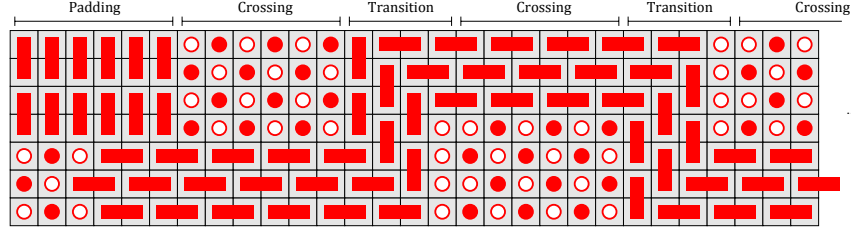


Figure 5.5: Lateral view on the construction, with $K = 6$ and $N = 7$, so that $q = q_1 = 4$ and $q_2 = 3$: this represents part of the subregion $[K + 2, K + 3] \times [0, M] \times [0, N]$ (see also Figure 5.3).

Figures 5.4 and 5.5 also make it clear that the paths need a length of q_1 (for the first kind) and q_2 (second kind) to transition from top to bottom and vice-versa. Since $q \geq \max(q_1, q_2)$, the paths have enough space to transition: any remaining space is filled with dominoes that are orthogonal to the paths, as shown in Figure 5.5 (this is possible because K is even).

Finally, notice that the external padding area has enough space for the curves to make turns, as indicated in Figure 5.3. It is also easy to see that the remainder of the box can be filled in a way that doesn't create any \vec{k} -effects (for instance, since q is even, the $q \times q \times N$ filler subregions can be tiled in a trivial way).

Let $t_{K,L,M,N}$ denote the tiling obtained from this construction: we claim that, in essence, only \vec{k} -effects in the contact zones count towards the twist. To see this, notice that the only areas outside contact zones where there is nonzero \vec{k} -effects between dominoes are the external padding area and (possibly) the

transition zones (for instance, if $q > q_1$ and q_1 is odd, there might be nonzero effects between the dominoes in the path and the dominoes that are used to fill the remaining space). For the transition zones, each cycle has an even number of transitions: since K and q are even, it is easy to see that the effects from two consecutive transitions cancel out. As for the external padding zones, the effects in the four corners of the cycles cancel out if N is even; if N is odd, however, and, say, q_i is even (exactly one of q_1, q_2 is even), then some effects that do not cancel, adding up to $K n_i q_i / 2 \leq K \max(n_1, n_2) q / 2 \leq (L + M) K N$.

By construction, the effects in a single $K \times K$ contact zone equal $(K^2 q_1 q_2) / 4$. Thus, letting $E = (L + M) K N$, we may write

$$\begin{aligned} \text{Tw}(t_{K,L,M,N}) &\geq \frac{n_1 n_2 K^2 q_1 q_2}{4} - E \\ &\geq \left\lfloor \frac{L - 2K + 2 \lceil N/4 \rceil}{2(K + 2 \lceil N/4 \rceil)} \right\rfloor \left\lfloor \frac{M - 2K + 2 \lceil N/4 \rceil}{2(K + 2 \lceil N/4 \rceil)} \right\rfloor K^2 \lceil N/2 \rceil \lfloor N/2 \rfloor - E, \quad (5-4) \end{aligned}$$

To see (i), let $N \geq 2$ be fixed. If, given L, M , we let $K = K(L, M) = 2 \lfloor \sqrt{\min(L, M)} \rfloor$, (5-4) yields that

$$\lim_{L, M \rightarrow \infty} \frac{\text{Tw}(t_{K,L,M,N})}{L M N^2} = \lim_{K \rightarrow \infty} \frac{K^2 \lceil N/2 \rceil \lfloor N/2 \rfloor}{4(K + 2 \lceil N/4 \rceil)^2 N^2} = \frac{\lceil N/2 \rceil \lfloor N/2 \rfloor}{4N^2},$$

which, together with Lemma 5.1, implies (i).

For (ii), let $L = \lfloor \lambda N \rfloor$, $M = \lfloor \mu N \rfloor$ and $K = K(\lambda, \mu, N) = 2N \lfloor \sqrt{\min(\lambda, \mu)} \rfloor$. Then, as $\lambda, \mu, N \rightarrow \infty$ we have $K/N \rightarrow \infty$ and $\frac{\text{Tw}(t_{K,L,M,N})}{L M N^2} \approx \frac{\lceil N/2 \rceil \lfloor N/2 \rfloor}{4N^2} \rightarrow 1/16$. \square

5.2

General bounds for boxes

Lemma 5.5. *Let L, M, N be integers, at least one of them even. Then*

$$\text{Tw}_{\max}(L, M, N) \leq \frac{L M N}{4} \max_{\substack{\alpha, \beta, \gamma \geq 0 \\ \alpha + \beta + \gamma = 1}} \min \left(\frac{N \alpha \beta}{\alpha + \beta}, \frac{M \alpha \gamma}{\alpha + \gamma}, \frac{L \beta \gamma}{\beta + \gamma} \right).$$

Proof. Let t be a tiling of an $L \times M \times N$ box, and let a, b, c denote the number of dominoes parallel to $\vec{\mathbf{i}}, \vec{\mathbf{j}}, \vec{\mathbf{k}}$, respectively: notice that $2a + 2b + 2c = L M N$.

For each pair of integers $0 \leq x < L, 0 \leq y < M$, let $a(x, y)$ (resp. $b(x, y)$) denote the number of dominoes parallel to $\vec{\mathbf{i}}$ (resp. $\vec{\mathbf{j}}$) which contain a cube of the form $C(x^\sharp, y^\sharp z^\sharp)$ for some z . Then $0 \leq a(x, y) + b(x, y) \leq N$ and $\sum_{x,y} a(x, y) = 2a$, $\sum_{x,y} b(x, y) = 2b$.

Notice that $\text{Tw}(t) \leq \frac{1}{4} \sum_{x,y} a(x,y)b(x,y)$. We claim that $\frac{1}{4} \sum_{x,y} a(x,y)b(x,y) \leq \frac{Nab}{2(a+b)}$. To see this, we will consider the following relaxed optimization problem: we want to find the maximum value of $\frac{1}{4} \sum_{x,y} \bar{a}(x,y)\bar{b}(x,y)$, subject to the conditions that $\bar{a}(x,y)$ and $\bar{b}(x,y)$ are nonnegative real numbers, $\bar{a}(x,y) + \bar{b}(x,y) \leq N$, $\sum_{x,y} \bar{a}(x,y) = 2a$, $\sum_{x,y} \bar{b}(x,y) = 2b$.

Let $(\bar{a}(x,y), \bar{b}(x,y))$ be such that $\sum_{x,y} \bar{a}(x,y)\bar{b}(x,y)$ is maximum. We claim that there is at most one pair (x,y) such that $0 < \bar{a}(x,y) + \bar{b}(x,y) < N$. To see this, suppose that (x_1, y_1) and (x_2, y_2) are two such pairs, and suppose $\bar{a}(x_1, y_1) + \bar{b}(x_1, y_1) \geq \bar{a}(x_2, y_2) + \bar{b}(x_2, y_2)$. Then for any $\epsilon > 0$ we have $(\bar{a}(x_1, y_1) + \epsilon)(\bar{b}(x_1, y_1) + \epsilon) + (\bar{a}(x_2, y_2) - \epsilon)(\bar{b}(x_2, y_2) - \epsilon) > \bar{a}(x_1, y_1)\bar{b}(x_1, y_1) + \bar{a}(x_2, y_2)\bar{b}(x_2, y_2)$, which contradicts the maximality of \bar{a}, \bar{b} .

The latter claim implies that there are exactly $\lceil (2a + 2b)/N \rceil$ pairs (x, y) such that $\bar{a}(x, y) + \bar{b}(x, y) > 0$, and exactly $\lfloor (2a + 2b)/N \rfloor = K$ pairs (x, y) where $\bar{a}(x, y) + \bar{b}(x, y) = N$; if we consider two of these K positions (x_1, y_1) and (x_2, y_2) , we see that we must have $\bar{a}(x_1, y_1) = \bar{a}(x_2, y_2)$ and $\bar{b}(x_1, y_1) = \bar{b}(x_2, y_2)$ (if that's not the case, it's easy to see that it cannot be a maximum), so that, in each of these K pairs, $\bar{a}(x, y) = Na/(a+b)$ and $\bar{b}(x, y) = Nb/(a+b)$. If the fractional part s of $(2a + 2b)/N$ is not zero, then there is exactly one position where $\bar{a}(x, y) = Nas/(a+b)$ and $\bar{b}(x, y) = Nbs/(a+b)$. Consequently,

$$\frac{1}{4} \sum_{x,y} \bar{a}(x,y)\bar{b}(x,y) = \frac{1}{4}(K + s^2) \frac{N^2 ab}{(a+b)^2} \leq \frac{2a+2b}{4N} \cdot \frac{N^2 ab}{(a+b)^2} = \frac{Nab}{2(a+b)},$$

establishing the first claim.

Finally, by symmetry (by looking at effects along other directions), we see that $\text{Tw}(t) \leq \frac{1}{2} \min \left(\frac{Nab}{a+b}, \frac{Mac}{a+c}, \frac{Lbc}{b+c} \right)$, and

$$\begin{aligned} \text{Tw}_{\max}(L, M, N) &\leq \frac{1}{2} \max_{\substack{a,b,c \geq 0 \\ a+b+c=LMN/2}} \min \left(\frac{Nab}{a+b}, \frac{Mac}{a+c}, \frac{Lbc}{b+c} \right) \\ &\leq \frac{LMN}{4} \max_{\substack{\alpha, \beta, \gamma \geq 0 \\ \alpha+\beta+\gamma=1}} \min \left(\frac{N\alpha\beta}{\alpha+\beta}, \frac{M\alpha\gamma}{\alpha+\gamma}, \frac{L\beta\gamma}{\beta+\gamma} \right), \end{aligned}$$

completing the proof. \square

Lemma 5.6. Suppose $N \leq M \leq L$, and suppose $(\bar{\alpha}, \bar{\beta}, \bar{\gamma})$ realize the maximum for the problem

$$\max_{\substack{\alpha, \beta, \gamma \geq 0 \\ \alpha+\beta+\gamma=1}} \min \left(\frac{N\alpha\beta}{\alpha+\beta}, \frac{M\alpha\gamma}{\alpha+\gamma}, \frac{L\beta\gamma}{\beta+\gamma} \right). \quad (5-5)$$

Then

$$\frac{N\bar{\alpha}\bar{\beta}}{\bar{\alpha} + \bar{\beta}} = \frac{M\bar{\alpha}\bar{\gamma}}{\bar{\alpha} + \bar{\gamma}} \leq \frac{L\bar{\beta}\bar{\gamma}}{\bar{\beta} + \bar{\gamma}}.$$

Proof. First, observe that $\bar{\alpha}\bar{\beta}\bar{\gamma} > 0$. Suppose, by contradiction, that $\frac{N\bar{\alpha}\bar{\beta}}{\bar{\alpha} + \bar{\beta}} > \frac{M\bar{\alpha}\bar{\gamma}}{\bar{\alpha} + \bar{\gamma}}$. Then $\bar{\beta} > \bar{\gamma}$, and we can pick a sufficiently small $\epsilon > 0$ such that the triple $(\bar{\alpha}, \bar{\beta} - \epsilon, \bar{\gamma} + \epsilon)$ satisfies $\frac{N\bar{\alpha}\bar{\beta}}{\bar{\alpha} + \bar{\beta}} > \frac{N\bar{\alpha}(\bar{\beta} - \epsilon)}{\bar{\alpha} + \bar{\beta} - \epsilon} > \frac{M\bar{\alpha}(\bar{\gamma} + \epsilon)}{\bar{\alpha} + \bar{\gamma} + \epsilon} > \frac{M\bar{\alpha}\bar{\gamma}}{\bar{\alpha} + \bar{\gamma}}$ and $\frac{L(\bar{\beta} - \epsilon)(\bar{\gamma} + \epsilon)}{\bar{\beta} + \bar{\gamma}} = \frac{L(\bar{\beta}\bar{\gamma} + \epsilon(\bar{\beta} - \bar{\gamma}) - \epsilon^2)}{\bar{\beta} + \bar{\gamma}} > \frac{L\bar{\beta}\bar{\gamma}}{\bar{\beta} + \bar{\gamma}}$, which is a contradiction. A similar analysis shows that we cannot have $\frac{L\bar{\beta}\bar{\gamma}}{\bar{\beta} + \bar{\gamma}} > \frac{M\bar{\alpha}\bar{\gamma}}{\bar{\alpha} + \bar{\gamma}}$, so that we necessarily have $\frac{N\bar{\alpha}\bar{\beta}}{\bar{\alpha} + \bar{\beta}} \leq \frac{M\bar{\alpha}\bar{\gamma}}{\bar{\alpha} + \bar{\gamma}} \leq \frac{L\bar{\beta}\bar{\gamma}}{\bar{\beta} + \bar{\gamma}}$.

Finally, if $\frac{N\bar{\alpha}\bar{\beta}}{\bar{\alpha} + \bar{\beta}} < \frac{M\bar{\alpha}\bar{\gamma}}{\bar{\alpha} + \bar{\gamma}} \leq \frac{L\bar{\beta}\bar{\gamma}}{\bar{\beta} + \bar{\gamma}}$, then clearly the triple $(\bar{\alpha} + \epsilon, \bar{\beta}, \bar{\gamma} - \epsilon)$ would have a strictly larger objective function for sufficiently small $\epsilon > 0$, and thus we must have $\frac{N\bar{\alpha}\bar{\beta}}{\bar{\alpha} + \bar{\beta}} = \frac{M\bar{\alpha}\bar{\gamma}}{\bar{\alpha} + \bar{\gamma}}$. \square

Corollary 5.7. *Suppose $N \leq M \leq L$, at least one of them even. Then*

$$\text{Tw}_{\max}(L, M, N) < \frac{1}{16} \left(1 - \frac{N}{4M}\right) LMN^2.$$

Proof. By Lemma 5.6, the maximum value of (5-5) can be bounded above by the problem

$$\max_{\substack{\alpha, \beta, \gamma \geq 0 \\ \alpha + \beta + \gamma = 1}} \frac{N\alpha\beta}{\alpha + \beta}, \quad \text{subject to } \frac{N\alpha\beta}{\alpha + \beta} = \frac{M\alpha\gamma}{\alpha + \gamma}. \quad (5-6)$$

Let $\mu = N/M$, so that $0 < \mu \leq 1$, and denote by $A(\mu)$ the maximum value of $\frac{\alpha\beta}{\alpha + \beta}$ subject to the condition that $\frac{\mu\alpha\beta}{\alpha + \beta} = \frac{\alpha\gamma}{\alpha + \gamma}$: we claim that $A(\mu) < \frac{1}{4}(1 - \mu/4)$. To see this, suppose $\frac{\alpha\beta}{\alpha + \beta} \geq \frac{1}{4}(1 - \mu/4)$ for some α, β : a straightforward calculation shows that $\alpha + \beta \geq 1 - \mu/4$, so that $\gamma = 1 - \alpha - \beta \leq \mu/4$ and so

$$\frac{\alpha\gamma}{\alpha + \gamma} < \gamma(1 - \gamma) < \frac{\mu}{4}(1 - \mu/4) \leq \frac{\mu\alpha\beta}{\alpha + \beta},$$

hence the triple α, β, γ cannot satisfy the condition $\frac{N\alpha\beta}{\alpha + \beta} = \frac{M\alpha\gamma}{\alpha + \gamma}$. Therefore, we have that the maximum of (5-6) is less than $\frac{N}{4}(1 - N/(4M))$. By Lemma 5.5,

$$\text{Tw}_{\max}(L, M, N) < \frac{LMN}{4} \cdot \frac{N}{4} \left(1 - \frac{N}{4M}\right),$$

completing the proof. \square

Corollary 5.8 (Case $L = M$). *Suppose $N \leq M$, at least one of them even, and let $\mu = N/M$. Then*

$$\text{Tw}_{\max}(M, M, N) \leq \frac{2-\mu}{8(4-\mu)} M^2 N^2.$$

In particular, $\text{Tw}_{\max}(N, N, N) \leq N^4/24$.

Proof. Suppose $(\bar{\alpha}, \bar{\beta}, \bar{\gamma})$ realize the maximum of (5-5) for $L = M$. A very similar analysis to the one done in the proof of Lemma 5.6 shows that $\frac{N\bar{\alpha}\bar{\beta}}{\bar{\alpha}+\bar{\beta}} = \frac{M\bar{\alpha}\bar{\gamma}}{\bar{\alpha}+\bar{\gamma}} = \frac{M\bar{\beta}\bar{\gamma}}{\bar{\beta}+\bar{\gamma}}$, so that $\bar{\alpha} = \bar{\beta}$ and $\frac{N}{2} = \frac{M(1-2\bar{\alpha})}{1-\bar{\alpha}}$. Writing $\mu = N/M$, we see that $\bar{\alpha} = \frac{2-\mu}{4-\mu}$ and so $\frac{\bar{\alpha}\bar{\beta}}{\bar{\alpha}+\bar{\beta}} = \frac{\bar{\alpha}}{2} = \frac{2-\mu}{2(4-\mu)}$. By Lemma 5.5, we're done. \square

Corollary 5.9 (Case $M = N$). *Suppose $N \leq L$, at least one of them even, and let $\lambda = N/L$. Then $\text{Tw}_{\max}(L, N, N) \leq C(\lambda)LN^3$, where*

$$C(\lambda) = \begin{cases} \frac{3-2\sqrt{2}}{4}, & \lambda \leq \frac{2+\sqrt{2}}{4}; \\ \frac{2\lambda-1}{8\lambda(4\lambda-1)}, & \frac{2+\sqrt{2}}{4} < \lambda \leq 1. \end{cases}$$

Proof. Let $(\bar{\alpha}, \bar{\beta}, \bar{\gamma})$ realize the maximum of (5-5) for $M = N$. By Lemma 5.6, $\frac{\bar{\alpha}\bar{\beta}}{\bar{\alpha}+\bar{\beta}} = \frac{\bar{\alpha}\bar{\gamma}}{\bar{\alpha}+\bar{\gamma}} \leq \frac{\bar{\beta}\bar{\gamma}}{\lambda(\bar{\beta}+\bar{\gamma})}$, so that $\bar{\beta} = \bar{\gamma}$. Therefore, the value $\max_{0 \leq \gamma \leq 1} \min \left(\frac{(1-2\gamma)\gamma}{1-\gamma}, \frac{\gamma}{2\lambda} \right)$, multiplied by N , equals the maximum in (5-5). Let $f(\gamma) = \frac{(1-2\gamma)\gamma}{1-\gamma}$ and $g(\gamma) = \frac{\gamma}{2\lambda}$.

Notice that f is strictly concave in $(0, 1)$. Since $f'(1 - \sqrt{2}/2) = 0$, it follows that this is the only maximum point of f . Let $\gamma^* \in [0, 1]$ be the largest value for which $f(\gamma^*) = g(\gamma^*)$ ($f(0) = g(0)$). Since for $\gamma \geq 1/2$ we have $f(\gamma) \leq 0 < g(\gamma)$, it follows that $\gamma^* < 1/2$ and $f(\gamma) < g(\gamma)$ whenever $\gamma > \gamma^*$. Therefore, if $\gamma^* \leq 1 - \sqrt{2}/2$, then $f(\gamma^*) < f(1 - \sqrt{2}/2) \leq g(1 - \sqrt{2}/2)$, thus the maximum value is given by $f(1 - \sqrt{2}/2)$. Otherwise, since g is always increasing and f is decreasing for $\gamma > 1 - \sqrt{2}/2$ (because it is concave), it follows that the maximum is given by $g(\gamma^*)$.

Solving the equation $f(\gamma) = g(\gamma)$ yields $\gamma^* = \max(\frac{2\lambda-1}{4\lambda-1}, 0)$, and $\frac{2\lambda-1}{4\lambda-1} = 1 - \sqrt{2}/2$ for $\lambda = \frac{2+\sqrt{2}}{4}$. Hence, the maximum is

$$\begin{cases} f(1 - \sqrt{2}/2) = 3 - 2\sqrt{2}, & \lambda \leq \frac{2+\sqrt{2}}{4}; \\ g\left(\frac{2\lambda-1}{4\lambda-1}\right) = \frac{2\lambda-1}{2\lambda(4\lambda-1)}, & \frac{2+\sqrt{2}}{4} < \lambda \leq 1. \end{cases}$$

By Lemma 5.5, we have

$$T_{\text{wmax}}(L, N, N) \leq \frac{LN^3}{4} \max_{0 \leq \gamma \leq 1} \min \left(\frac{(1-2\gamma)\gamma}{1-\gamma}, \frac{\gamma}{2\lambda} \right) \leq C(\lambda)LN^3,$$

completing the proof. \square

We shall now finish the discussion with a construction that yields a lower bound for the maximum twist of boxes. Let $a, b, c, d \in \mathbb{N}$. The *solenoid* with parameters (a, b, c, d) is a tiling of the box $\mathcal{B} = [0, 2b+2c] \times [0, 2b+d] \times [0, a+2c]$ whose twist is $\lceil abcd/2 \rceil$.

A *wire loop* is a region which, after translation by vectors of integer coordinates and permutations of the axes, equals $([0, m] \times [0, n] \times [0, 1]) \setminus ((1, m-1) \times (1, n-1) \times [0, 1])$ as illustrated by Figure 5.6. Notice that a wire loop has exactly two tilings.

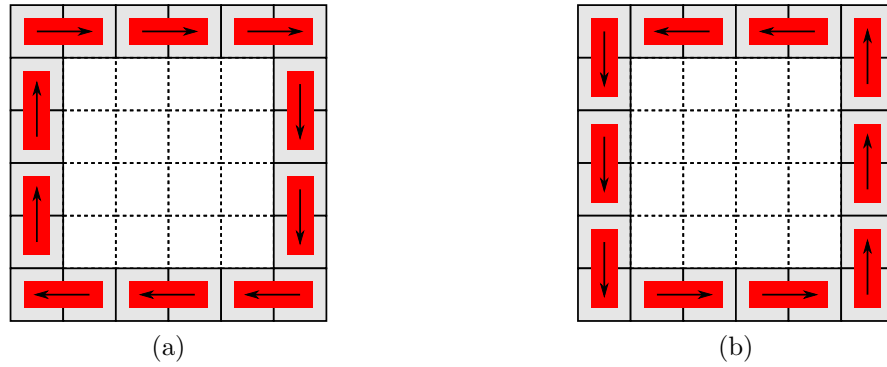
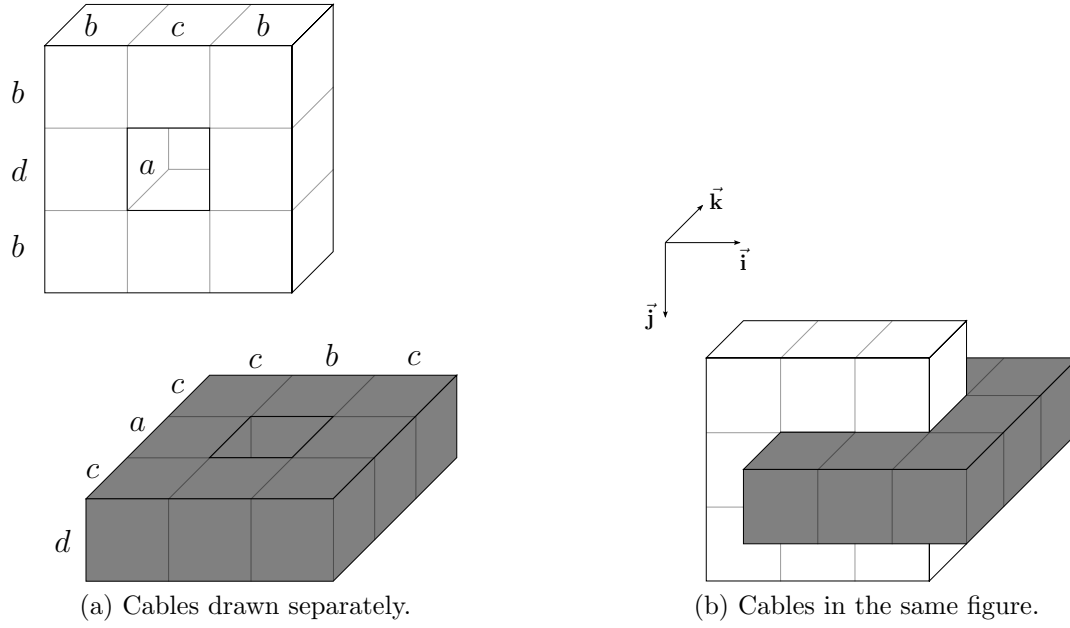
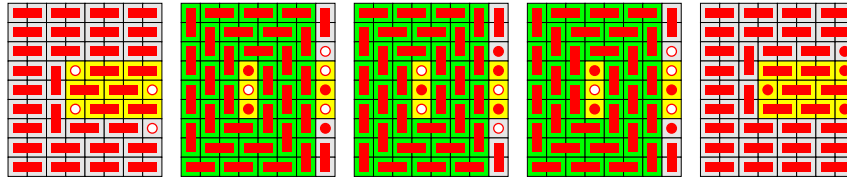


Figure 5.6: The two tilings of a wire loop. The vector $\vec{v}(d)$ is shown for each domino d .

Figure 5.7 shows the basic idea of the solenoid construction. We consider the *cable loops*

$$\begin{aligned} L_0 &= ([0, 2b+c] \times [0, 2b+d] \times [c, a+c]) \setminus ((b, b+c) \times (b, b+d) \times [c, a+c]), \\ L_1 &= ([b, 2b+2c] \times [b, b+d] \times [0, a+2c]) \\ &\quad \setminus ((b+c, 2b+c) \times [b, b+d] \times (c, a+c)), \end{aligned}$$

illustrated in Figure 5.7. Notice that L_0 is the disjoint union of ab wire loops, whereas L_1 is the disjoint union of cd wire loops. Each of these wire loops can be tiled in such a way that if W_0 is a wire loop in L_0 with tiling t_{W_0} and W_1 is a wire loop in t_1 with tiling t_{W_1} , then $T^{\vec{i}}(t_{W_0}, t_{W_1}) + T^{\vec{i}}(t_{W_1}, t_{W_0}) = 1/2$. If we consider the tilings t_0 of L_0 and t_1 of L_1 formed by individual tilings of each wire loop, then $T^{\vec{i}}(t_0, t_1) + T^{\vec{i}}(t_1, t_0) = (abcd)/2$. Figure 5.8 shows an example of this construction.

Figure 5.7: The cable loops L_0 (white) and L_1 (grey).Figure 5.8: A solenoid with parameters $(3, 3, 1, 3)$. L_0 is highlighted in green, while L_1 is highlighted in yellow. Notice that the twist of this tiling is $14 = \lceil 3 \cdot 3 \cdot 1 \cdot 3/2 \rceil$.

A reasonably straightforward case-by-case analysis shows that, if at least one of the parameters a, b, c, d is even, the remainder of the box can be tiled in such a way that the twist of the solenoid is exactly $abcd/2$ (most dominoes will be parallel to \vec{i} , and we need to check that the effects between others cancel out). If all dimensions are odd (as in Figure 5.8), then everything cancels out with the exception of two pairs of dominoes with positive sign in the twist, hence yielding $\lceil abcd/2 \rceil$.

We shall now use this construction to find a lower bound for all boxes. First, an auxiliary Lemma:

Lemma 5.10. *Let $\mathcal{B} = [0, L] \times [0, M] \times [0, N]$ be a box, with N even. Then $\max \text{Tw}(\mathcal{B}) \geq \lfloor L/3 \rfloor \lfloor M/3 \rfloor N/2$.*

Proof. Consider the boxes $\mathcal{B}_{i,j,k} = [3i, 3(i+1)] \times [3j, 3(j+1)] \times [2k, 2(k+1)]$ for $0 \leq i < \lfloor L/3 \rfloor$, $0 \leq j < \lfloor M/3 \rfloor$, $0 \leq k < N/2$. Since the complement $\mathcal{B} \setminus (\bigcup_{i,j,k} \mathcal{B}_{i,j,k})$ is tileable with every domino parallel to \vec{k} , we can clearly

construct a tiling t whose twist is $\sum_{i,j,k} \text{Tw}_{\max}(3, 3, 2) = \lfloor L/3 \rfloor \lfloor M/3 \rfloor (N/2)$ (see Example 3.5). \square

Remark 5.11. *Lemma 5.10 also implies that the only tileable flip connected boxes are those of dimension $L \times M \times 1$ and $L \times 2 \times 2$ (and rotations of those boxes). It is easy to show that these boxes are flip connected: $L \times M \times 1$ boxes are essentially plane regions, and one can show by induction that $L \times 2 \times 2$ boxes are flip connected. For any other tileable $L \times M \times N$ box, we can after a rotation assume that $L, M \geq 3$, $N \geq 2$ and that N is even, so that $k = \lfloor L/3 \rfloor \lfloor M/3 \rfloor N > 0$. Since all the elements in the sequence differ by positive trits, it follows that the box has at least $k + 1 > 1$ flip connected components.*

Lemma 5.12. *If $L, M, N \geq 2$, at least two of them greater than or equal to 3 (and at least one of them even), then $\text{Tw}_{\max}(L, M, N) \geq (1/162)LMN \min(L, M, N)$.*

Proof. Assume that $N \leq M \leq L$. If $N < 4$, then Lemma 5.10 suffices: if $N = 2$, $\lfloor L/3 \rfloor \lfloor M/3 \rfloor N/2 \geq LMN/50 \geq LMN^2/100$; if $N = 3$, and, say, L is even, then $\lfloor N/3 \rfloor \lfloor M/3 \rfloor L/2 \geq LMN/30 \geq LMN^2/90$. Therefore, we may assume that $N \geq 4$.

In order to construct the most efficient solenoid, we rotate the box and consider $\mathcal{B} = [0, N] \times [0, M] \times [0, L]$. Let $b = \lfloor N/4 \rfloor$, $c = \lfloor (N+2)/4 \rfloor$, $a = L - 2c$ and $d = M - 2b$. Let t be the tiling of \mathcal{B} obtained from the solenoid construction with parameters a, b, c, d (and $[N - 2b - 2c, N] \times [0, M] \times [0, L]$ is tiled with all dominoes parallel to each other).

Now

$$\frac{\text{Tw}(t)}{LMN^2} = \frac{\lceil \frac{abcd}{2} \rceil}{LMN^2} \geq \frac{bc}{2N^2} \cdot \frac{M - 2b}{M} \cdot \frac{L - 2c}{L} \geq \frac{bc}{2N^2} \cdot \left(1 - \frac{2b}{N}\right) \left(1 - \frac{2c}{N}\right).$$

Let $g(N)$ denote the last expression: we see that $g(4) = 1/128$, $g(5) = 9/1400$, $g(6) = 1/162$, $g(7) = 15/2401$, which are all greater than or equal to $1/162$. We now want to see that $g(N+4) \geq g(N)$. Clearly $g(4k) = 1/128$ for any $k > 0$. For the other cases, we see that for $i = 1, 2, 3$, we have $g(4k+i+4) - g(4k+i) = p_i(k)/(2(4k+i+4)^4(4k+i)^4)$, where $p_1(k) = (4k+3)(64k^4 + 192k^3 + 180k^2 + 54k + 3)$, $p_2(k) = 256(k+1)^3(4k^2 + 8k + 1)$, $p_3(k) = 2(k+1)(2k+3)(4k+5)(80k^2 + 200k + 81)$. Since clearly $p_i(k) > 0$ for $k > 0$, we see that $g(N+4) \geq g(N)$ and thus $\text{Tw}(t)/(LMN^2) \geq 1/162$. \square

Proof of Theorem 4. The general lower and upper bounds follow directly from Lemmas 5.1 and 5.12. Lemmas 5.4 and Corollary 5.8 (using $L = M = N$) imply that, if $h(L, M, N) = \text{Tw}_{\max}(L, M, N)/(LMN \min(L, M, N))$, then

$$\limsup_{L, M, N \rightarrow \infty} h(L, M, N) = \frac{1}{16} \text{ and } \liminf_{L, M, N \rightarrow \infty} h(L, M, N) \leq \frac{1}{24},$$

completing the proof. □

Glossary

- B** The set of all positively oriented bases formed by vectors of Φ .
- $\text{color}(v)$ The color of some object (a cube, a square, a vertex, etc): 1 if it is black, and -1 if it is white.
- cylinder** Region of the form $\mathcal{D} \times [0, N]$ (possibly rotated), where $\mathcal{D} \subset \mathbb{R}^2$ is a connected and simply connected planar region. Same as multiplex.
- Δ The set $\{\vec{\mathbf{i}}, \vec{\mathbf{j}}, \vec{\mathbf{k}}\}$.
- $A_0 \sqcup A_1$ The union of two disjoint sets A_0 and A_1 .
- duplex region** Region of the form $\mathcal{D} \times [0, 2]$, where $\mathcal{D} \subset \mathbb{R}^2$ is a connected and simply connected planar region.
- embedding** In general, an embedding of a tiling t of \mathcal{R} in a larger region $\mathcal{R}' \supset \mathcal{R}$ is a tiling of \mathcal{R}' which coincides with t in \mathcal{R} . For specific uses, see Sections 3.5, 3.7 and 4.6.
- ghost curve** Curve connecting a source to a sink in a two-story region. See page 19.
- jewel** Projection of a domino that is parallel to the axis of a duplex region. See page 16.
- $\text{Link}(\gamma_0, \gamma_1)$ The linking number between two curves γ_0 and γ_1 .
- multiplex** Region of the form $\mathcal{D} \times [0, N]$ (possibly rotated), where $\mathcal{D} \subset \mathbb{R}^2$ is a connected and simply connected planar region. Same as cylinder.
- Φ The set $\{\pm\vec{\mathbf{i}}, \pm\vec{\mathbf{j}}, \pm\vec{\mathbf{k}}\}$.
- (\vec{u} -)pretwist** See $T^{\vec{u}}(t)$.
- $P_t(q)$ Polynomial invariant for regions with two floors. See pages 17 and ??.
- n^\sharp Equals $n + 1/2$.
- sock** System of cycles. See page 27.

$\tau^{\vec{u}}(d_0, d_1)$ The effect of the domino (or segment) d_0 on the domino (or segment) d_1 along \vec{u} : see pages 41 and 48.

$\tau_{a,b}^\beta(\ell_0, \ell_1)$ The slanted effect of the segment ℓ_0 on the segment ℓ_1 with parameters $\beta \in \mathbf{B}$ and $a, b \in \mathbb{R}$. See page 49.

$T_{a,b}^\beta(A_0, A_1)$ Sums of slanted effects $\tau_{a,b}^\beta(\ell_0, \ell_1)$ for all segments $\ell_0 \in A_0, \ell_1 \in A_1$. See page 51.

$T_{a,b}^\beta(A)$ Equals $T_{a,b}^\beta(A, A)$: see page 51.

$T^{\vec{u}}(t), T^{\vec{u}}(A)$ The \vec{u} -pretwist of a tiling t (see page 42); also, if A is an arbitrary set of segments, this equals $T^{\vec{u}}(A, A)$: see page 51.

$T^{\vec{u}}(A_0, A_1)$ The sum of effects of segments of A_0 on segments of A_1 along \vec{u} . See page 51.

$\text{Tw}(t)$ Integer that is invariant by flips in cylinders. See Definition 4.4 on page 43.

$\text{Tw}_{\max}(L, M, N)$ The maximum value of the twist on the set of tilings of an $L \times M \times N$ box.

$\text{wind}(\gamma, p)$ The winding number of a planar curve γ around a point $p \in \mathbb{R}^2$.

$\text{Wr}(\gamma, \vec{u})$ The directional writhing number of a curve γ in the direction of a vector \vec{u} . See page 53.

$\text{Wr}^\pm(\gamma)$ A particular directional writhing number. See page 57.

Bibliography

- [1] Colin C. Adams. *The knot book: an elementary introduction to the mathematical theory of knots*. American Mathematical Soc., 2004.
- [2] David G. Alciatore and Rick Miranda. A winding number and point-in-polygon algorithm. Technical report, Colorado State University, 1995.
- [3] Olivier Bodini and Damien Jamet. Tiling a Pyramidal Polycube with Dominoes. *Discrete Mathematics & Theoretical Computer Science*, 9(2), 2007.
- [4] Mihai Ciucu. An improved upper bound for the three dimensional dimer problem. *Duke Math J*, 94:1–11, 1998.
- [5] Henry Cohn, Noam Elkies, James Propp, et al. Local statistics for random domino tilings of the Aztec diamond. *Duke Mathematical Journal*, 85(1):117–166, 1996.
- [6] John H. Conway and Jeffrey C. Lagarias. Tiling with polyominoes and combinatorial group theory. *Journal of combinatorial theory, Series A*, 53(2):183–208, 1990.
- [7] Noam Elkies, Greg Kuperberg, Michael Larsen, and James Propp. Alternating-sign matrices and domino tilings (Part II). *Journal of Algebraic Combinatorics*, 1(3):219–234, 1992.
- [8] Shmuel Friedland and Uri N. Peled. Theory of computation of multidimensional entropy with an application to the monomer–dimer problem. *Advances in applied mathematics*, 34(3):486–522, 2005.
- [9] F. Brock Fuller. The Writhing Number of a Space Curve. *Proc. Nat. Acad. Sci. USA*, 68(4):815–819, 1971.
- [10] J. M. Hammersley. Existence theorems and Monte Carlo methods for the monomer-dimer problem. In F.N. David, editor, *Research Papers in Statistics: Festschrift for J. Neyman*, pages 125–146. Wiley, 1966.

- [11] William Jockusch, James Propp, and Peter Shor. Random domino tilings and the arctic circle theorem. *arXiv:math/9801068*, 1995.
- [12] P. W. Kasteleyn. The statistics of dimers on a lattice: I. The number of dimer arrangements on a quadratic lattice. *Physica*, 27(12):1209 – 1225, 1961.
- [13] Richard Kenyon, Andrei Okounkov, et al. Planar dimers and Harnack curves. *Duke Mathematical Journal*, 131(3):499–524, 2006.
- [14] Richard Kenyon, Andrei Okounkov, and Scott Sheffield. Dimers and amoebae. *Annals of mathematics*, pages 1019–1056, 2006.
- [15] Joakim Linde, Cristopher Moore, and Mats G. Nordahl. An n -dimensional generalization of the rhombus tiling. *Discrete Mathematics and Theoretical Computer Science Proceedings AA*, pages 23–42, 2001.
- [16] Pedro H. Milet and Nicolau C. Saldanha. Additional material for *Domino tilings of three-dimensional regions*. <http://www.nicolausaldanha.com/multiplex/index.html>.
- [17] Pedro H. Milet and Nicolau C. Saldanha. Flip invariance for domino tilings of three-dimensional regions with two floors. To appear in *Discrete & Computational Geometry*. doi:10.1007/s00454-015-9685-y.
- [18] Pedro H. Milet and Nicolau C. Saldanha. Domino tilings of three-dimensional regions: flips, trits and twists. *arXiv:1410.7693*, 2014.
- [19] Igor Pak and Jed Yang. The complexity of generalized domino tilings. *The Electronic Journal of Combinatorics*, 20(4):P12, 2013.
- [20] Dana Randall and Gary Yngve. Random three-dimensional tilings of Aztec octahedra and tetrahedra: an extension of domino tilings. In *Proceedings of the eleventh annual ACM-SIAM symposium on Discrete algorithms*, pages 636–645. Society for Industrial and Applied Mathematics, 2000.
- [21] Nicolau C. Saldanha, Carlos Tomei, Mario A. Casarin Jr., and Domingos Romualdo. Spaces of domino tilings. *Discrete & Computational Geometry*, 14:207–233, 1995.
- [22] Nicolau C. Saldanha and Carlos Tomei. An overview of domino and lozenge tilings. *Resenhas IME-USP*, 2(2):239–252, 1995.

- [23] William P. Thurston. Conway's Tiling Groups. *The American Mathematical Monthly*, 97(8):pp. 757–773, 1990.